UNIVERSITY OF SÃO PAULO

PHARMACEUTICAL SCIENCES FACULTY

Department of Clinical and Toxicological Analysis

Graduate Program in Pharmacy (Physiopathology and Toxicology)

A non-targeted proteomics investigation of cylindrospermopsin-induced hepatotoxicity

Carlos Andrey González Blanco

Manuscript presented for the degree of P.h.D.
Professor Advisor: Assoc. Prof. Ernani Pinto

São Paulo

2017

UNIVERSIDADE DE SÃO PAULO
FACULDADE DE CIÊNCIAS FARMACÊUTICAS
Departamento de Analises Clinicas e Toxicológicas
Programa de Pós-graduação em Farmacia (Fisiopatologia e Toxicologia)

Uso de uma estratégia proteômica não-direcionada para investigar a hepatotoxicidade producida pela cilindrospermopsina

Carlos Andrey González Blanco

Versão corrigida da Tese conforme resolução CoPGr 6018

Tese para obtenção do Título de Doutor
Orientador: Prof. Assoc. Ernani Pinto

São Paulo
2017

CARLOS ANDREY GONZÁLEZ BLANCO

A non-targeted proteomics investigation of cylindrospermopsin-induced hepatotoxicity

Comissão Julgadora

da

Tese para obtenção do Título de Doutor

Prof. Assoc. Ernani Pinto

orientador/presidente

_____

1o. examinador

_____

2o. examinador

_____

3o. examinador

_____

4o. examinador

São Paulo, _____ de _____ de 2017

Ficha Catalográfica
Elaborada pela Divisão de Biblioteca e
Documentação do Conjunto das Químicas da USP

González Blanco, Carlos Andrey
G642n
A non-targeted proteomics investigation of cylindrospermopsin-induced hepatotoxicity / Carlos Andrey González Blanco. - São Paulo, 2017.
156 p.

Tese (doutorado) - Faculdade de Ciências Farmacêuticas da Universidade de São Paulo. Departamento de Análises Clínicas e Toxicológicas.

Orientador: Pinto, Ernani

1. Toxicologia. 2. Toxinas de microorganismos. 3. Interação metabolito e proteina. 4. Proteomica . I. T. II. Pinto, Ernani , orientador.

“The map is not the territory”.

A. Korzybski

Acknowledgement

I would like to thank my thesis advisor Prof. Ernani for his unconditional support and friendship. Throughout the years, I saw you taking risks in projects and making daring decisions in your academic career, which always turned up right. The audacity I saw in your work inspired me to strive harder and try out new ideas.

I would also like to thank all the students I met throught the years at prof. Ernani`s lab, all of which are and will always be great friends; I learned something from each and every one of you. Special credit to my friends Felipe and Fabiane Dörr for your counseling on chromatography and MS related topics. Kazumi, Teras, Raquel, Fernanda and Jõao, thank you all for your friendship and warmth. Finally thanks Faby dos Anjos for being my first friend at the lab; thanks for your guidance and love.

Thanks to Prof. Ana Campa (and all of her bright students), as well as the staff at the Clinical and Toxicological Analysis Department (Farmaceutical Sciences Faculty - USP). Every FACS analysis was done under close supervision of our Department's expert Renata. I would also like to express my gratitude to prof. Eduardo Reis at the Chemistry Institute (USP) and his student Diogo for welcoming me in your molecular biology lab. Thanks to Gaby at INCOR (Medicine Faculty – USP) for your help on my first SILAC experience. I am also indebted to Valdemir and Karina at Fleury Medicine and Health Group; Val this project would not have been possible without your insights and analytical elegance.

Thanks to the students, PI's, and staff of the Biochemistry and Biophisics Lab. and also of LETA, at the Butantan Institute. Special thanks to Ana Olivia, Rose, Adrian and Douglas. Patricia, thanks for your friendship and for all your help and care specially on the experiments on my last months in SP. This project was achieved for the most part thanks to the support and the invaluable scientific guidance of Janice Onuki throught the years.

Yuri, Karol, Raul, Karina and Ernesto thanks for your unconditional friendship; I am in great debt to each and every one of you.

I would also like to express my gratitude to prof. Pierre Thibault at IRIC (Université de Montréal) for welcomimg me in his proteomics group. Thanks to Sybille, Eric, Peter, Chong-Yang, Francis, Christina and everybody I met at Thibault's lab around those months.

Cheers to all of my good friends and colleagues of theToxicology laboratory at the Department of Forensic Sciences, Costa Rica. You always inspired me to become a better scientist.

Finally, I would like to express profound gratitude to Mom, Dad, Kim and Fabi for providing me with boundless support and love during the course of learning, unlearning, researching and throughout the writing of this manuscript.

Thank you.

Carlos.

ABSTRACT

GONZALEZ, C. A. B. **A non-targeted proteomics investigation of cylindrospermopsin-induced hepatotoxicity**. 2017. Thesis (PhD) – Pharmaceutical Sciences Faculty, São Paulo University, São Paulo, 2017.

Cyanobacteria is perhaps the phylum that profit the most from the escalating hypereutrophication of continental waters. The resulting cyanobacterial blooms may accumulate a variety of potent toxins. Cylindrospermopsin (CYN) is a cyanotoxin known for inhibiting protein synthesis, and producing oxidative stress as well as DNA damage in eukaryotic cells. Since the toxin's molecular mechanisms and targets are still unclear, we purified the cyanotoxin from our lab strains and employed a shotgun proteomics approach to reveal the major changes in HepG2 cells at sublethal doses of CYN (1 μM for 6, 12 and 24h). Metabolically labeled cells were stimulated and lysed after each treatment, their tryptic digests were separated by nano HPLC and analyzed by high-resolution tandem mass spectrometry (HRMS) on data dependent acquisition mode. We scanned an average of 4000 proteins in every sample throughout the three timepoints. Cholesterol biosynthesis and transport was mostly downregulated throughout the timepooints of the experiment. Downregulation of proteins related to ubiquitination (e.g. UBE2L3) and proteolysis pathways (e.g. PSMA2) was observed in the proteomics dataset, and these results were validated by western blot. Transcription, translation and cell cycle processes showed convoluted regulation dynamics involving known cell cycle regulators like PCNA. Downregulation of mitochondrial enzymes, oxidative stress and damage to the mithochondrial inner membrane was early evidenced after a 6 hrs treatment and validated using a JC-1, a mitochondrial membrane potential probe. The resulting dataset gives us a first glimpse of the protein groups affected at the early stage of CYN cell intoxication.

Keywords: Cyanotoxins, cyanobacteria, cylindrospermopsin, proteomics, toxicity, apoptosis, SILAC.

RESUMO

GONZALEZ, C. A. B. Uso de uma estratégia proteômica não-direcionada para investigar a hepatotoxicidade producida pela cilindrospermopsina. Tese (Doutorado) – Faculdade de Ciências Farmacêuticas, Universidade de São Paulo, São Paulo, 2017.

Cianobactéria é o filo que mais se beneficia da crescente hipereutrofização das águas continentais. As florações de cianobactérias resultantes podem acumular potentes toxinas. A Cilindrospermopsina (CYN) é uma cianotoxina conhecida por inibir a síntese protéica e produzir estresse oxidativo, além de danos ao DNA em células eucarióticas. Os mecanismos moleculares e alvos de toxicidade aguda desta toxina ainda não são claros. Por esse motivo adoptamos uma abordagem de proteômica quantitativa baseada em descoberta para revelar as principais alterações nas células HepG2 em doses subletais de CYN (1 μM para 6, 12 e 24h). As proteinas dos hepatócitos foram marcadas metabolicamente, foram estimuladas com a toxina e os digestos trípticos foram analisados por espectrometria de massa em tandem de alta resolução (HRMS) no modo de aquisição dependente de dados. Escaneamos uma média de 4000 proteínas ao longo dos intervalos de tempo. A biosintese e transporte do colesterol foi inibida durante a maior parte do tratamento com a toxina. Proteínas e enzimas relacionadas com o processo de ubiquitinação (ex. UBE2L3) e proteólise (ex. PSMA2) foram inibidas, e alterações nas proteínas envolvidas nesses processos foram validadas por meio de Western Blot. Os processos de transcrição, tradução e ciclo celular mostraram uma dinâmica de regulação complexa, envolvendo reguladores e disruptores do ciclo celular como por exemplo PCNA. Danos à membrana mitocondrial e evidência de estresse oxidativo foram detectados após 6 horas de tratamento, e essas mudanças no proteoma foram validados por meio do corante JC-1 (test que detecta mudanças no potencial da membrana mitocondrial). O banco de dados resultante nos dá um primeiro vislumbre das proteinas afetados no estágio inicial da intoxicação celular pela CYN.

.

Palavras-chave: Cianotoxinas, cianobactérias, cilindrospermopsina, proteômica, toxicidade, apoptose, SILAC.

LIst of Figures

LIST OF ABBREVIATIONS AND ACRONYMS

7D-CYN: 7-deoxy-cylindrospermopsin

7D-desulfo-CYN: 7-deoxy-desulfo-cylindrospermopsin

ACN: acetonitrile

APC: allophycocyanin (red laser fluorophore)

Arg: L-arginine

BCA: bicinchoninic acid

C18 column: column with an octadecyl carbon chain-bonded silica stationary phase

CID: collision-induced dissociation

CENA: center for nuclear energy in agriculture

CO_2: carbon dioxide

CH_2CL_2: dichloromethane

CYN: cylindrospermopsin

CYP450: Cytochrome P450

Cys: L-cystein

DAD: diode array detector

DMEM: Dulbecco´s Modified Eagle Medium

DMSO: dimetilsulfoxide

DNA: deoxyribonucleic acid

EDTA: ethylenediamine tetra-acetic acid

EIC: Extracted ion chromatogram

ELISA: enzyme-linked immunosorbent assay

FMO: fluorescence minus one

FA: formic acid

FBS: fetal bovine serum

FC: fold change

FDR: false discovery rate

GNPC: graphitized non-porous carbon

GO: gene ontology

GOBP: gene ontology biological process

GOCC: gene ontology cellular componente

GOMF: gene ontology molecular function

H: heavy labeled cells (cells with >95% incorporation of Arg $^{13}C_6$ $^{15}N_4$ and Lys $^{13}C_6$ $^{15}N_2$)

HCD: high-energy collision dissociation

HPLC: high performance liquid chromatography

HPLC-DAD: high performance liquid chromatography with diode array detection

HPLC-MS^2: high performance liquid chromatography coupled to tandem mass spectrometry

hr: hour

ICAT: isotope-coded affinity tags

ip: intra peritoneal

IRD: Institute of Renal Diseases

IRIC: Institute for Research in Immunology and Cancer

K: L-lysine

KEGG: Kyoto encyclopedia of genes and genomes.

L: light labeled cells (cells with >99% incorporation of normal amino acids)

LD_{50}: median lethal dose

Lys: L-lysine

M: medium labeled cells (cells with >95% incorporation of Arg 13C6 and Lys 4,4,5,5-D4)

MeOH: methanol

MS: mass spectrometry

MS^2: tandem mass spectrometry

MTT: 3-(4,5-dimethylthiazolyl-2)-2,5-diphenyltetrazolium bromide

N_2: nitrogen

NADPH: nicotinamide adenine dinucleotide phosphate

NH_2: amine group

O_2: oxigen

PAC: powdered activated carbon

PARP: poly ADP ribose polymerase

PBS: phosphate buffered saline

PCA: principal component analysis

PE: phycoerytrin (blue laser fluorophore)

PI: propidium iodide

PP1/2A: protein phosphatase 1/2A

PRH: primary rat hepatocites

R^2: coeficient of determination

R: L-Arginine

RNA: ribonucleic acid

ROS: reactive oxygen species

RT: room temperature

SCX: strong cation exchange

SD: standard deviation

SDC buffer: sodium deoxycholate buffer

SDS-PAGE: sodium dodecyl sulfate - polyacrylamide gel electrophoresis

SILAC: stable isotope labeling by amino acids in cell culture

SPE: solid phase extraction

SPR: surface plasmon resonance

TMT: tandem mass tag

TABLE OF CONTENTS

1.0 INTRODUCTION

The production of toxins by harmful blooms of cyanobacteria has become a major problem for countries whose drinking and recreational water supplies come from lakes or open-air water reservoirs (MOREIRA, AZEVEDO, ET AL., 2013).

The cyanotoxin cylindrospermopsin (CYN) is a worldwide health risk. *Cylindrospermopsis raciborskii* and other species capable of synthesizing this molecule have been reported in water bodies of tropical areas and temperate regions of Australia, North America, South America, New Zealand and Europe. However, cyanobacterial species capable of producing CYN and CYN structural variants are found in almost all latitudes of the world (GALLO, FABBROCINO, ET AL., 2009, BITTENCOURT-OLIVEIRA MDO, PICCIN-SANTOS, ET AL., 2014).

Exposure to CYN produces a fatty liver and hepatonecrosis in experimental animals, with extrahepatical lesions of variable location and severity. The primary toxic effect of this alkaloid appears to be irreversible protein synthesis inhibition, oxidative stress and deoxyribonucleic acid (DNA) damage. Nevertheless, a comprehensive and specific mechanism is yet unclear (MOREIRA, ET AL., 2013, SADLER, 2015).

The site of action of this toxin is not known. A biological target or targets would help us to better understand mechanism(s) of cell damage, leading to identification of biomarkers of exposure and effect. High output techniques, like modern proteomics, can yield useful quantitative information on the effect of xenobiotics on a biological system.

In this study we intent to quantify the effects of CYN on the proteome and of human hepatoma cells (HepG2). Knowing which proteins groups are specifically upregulated or downregulated by the toxin in cultured hepatocytes will contribute to the understanding of why the liver is one of the most affected organs by CYN in poisoned animals.

In the pharmaceutical field the knowledge generated by the study may be useful for the preparation of therapeutic drugs for the purpose of specific regulation of metabolic pathways or causing programmed cell death in cancer cells for example.

In the environmental research field a detailed insight of the mechanism of action of this toxin, will contribute to the understanding of the environmental impact that could result from the release of this toxin in animal populations, freshwater plants

and microorganisms. In addition, a better understanding of the CYN mechanism could lead to its potential use in the fields of agriculture, veterinary or biotechnology.

The major steps for the accomplishment of the current project are described in Figure 1.

Figure 1 - Schematic workflow of the major stages of the current research project.

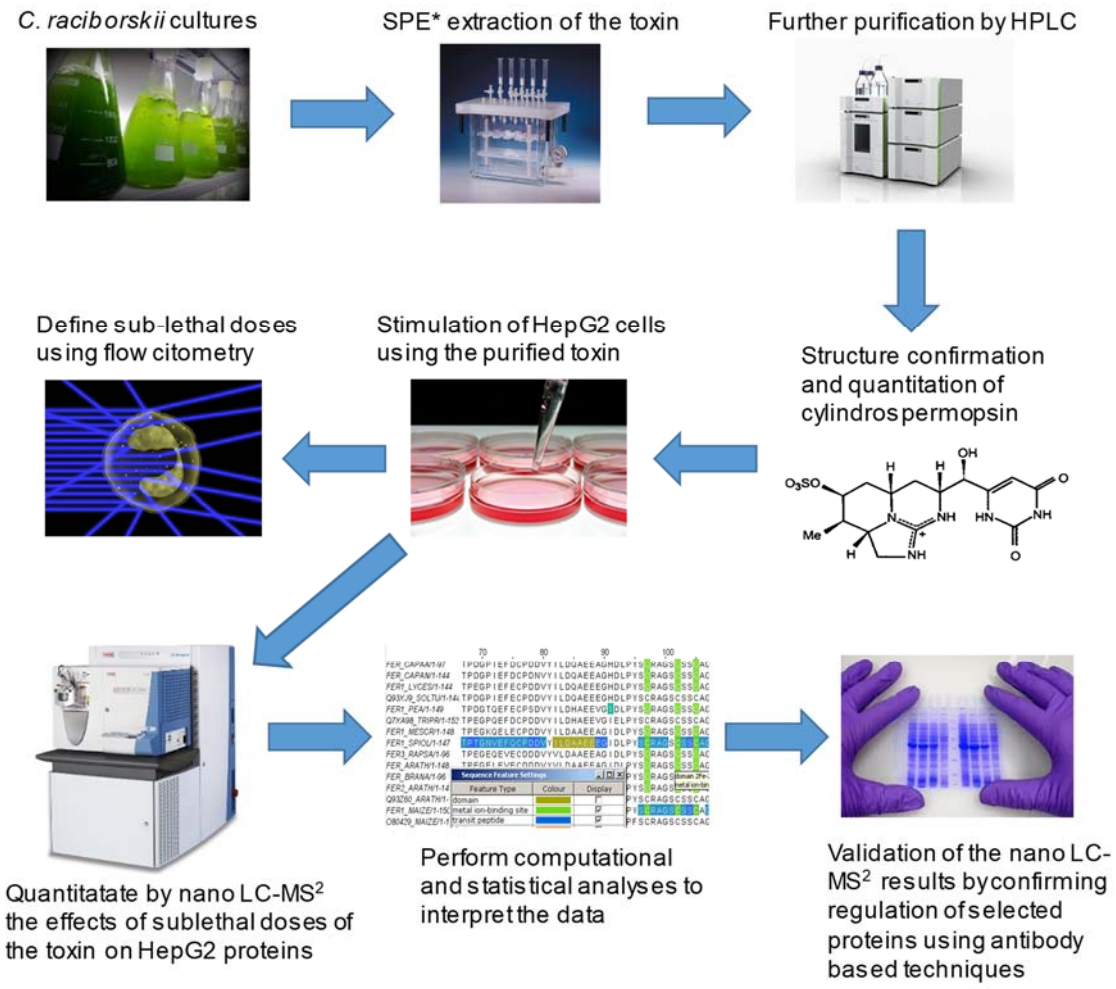

*SPE: solid phase extraction

2.0 LITERATURE REVIEW

2.1 Impact of cyanotoxins in Brazilian freshwaters

The large-scale production of toxins by harmful cyanobacteria or "blue-green algae bloom" has become an important issue for countries whose freshwater supply comes from lakes, ponds or large artificial water reservoirs in the open. In Brazil the problem of cyanobacteria and their toxins in water is widely known, and is a matter of public health policies. The accident occurred at the Institute of Renal Diseases (IRD) in Caruaru, Pernambuco, during the month of February 1996 transformed the history and clinical hemodialysis practice. Contamination of water used for dialysis with microcystin (one cyanotoxin), caused the death of at least 65 patients. This incident made it clear that studies on harmful algae and their secondary metabolites is a relevant topic in the scientific community in Brazil (AZEVEDO, CARMICHAEL, ET AL., 2002).

Due to the frequent contamination of drinking water with cyanotoxins that can cause serious heakth issues, the No.2.914 regulatory guidelines published on 2011 (Ministry of Health, Brazil) established as mandatory microcystins and saxitoxins analysis. It also states that, when detecting the presence of potentially CYN and anatoxin-a (s) producing cyanobacteria, it is recommended to screen the prescence of these toxins. According to these regulation, the maximum acceptable concentration for CYN in drinking water is 1.0 µg/L.

Figure 2 - Images showing: (A) the filamentous cyanobacteria *Cylindrospermopsis raciborskii* 400x, (B) the colonial *Microcystis sp*. 400x, (C) a typical cyanobacterial laboratory culture, and (D) a harmful cyanobacterial bloom at a water reservoir in Americana, São Paulo.

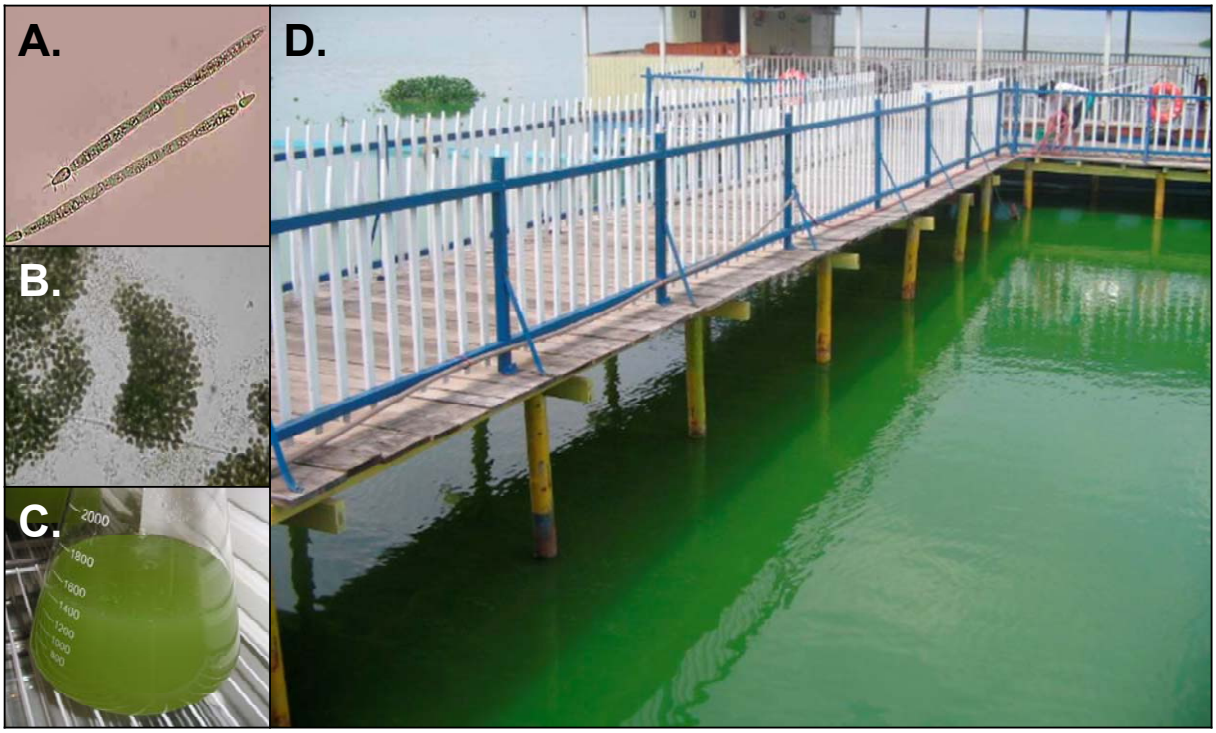

The most common group of cyanotoxins are the hepatotoxins: microcystins, nodularins and CYN (Figure 3). The cyclical heptapeptides called microcystins (MC) cause toxic effects in hepatocytes by inhibiting phosphatase PP1 and PP2A enzymes. Consequently, the inactivation of these enzymes mantain the cytoskeletal proteins in a hyperphosphorylated state promoting disruption and disintegration of the hepatocytes (YOSHIZAWA, MATSUSHIMA, ET AL., 1990). *Microcystin aeruginosa* is the main producing species MCs, however they are also synthesized by other cyanobacterial genera. Structural analogues of MC-LR are the most commonly reported MC in the scientific literature (PEARSON, MIHALI, ET AL., 2010) and have an L-leucine residue at position R1 and L-arginine at position R2 (fig. 3). The nodularins (NOD) are cyclic pentapeptides whose mechanism of toxicity and pathology are identical to those of MCs. CYN has cytotoxic activity especially in the liver of mammals (TERAO, OHMORI, ET AL., 1994). It is a potent inhibitor of protein synthesis, has genotoxic action and also induces oxidative stress with production of reactive oxygen species (ROS) (FROSCIO, HUMPAGE, ET AL., 2003).

Figure 3 - Chemical structure of the most common cyanobacterial toxins.

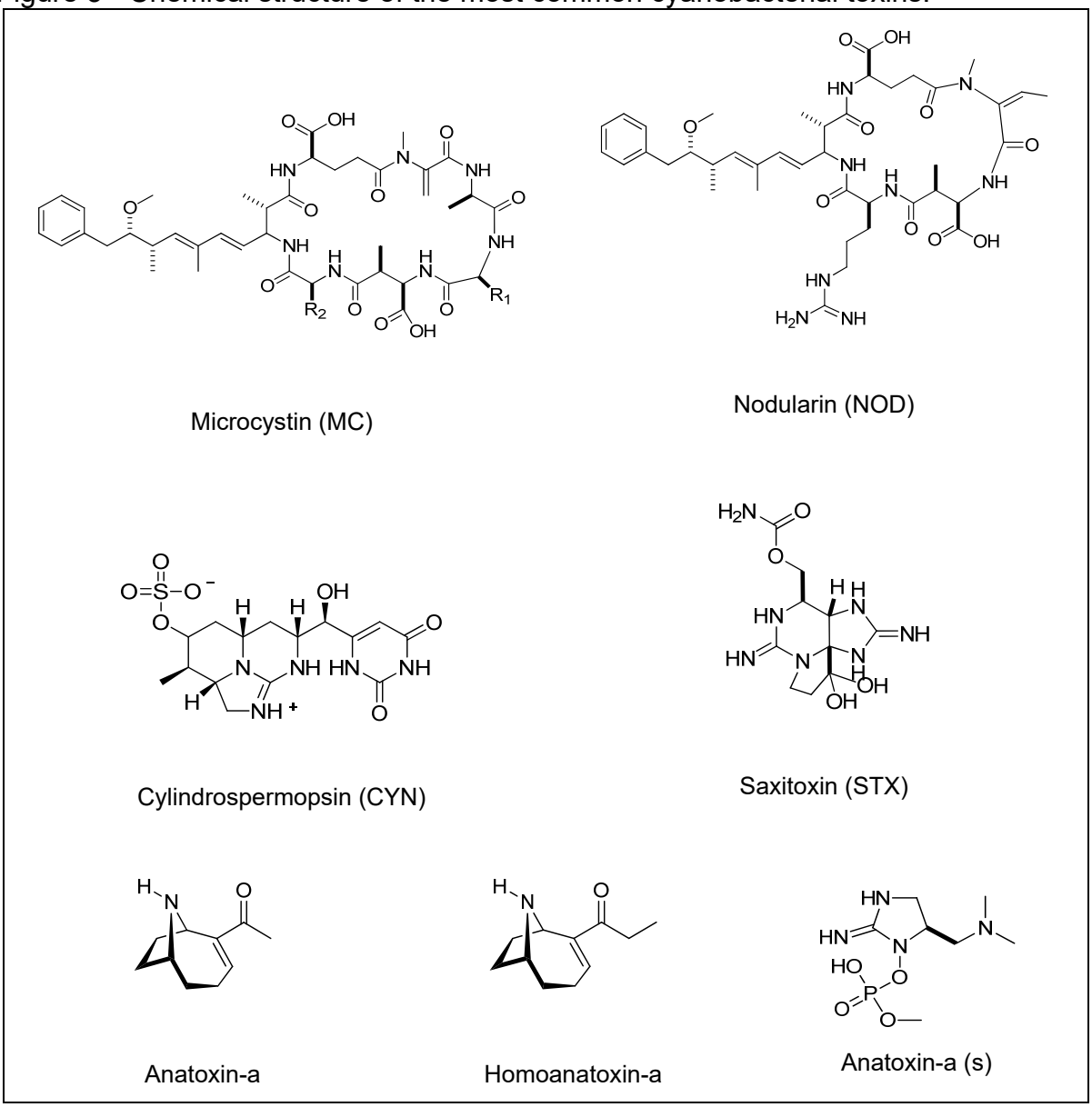

Cyanobacteria also produce neurotoxic alkaloids such as anatoxin-a, homoanatoxin-a, anatoxin-a(s) and saxitoxin (Figure 3). After causing extensive mortality in freshwater animals, saxitoxins (STX) and its analogues were isolated from the genera *Anabaena spp., Cylindrospermopsis spp., Aphanizomenon spp., Planktothrix spp.* and *Lyngbya spp.*. Anatoxin-a (s) is an organophosphorus compound which acts as a potent irreversible inhibitor of cholinesterase enzyme. Anatoxin-a and homoanatoxin-a are bicyclic secondary amines of low molecular weight that cause rapid death in animals, and both are agonists of nicotinic acetylcholine receptors (HUMPAGE, 2008).

Cyanotoxins represent a major public health problem worldwide, with an increasingly common occurrence due to eutrophication processes in natural and artificial water reservoirs.

2.2 Cylindrospermopsin: general information

The most widely known reported incident of intoxication attributed to CYN occurred in 1979 on a water reservoir on Palm Island (northern Queensland, Australia) that was the source of chlorinated, unfiltered drinking water for it's residents. In this event, 148 residents were hospitalized with hepatitis-like symptoms. Kidney malfunction along with bloody diarrhea and urine were reported. In 20% of the patients, kidney damage was severe and with bloody urine. Other sympthoms included severe damage to the gastrointestinal epithelium, severe electrolyte loss and hypovolemic shock. *C. raciborskii* extracts isolated from the reservoir caused the same pathology observed in humans when injected intraperitoneally (i.p.) to mice (GRIFFITHS AND SAKER, 2003).

2.2.1 Chemical structure of CYN and analogs

The alkaloid named CYN (glassy solid powder) is a sulfate ester of a tricyclic guanidine moiety with a uracil ring, and has a molecular mass of 415.43 g/mol. It is a zwitterionic molecule with high solubility in water. The gross structure of CYN was solved by mass spectrometry (MS) and nuclear magnetic resonance (NMR), first by Ohtani et al. (1992).

Other CYN variants have been described, including 7-deoxy-cylindrospermopsin (7-deoxy-CYN) a frequently reported toxic analog. As seen on figure 4 the pyrimidine ring is postulated as an essential component for the toxicity of CYN (BANKER, CARMELI, ET AL., 2001). Animals injected i.p. with CYN variants containing the unmodified uracyl group, yielded lower median lethal dose (LD_{50}) values. It is important to notice that CYN lethal toxicity is slow and ocurred after 5 days in the treated mice.

Figure 4 – Structures and LD_{50} ($\mu g.kg^{-1}$) of CYN, analogs and oxidation products.

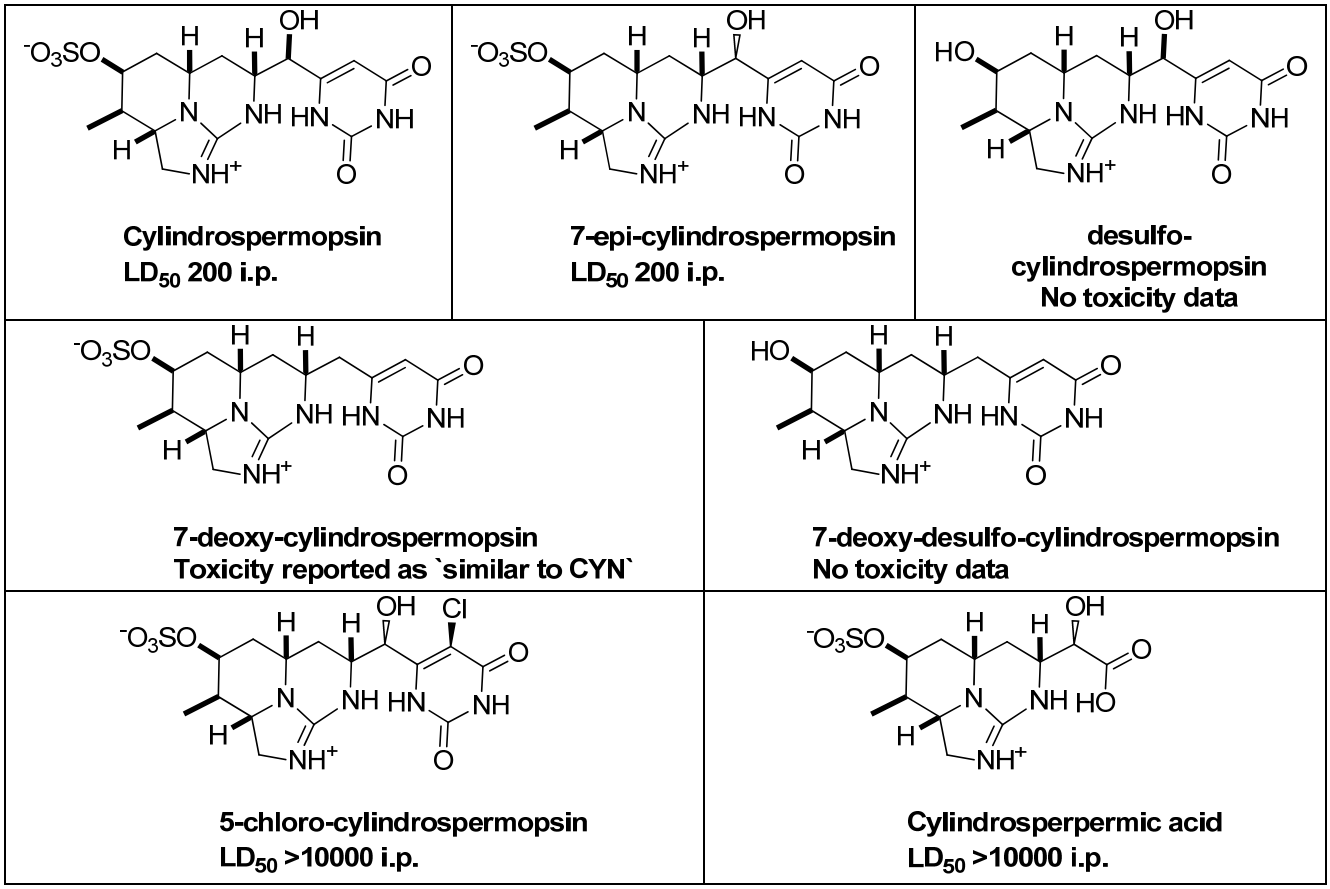

Adapted from Banker et al., 2001.
LD_{50} in mouse was estimated 5 days after the xenobiotic administration.
i.p.= intraperitoneal

2.2.2 Ocurrence and producing organisms

Even though *C. raciborskii* was the first species reported as a producer of CYN, other cyanobacteria species have been identified as CYN producers: *Umezakia natans, Aphanizomenon ovalisporum, Anabaena bergii, Raphidiopsis curvata, Aphanizomenon flos-aquae, Anabaena lapponica* and *Lyngbya wollei* (MOREIRA, AZEVEDO et al. 2013).

Although this cyanotoxin has been reported in North America, Europe, Asia and Oceania, the confirmation of CYN producing cyanobacteria in Brazilian fresh waters is still controversial. Even though several authors have reported the presence of the toxin in samples from Brazilian water reservoirs (BITTENCOURT-OLIVEIRA MDO, PICCIN-SANTOS et al. 2014), the isolation and laboratory culture of a CYN producing cyanobacterial strain from Brazilian freshwaters has not been published to date.

Cyanotoxins are secondary metabolites; compounds that are not used by the organism for its primary processes (cell division or metabolism). Most of the biomolecules considered as secondary metabolites isolated from cyanobacteria belong to large classes of natural products that are polyketides, nonribosomal peptides or a mixture of both. Biosynthesis of these compounds is performed by a family of multi-enzymatic complexes called nonribosomal peptide synthetases and polyketide synthases organized into repeated functional units known as modules. Translation and transcription of these modules are independent from the messenger ribonucleic acid (PEARSON, ET AL., 2010). The characterization of the gene cluster responsible for the biosynthesis of CYN in *C. raciborskii* and a complete biosynthetic pathway proposal has been described (MIHALI, KELLMANN, ET AL., 2008).

2.2.3 Detection methods on environmental samples

High Performance Liquid Chromatography with Diode Array detection (HPLC-DAD) is a good option for the detection of CYN's and its analogues, taking advantage of the characteristic UV spectra (λ_{max} 262 nm) of the uracyl moiety. Sample cleanup must be implemented along with HPLC–DAD to remove co-eluting contaminants (LAWTON AND EDWARDS, 2008).

The confirmation method of choice is LC–MS^2 because it provides structural confirmation and sensitive quantification by monitoring the transition from the $[M+H]^+$ precursor ion (416 m/z) to the major MS2 fragment 194 m/z. (EAGLESHAM, NORRIS, ET AL., 1999).

2.3 CYN toxicity

CYN could be considered as having an intermediate toxicity. It's LD_{50} (ip) in mouse is approximately 200 µg/Kg. As a means of comparison, saxitoxin has an average LD_{50} (ip) of 10 ug/Kg in mouse (MOREIRA, ET AL., 2013).

In the following sections (2.3.1 - 2.3.3) we summarize the main toxic mechanisms proposed for CYN and the respective supporting evidence .

It's important to point out that the oral route is the most important administration route for CYN and its analogs. It is not known how the toxin enters the target cells *in vivo* (mainly hepatocytes), nor *in vitro*. The bile acid transport system in

the hepatotoxin-induced toxicities may have some involvement. Some authors believe that with its smaller molecular weight, passive diffusion might be one of the possible mechanisms for CYN uptake into hepatocytes. This was supported by incubating a cell line devoided of bile acid transport system, with CYN, which showed cytotoxic effects (CHONG, WONG, ET AL., 2002).

2.3.1 Toxicity and pathology of CYN on mammals and vertebratres

This toxin acts slowly, even in high concentrations. For example for the LD_{50} with 2 $mg.kg^{-1}$ i.p., mice usually die in 24 hrs. For the LD_{50} with 0,2 $mg.kg^{-1}$ ip, mice die in 5-7 days (MOREIRA, ET AL., 2013).

The pathological effects of CYN isolated from a *Umezakia natans* on mice are well described. The main target of CYN was the liver. Other organs (thymus, kidneys, heart, etc) were also reportedly affected. According to the authors there were at least four consecutive phases of the pathological changes in the liver. In the initial phase inhibition of the protein synthesis was detected, on the second phase of membrane proliferation followed, on a third phase there was accumulation of fat droplets, followed by a final phase of cell death. The authors demonstrated inhibition of the protein synthesis using globin synthesis in rabbit reticulocytes system. All pathological phases were documented by optical and electronic microscopy coupled with other biochemical techniques (TERAO, ET AL., 1994).

2.3.2 Toxicity and pathology of CYN on other organisms

Although the majority of *in vivo* tests with CYN uses mice as animal model, invertebrates, microorganisms and plants may also be used as an animal model. This is the case, for example, of the insect *Locusta migratoria migratorioides* in these toxicity tests, because in addition to provide cost-effective advantages, the use of insects enables the observation of the toxin effects in a more sensitive way and in a larger amount of animals. In this scenario researchers could design experiments in insects that wouldn't be possible in mammals. (MOREIRA, ET AL., 2013).

2.3.3 Toxicity mecanisms of CYN according to in-vitro evidence

The toxic effects of CYN on *in vitro* cell lines and other biological models had been studied using diffferent techniques depending on the objective of the specific experiment. On the following sub-sections, we will briefly present the most relevant proposed mechanisms for cell injury caused by CYN.

Regarding our following experiments, some relevant information on the acute toxic effect of CYN on primary rat hepatocites (PRH) and HepG2 have been published. The levels of apoptosis (or programmed cell death) described in literature differ according to the compound concentration, exposure time and the cell model used. Based on this information, Lopez-Alonso et al. (2013) presented results of apoptosis at 200 mM and after 12 hours of primary rat hepatocytes treatment. In addition, Alja et al. (2013) showed cell damage in HepG2 cells at 2.4 µM after 24 hours of treatment, including genotoxic effects.

2.3.3.1 Protein synthesis inhibition

Considering that the inhibition of protein synthesis precedes the effects of CYN toxicity in primary rat hepatocytes, several studies have been published in an attempt to clarify the main routes involving irreversible inhibition of protein synthesis, both in eukaryotes as in prokaryotes, in which the CYN was involved.

Using a rabbit reticulocytes, experiments confirmed that the irreversible inhibition of protein synthesis in immature erythrocytes was caused by the interference of CYN on second stage of cellular translation process, that is, in the elongation step (FROSCIO, ET AL., 2003).

Despite its higher protein synthesis inhibition in eukaryotic cells, 1000 times more than in prokaryotes (FROSCIO, HUMPAGE, ET AL., 2008), it is believed that CYN's target may not be the ribosome itself, but rather one of the soluble proteins that are related to the eukaryotic translation system (TERAO, ET AL., 1994, FROSCIO, ET AL., 2008).

2.3.3.2 Metabolic activation of CYN and Oxidative Stress

There is evidence in literature leading to believe that metabolic transformation could be the onset of the major or secondary toxic effects of CYN on cells. Some authors consider that the CYN parent compound is responsible for the inhibition of protein synthesis, whereas cytochrome P450 (CYP450) metabolism of CYN produces cytotoxic endproducts capable of producing oxidative stress and cell damage (BAZIN, MOUROT, ET AL., 2010).

CYN acute toxicity was successfully diminished by Inhibition of CYP450's activity (using ketoconazole, proadifen), but not the effects on protein synthesis, implying that the two events had no association. This studies of the effects of CYP450 inhibitors on the acute toxicity induced by CYN reinforced the theory that bioactivation contributes to the cytotoxicity of this toxin in liver cells (FROSCIO, ET AL., 2003). Also reinforcing this idea is the fact that cell lines expressing low levels of CYP450s, such as HepG2 or HeLa were more resistant to the cytotoxic effects of CYN than primary hepatocytes. For example in the KB cell line (HeLa like cells) cell death was detected after 72 hrs using 2 µM of CYN (CHONG, ET AL., 2002).

Other related field of study is the relevance of reduced glutathione (GSH) on the oxidative stress outcome produced by CYN stimulation. It was shown that the depletion of GSH (either by conjugation with CYN, or by inhibition of its synthesis by CYN) is unlikely to be of primary importance in the toxicity in mouse (NORRIS, SEAWRIGHT, ET AL., 2002).

In a related matter distribution tests of ^{14}C CYN in mouse showed the presence of radiolabelled CYN in protein precipitates of urine and liver tissue, confirming the hypothesis of protein adduct formation, in which protein binds to the either the CYN metabolite or the toxin itself for its elimination (NORRIS, ET AL., 2002).

2.3.3.3 DNA damage and carcinogenicity

On animal studies, CYN mediated carcinogenesis has not been well evaluated, and therefore the mechanisms of CYN carcinogenicity *in vivo* are not well understood (ZEGURA, STRASER, ET AL., 2011).

On the other hand several *in vivo* studies had shown that CYN possess both clastogenic and aneugenic activity (ZEGURA, ET AL., 2011). Several genotoxic studies

had been carried out in HepG2 cells. In this lineage, CYN induced DNA double strand breaks in after a 72 hour exposure at a concentration of 1.2 μM (ALJA, ET AL., 2013).

The inference that CYN itself does not react directly with cellular DNA but its metabolism can lead to genotoxic products was reported by Fessard and Bernard (2003), after their experiments with hamster ovary cells. Later this was reinforced by studies in HepG2 cells, when authors saw that an increase in DNA damage was found to be dose dependant in cells treated with doses of CYN (0.05–0.5 mM) for 18 hours. In this study CYP450 inhibitors were also used in order to explore the relevance of CYN metabolites in the DNA toxicity.

CYN exposure induced early responses in the genome at 0.5 $\mu g.mL^{-1}$ (sub-cytotoxic concentration) in HepG2 cells during 12 and 24 hour treatments. There is evidence of signaling of the transcription factors P53 and NF-jB by CYN stimulation. Other upregulated genes were: growth arrest and DNA damage inducible genes (GADD45A and GADD45B), cyclin-dependent kinase inhibitors (CDKN1A and CDKN2B), checkpoint kinase 1 (CHEK1), and genes involved in DNA damage repair (XPC, ERCC4 and others). Upregulation of DNA damage repair genes and cell cycle arrest might have a connection with previus evidence of double strand break and genotoxicity. Genes coding for metabolic enzymes involved in phase I (CYP1A1, CYP1B1, ALDH1A2, CES2) and phase II (UGT1A6, UGT1A1, NAT1, GSTM3) metabolism were upregulated. The upregulation of these metabolic genes might indicate a detoxification response of the cell and the potential activation of CYN into a more reactive metabolite (STRASER, FILIPIC, ET AL., 2013).

2.3.3.4 Other proposed mechanisms

Although the already mentioned toxicity mechanisms are well studied by the scientific community, some authors propose other possible toxic mechanisms. Some authors point out that CYN might work as an enzyme inhibitor by competing for the UDP (uridine diphosphate) binding site. These authors also propose that CYN could have pro-oxidant activity by inhibiting the formation of vitamin C (BANKER, ET AL., 2001).

In vitro studies show that CYN acts as a non-competitive inhibitor of the uridine monophosphate (UMP) synthase complex. However, the reported evidence on *in vivo* related experiments do not support a general inhibition of UMP synthesis (LOOPER, RUNNEGAR, ET AL., 2006).

Recent studies show that CYN can decrease the NADPH (nicotinamide adenine dinucleotide phosphate-oxidase) oxidase-mediated production of ROS. This would reduce the ability of white blood cells to fight pathogens. Authors used concentrations from 0.024 - 2.4 µM CYN for exposures of less than 1 hour (PONIEDZIALEK, RZYMSKI, ET AL., 2014).

2.4 The use of modern proteomics techniques applied to toxicology

Toxicology is a multidisciplinary subject and profits from any analytical or biological advancement to understand the effect of toxicants in biological systems. The modern tendencies to analyze a biological event use high-throughput screenings (e.g., "omics" techniques) to gain informative and quantitative data on the matter. In this context, toxicology can benefit greatly from quantitative proteomics. The comprehensive data resulted from a proteomics experiment can help the researcher to better understand the potential toxic mechanisms, toxicity pathways, biomarkers, and assessment of adverse contact with a toxicant. Recently the application of "omics" technologies to toxicology has been given the name: systems toxicology. Systems Toxicology resides at the crossroads of systems biology with toxicology and chemistry. Quantitative proteomics by LC-MS^2 can elucidate complex patterns of toxic action. In order to enable a more mechanism-based and predictive toxicological assessment, toxicological studies need to acquire measurements at molecular resolution. In this scenario, proteomic measurements are an essential component for the implementation of this approach because protein alterations closely reflect the physiological response of a biological system to an external insult. (TITZ, ELAMIN, ET AL., 2014).

2.5 Contemporary approaches to shotgun proteomics studies

Shotgun proteomics identifies proteins based on the tandem mass spectra of their peptides, and it is named after its homolog in genomics "shotgun sequencing". The proteins, are identified from the MS^2 (tandem mass spectrometry) spectra of the peptides produced from the protein digestion. Matching the MS^2 spectra to peptide sequences is the fundamental computational challenge of MS (mass spectrometry) based proteomics. This complicated computational match is what eventually determines the success of shotgun proteomics (HUNT, YATES, ET AL., 1986).

On a shotgun proteomics experiment, the proteins in a sample are digested and the resulting peptides are separated prior to MS^2 analysis. LC-MS^2 is commonly used to identify the peptides (MS1), and then match them back to proteins. Modern shotgun proteomics is achievable nowadays because of recent improvements in MS instrumentation, protein and peptide separation techniques, computational software, and the availability of open sequence databases for proteins of many species (NESVIZHSKII AND AEBERSOLD, 2005).

2.5.1 Chemical labeling, metabolic labeling and label free techniques

Many methods have been developed specifically for quantitative proteomics to obtain high proteome coverage, accurate quantification, and wide implementation for different types of samples (BANTSCHEFF, LEMEER, ET AL., 2012). The most simple and less expensive of all is label free quantitation (LFQ). LFQ can quantitate proteins without using any isotopic or chemical modification of proteins or peptides. This can be achieved by correlating protein abundance with: mass spectrometric signal intensities of peptides, or spectral counting (number of MS^2 spectra matched to peptides and proteins). In a general point of view, label-free approaches have limited quantification performance in terms of accuracy, precision, and reproducibility. On the other hand, label-free methods usually provides the deepest proteome coverage compared to other techniques (BODZON-KULAKOWSKA, BIERCZYNSKA-KRZYSIK, ET AL., 2007, LEUNG, MAN, ET AL., H.-C. E. LEUNG 2012).

In order to improve quantification, many approaches were developed, founded in isotopic and isobaric labeling of proteins and peptides. Some general labeling types are metabolic labeling, enzymatic labeling, and chemical labeling.

In metabolic labeling, stable isotopes of atoms like carbon and nitrogen are incorporated into proteins. This is accomplished by growing cells in special media containing, for example, isotopically labeled essential amino acids. This technique is called SILAC (stable isotope labeling by amino acids in cell culture). Metabolic labeling allows samples grown in different states to be combined after treatment, so that they can be processed together prior to LC-MS^2. Any losses or bias due to sample processing would change to the same extent in the mixed sample, resulting in peptide intensity ratios that closely resemble the protein proportions of the original samples (LEUNG, ET AL., H.-C. E. LEUNG 2012). On the downside, this technique is expensive

and not all cultured cells can incorporate 99% of the labeled aminoacids (for example PRH). It is also important to notice that when using multiplex SILAC (e.g., triple SILAC) the sample becomes much more complex since the same peptide is represented as three different isotopomers. Because of the complexity of this ion scanning, the number of unique peptide identification is reduced.

Not all biological systems are suitable to an efficient metabolic labeling, for example primary hepatocytes. To get around this complication, chemical or enzymatic methods have been developed to label proteins or peptides during sample processing. For example, after cell lysis, primary rat hepatocite proteins can be derivatized during the sample preparation using isotope-coded affinity tags (ICAT). When comparison of multiple labeling states becomes difficult to interpret, one can use multiplexed sets of reagents for quantitative proteomics. Isobaric mass tagging reagents and protocols, like ITRAQ (isobaric tag for relative and absolute quantitation) and TMT (tandem mass tag) TMT are commercialy available (THOMPSON, SCHAFER, ET AL., 2003, ROSS, HUANG, ET AL., 2004) .

Each one of these quantitative techniques has its own strengths and limitations, which must be considered when planning an experiment. Other important factors must be taken into account like budget, type of biological model and laboratory instrumentalization.

2.5.2 Sample preparation for a shotgun proteomics analysis of mammalian cells

When quantitating hundreds or thousands of analytes in a complex matrix by LC-MS^2, sample preparation is one of the most important steps to ensure reliable results. Because in quantitative proteomics, we are usually looking for minor differences between experimental and control samples, reproducibility is essencial for trustworthy results. (BODZON-KULAKOWSKA, ET AL., 2007).

The common shotgun proteomics by LC-MS^2 workflows analyze peptides, in contrast to gel electrophoresis separations, which are usually used to analyze intact proteins. Peptides are easier to fractionate by LC and ionize by electrospray, compared to intact proteins. They also fragment more efficiently than proteins, and the resulting spectra is easier to interpret. An average sample preparation protocol for shotgun proteomics involves: lysing of the cells in a detergent or lysis buffer, protein dosage, reduction and alkylation of cysteines, digestion of the sample into peptides, desalting

and concentration of the peptides, and finally injection into a LC-MS^2 high resolution instrument (BANTSCHEFF, ET AL., 2012).

2.5.3 Analysis of complex peptidic samples by LC-MS^2

Modern advances in mass analyzers instrumentation have reduced acquisition time and increased resolution and sensitivity, which have made quantitative proteomics into a high-throughput technique (NEUHAUSER, NAGARAJ et al. 2013).

In the mass spectrometer, the charged parent peptides are broken into smaller fragments, producing fragments of differing masses. This peptide fragmentation spectra, will later be automatically identified in databases using sequence-specific b- or y-ions. In a tripsinized sample, b- and y- ions are commonly generated by breaking peptides within peptide bonds by collision induced dissociation (CID) or high-energy collision dissociation (HCD). This will produce a mass ladder of many fragments that can then be measured by the mass spectrometer. As mentioned earlier, this experimental spectra is identified by computationally matching it to predicted MS^2 spectra in one or several species-specific databases. (MARCOTTE, 2007, ROEPSTORFF, 1985)

The great computational challenge is to process large databases of acquired MS^2 data to reconstruct the parent peptides that gave rise to observed spectra. A variety of free and licensed software tools to assign peptides to MS^2 and statistically validate the reported peptide assignment are available. Once this challenge is complete, another ultimate strife arises, because the main goal of the whole experiment is to match the reconstructed peptides to the original proteins in the sample (NESVIZHSKII and AEBERSOLD 2005).

2.5.4 Computational analysis of proteomics MS^2 datasets

As stated earlier, using the resulted MS^2 spectra to reassemble peptide sequences is the main computational issue of mass spectrometry–based proteomics. The MS^2 data of a complicated experiment usually undergoes several steps to become an interpretable dataset, and this steps does not always involve peptide identification by Mascot (one of the most common softwares confined for peptide identification).

Several bioinformatics softwares available nowadays can perform a full analysis starting from the raw data of all the samples of an experiment to the report of the whole quantitative data of the experiment in one data sheet only, including the false discovery rate (FDR) calculations. An example of a free software that can efficiently perform the full analysis of an experiment is MaxQuant. According to Neuhauser et al. (2013), MaxQuant allows processing of raw MS data files, incorporates its own probabilistic search engine called Andromeda and can be complemented with the Perseus software for statistical and biological significance analysis. The MaxQuant software was initially developed for the efficient analysis of SILAC experiments but recently it has been adapted for the processing of label free and nonmetabolic labeling proteomics experiments.

2.5.5 Validation of discovery proteomics experiments

A small group of proteins quantified by shotgun discovery proteomics of complex samples must be validated by an orthogonal method in order to confirm the changes detected by the mass spectrometer.

Some of the common approaches to validate proteomics MS^2 data can be the use of other omics techniques (e.g., metabolomics), other biochemical detection strategies using antibodies (Western blot, ELISA, immunofluorescence techniques), molecular biology techniques like polymerase chain reaction (PCR) or chemical techniques like surface plasmon resonance (SPR).

In regard to the quantified level of the protein (fold change) validation can be performed using independent orthogonal techniques as mentioned above, or repeating the experiment with a targeted proteomics experimental strategy (NESVIZHSKII, VITEK et al. 2007).

3.0 OBJECTIVES

3.1 General objective

This study aims to identify proteins that display significant changes in abundance upon a CYN sub-lethal treatment on HepG2 cells, by performing a relative quantitation by nanoscale LC-MS^2. The minimum proteome coverage expected is 10%.

3.2 Specific objectives

(i) To implement a high purity isolation method for CYN from toxic *Cylindrospermopsis raciborskii* cultures.

(ii) To determine by flow cytometry the concentrations of CYN that produce apoptosis and/or necrosis on HepG2 cells, in order to use sublethal working concentrations of CYN on the proteomics studies. A 48-hour treatment will be the maximum time interval considered for the necrosis/apoptosis tests.

(iii) To quantify by nanoscale LC-MS^2 the effects of previously tested sublethal dosis of CYN on the upregulation and downregulation of proteins from the overall protein groups expressed by HepG2 cells. A 48-hour treatment will be the maximum time interval considered for the proteomics tests.

(iv) To validate the nanoscale LC-MS^2 results by confirming upregulation and downregulation of selected proteins from CYN-treated *in vitro* hepatocytes, using orthogonal techniques.

4.0 MATERIALS AND METHODS

4.1 *Cylindrospermopsis sp.* 11K strain maintenance

Cylindrospermopsis raciborskii strain 11K was a gift from prof. Marli Fatima Fiori at the Center for Nuclear Energy in Agriculture, USP Campus Luiz de Queiroz, Piracicaba. This Australian CYN producing strain was maintained in our laboratory using the ASM-1 culture medium proposed by Gorham et al., 1964, with some modifications (BORTOLLI, 2011). In the same manner, a brazilian non-CYN producing strain (*C. raciborskii* ITEP 18) was grown and used as matrix for CYN spiked-in extractions during the implementation of the SPE protocol.

The cyanobacteria were cultured inside an incubator at the desired final volume (1 L – 4 L) with a working temperature of 22 °C, a 12 hours light/dark interval, and a light intensity of 30 to 50 µmol (calibrated by Li-cor 250 quantameter).

4.2 Toxin isolation

Samples of *C. raciborskii* broth were centrifuged (12857 *g*, 10 min, 4 °C) and the supernatant (medium) was collected. The resulting biomass was frozen at -20º prior to liofilization. Next we filtrated the culture medium sample through a 0.44 µm membrane, to avoid clogging of the SPE cartridges.

Liofilized biomass was also tested as a matrix for toxin extraction. After weighting the liofilized sample, cells were lised with 50% MeOH, centrifuged (12857 g, 10 min, 4 °C), filtered through a 0.44 µm membrane and diluted to approximately 1% MeOH. Clean up methods prior to SPE were tested (liquid-liquid extraction, QuEChERS, etc.) and even though some of them improved the chromatograms, there was always loss of analytes compared to the 50 % MeOH extracts.

4.2.1 Toxin extraction using C18 and HLB SPE columns

Filtered samples were passed through the desired cartridge: Supra Clean C18 (Perkin-Elmer®), Strata C18 (Phenomenex®), Oasis HLB and C18 Sep-Pak (Waters®). The pre-conditioning steps included activation and washing with MeOH (5 mL) and 1% MeOH (5mL), respectively. Three elution steps with aqueous solutions

were tested: (i) 10% MeOH (1.5 mL), (ii) 50% MeOH (1.5 mL) and (iii) 100% MeOH (1.5 mL). All eluted fractions were evaporated with nitrogen and resuspended in MeOH or MilliQ water (200 µL) for further HPLC analysis.

4.2.2 Toxin extraction using PAC

For this assay we prepared 15 mL falcon plastic tubes containing 200 mg of powdered activated carbon (PAC). This tube was conditioned with 100% MeOH (2 mL), which was later removed by aspiration. *Cylindrospermopsis sp.* culture supernatant (10 mL) was added to the previous activated charcoal, vortexed and centrifuged (12857 g, 5 min, RT). After centrifugation, the supernatant was collected and dried for further HPLC-DAD analysis. On the other hand, the analytes adsorbed to the charcoal were eluted twice using extraction solutions described in the literature (MEOLA AND VANKO, 1974) for this kind of protocol: (i) 5% formic acid (FA) in MeOH (1 mL), (ii) ethyl ether (1 mL), (iii) dichloromethane**:**MeOH (80**:**20, v/v) in 10 mmol.L^{-1} trifluoroacetic acid (1 mL), (iv) acetonitrile (1 mL), (v) 10% MeOH in water (1 mL). All the eluted supernatants (2 ml) were evaporated in nitrogen, resuspended in MeOH (200 µL) and filtered on Millex filter (Millipore®) for further HPLC-DAD analysis.

4.2.3 HPLC-DAD quantitative analysis

A volume of 5 uL from each resuspended sample were injected into a HPLC (Shimadzu LC20AD) using a Synergi 4 µm Hydro-RP 80A, 150 x 4.6 mm (Phenomenex®) HPLC column. The mobile phase consisted of 5 mmol/L ammonium acetate buffer with 0.05% FA. Several gradient elutions using MeOH were tested with a flow of 0,2 mL/min according to Eaglesham et al. (1999) and Gallo et al. (2009). The gradient elution of the final method started at 100% aqueous mobile phase with a gradual increase up to 80 % MeOH at 15 minutes. The detection was set at λ = 262 nm (200 – 600 nm) using a Diode Array Detector (Shimadzu SPD-M20A).

4.2.4 HPLC-DAD purification of concentrated samples.

Usually a volumes of 200 – 600 mL from SPE extracts resuspended in MillIQ grade H_2O were injected into the HPLC (Shimadzu LC20AT) using a Luna 5 µm C18

100A, 250 x 10 mm (Phenomenex®) HPLC column. The mobile phase consisted of MilliIQ grade H_2O. Similar to section 4.2.3 a gradual increase of the MeOH from 5% to 80% was achieved during 35 min. The detection was set at λ = 262 nm (200 – 600 nm) using a Diode Array Detector (Shimadzu SPD-M20A) coupled to a fraction collector (Shimadzu FRC-10A).

4.2.5 Confirmation analysis using HPLC-DAD-QTOF

Confirmation of CYN and structural analogs was carried out on a Shimadzu Prominence Liquid Chromatography system coupled to a quadrupole time-of-flight mass spectrometer (Micro TOF-QII; Bruker Daltonics, MA, USA) with an ESI interphase. The samples were separated through a Synergi 4 µm Hydro-RP 80A, 150 x 4.6 mm (Phenomenex®) HPLC column, protected with a guard column of the same material. The gradient elution of the final method started at 100% aqueous mobile phase with a gradual increase up to 80 % MeOH at 15 minutes (flow 0.2 mL/min). The ionization source conditions were as follows: positive ionization, capillary potential of 3500 V, temperature and flow of drying gas (nitrogen) of 300 °C and 5 mL/min respectively, and a nebulizer pressure of 35 psi. Mass spectra were acquired using electrospray ionization in the positive mode over the range of *m/z* from 50 to 3000. The Q/TOF instrument was operated in MS1 scan mode, or MS2 MRM mode as needed. In the MRM mode collision-induced dissociation CID experiments were performed using the following collision energies for fragmentation: 20 eV, 35 eV and 40 eV.

4.3 Defining sub-lethal CYN working ranges for HepG2 cells

4.3.1 Standardization of a flow citometry test to measure necrosis and apoptosis

4.3.1.1 Cell culturing of HepG2 cells

The HepG2 cells (ATCC® number: HB-8065™) were purchased from the Rio de Janeiro Cell Bank, and maintained in DMEM high glucose (Gibco®) supplemented with 10% fetal bovine serum (FBS) at 37 °C with 5% CO_2. Initially, to thaw the cells, one aliquot of 1 mL of frozen HepG2 containing approximately 1 x 10^6 cells was rinsed twice with 5 mL of medium, centrifuged (250 g, 15 min, 4 °C) and kept incubated in a

25 cm^2 culture flask at 37 ºC and 5% CO_2. After reaching 80% confluence in the flask, the medium was removed and 5 mL of PBS was added. The PBS was removed inmediatly and the adhered HepG2 cells were detached from the flask using 1 - 2 mL of 2,5 g/L trypsin solution during 5 minutes. Trypsin was inactivated with DMEM medium (5 mL containing 10% FBS), and centrifuged 250 g, 15 min, 4 °C). The pellet was resuspended in high glucose DMEM and transferred to 75 cm^2 bottles. The replication of the cells was repeated until the desired number of cells was reached.

4.3.1.2 Propidium iodide (PI) and Annexin V staining

The capacity of CYN to produce necrosis and apoptosis on (non metabolically labeled) HepG2 cells was quantitated using two staining techniques for flow cytometry, propidium iodide (PI) (BD Pharmingen™) and Annexin V (BD Pharmingen™), respectively. Cells where treated using various CYN concentrations (based on the available literature) during time intervals up to 48 hours.

Due to the fisiological variability of each cultured cell type and the variability of the composition of the Annexin V reagent, two volumes of annexin V were tested (2.5 and 5 µL). To standardize a positive control of apoptosis, HepG2 cells were treated for 24 and 48 hours with 10 % DMSO, 20% MeOH and 32 $mg.mL^{-1}$ cisplatin, according to Qin and Ng. (2002) and Gao et al. (2012), with some modifications.

On the other hand, the PI staining solution easily stains the DNA of necrotic mammalian cells using 2 µL of this reagent, according to the revised literature and preliminary tests. The induction of necrosis on the HepG2 cells was carried out using 20% MeOH for 24 hours. The final double-staining (PI + Annexin V) protocol is described on the supplementary material 8.2.

4.3.1.3 Flow cytometer analysis

10.000 events were acquired on the flow cytometer FACS Canto II (BD Bioscences®) using the BD FACS Diva™ software. The excitation wavelength was in λ_{EX} 633 and 480 nm, and emission at λ_{EM} 660 and 617, for allophycocyanin (Annexin-V reagent) and PI reagent respectively. Positive controls for apoptosis and necrosis were used to perform the compensation of the samples as well as fluorescence minus

one (FMO), in order to differentiate the negative and positive gate. On the other hand, negative control unlabelled cells were used to evaluate the autofluorescence.

4.4 Preliminary Discovery Proteomics using 0,1 - 1μM of CYN

4.4.1 Cell culturing of HepG2 cells (Light)

HepG2 cells were grown in DMEM high glucose (Gibco®), following the steps described in section *4.3.1.1*.

4.4.2 Cell culturing of HepG2 cells using SILAC

The overall SILAC cell culturing and reagents preparation was carried out according to Ong and Mann (2006). Depending on the experiment, HepG2 cells were grown in only light (L) & heavy (H), or in light & medium (M) & heavy SILAC broth for 12 divisions following the steps described in section *4.3.1.1*. For the preparation of the medium and heavy SILAC broths, we used an adaptation of Ong and Mann (2006), and Bendall et al. (2008) described in the supplementary material 8.3.

4.4.3 Sample preparation for LC-MS^2 analysis using the sodium deoxycholate protocol

Cells were detached from 6 well plates using 300 μL of 2,5 g/L trypsin solution for approx. 30 seconds. Trypsin was inactivated with DMEM medium (containing 10% FBS), and centrifuged 250 g, 10 min, 4 °C. Following the cell collection, we mixed L, M and H in 1 tube for every time point. We centrifuged 250 g, 10 min, 4 °C. The pellets were washed twice with ice cold PBS and stored at -80 °C so that all of the cell pellets could be lysed and processed at the same time.

All of the cell pellets were processed using the “Protein Digestion in Sodium Deoxycholate (SDC) buffer” protocol (supplementary material 8.4). Fractionation of samples was performed using the protocol on supplementary material 8.5.

4.4.4 Nanoscale LC-MS^2

10 uL (equivalent to 2 ug of tryptic digest) of each sample was loaded by onto a Easy-nLC 1000 (Thermo® Fisher Scientific) ultrahigh pressure liquid chromatography pump, equipped with a C18 capillary column 15cm x 150um diameter that was packed in house with C18 resin. Peptides were eluted with a 56 min gradient covering 5−40% of buffer B (buffer A: 0.2% FA; buffer B, 0.2% FA and 99.8% ACN; flow rate: 600 nL.min^{-1}). The chromatographic elute was electrosprayed directly into an Orbitrap Q Exactive Plus mass spectrometer (Thermo® Fisher Scientific) using a nanospray source with a spray voltage set at 1.6 kV. The mass spectrometric analysis was carried out in a data-dependent mode. For each cycle one full MS scan of m/z 300 - 2000 was acquired in the Orbitrap at a resolution of 70000 at m/z 200 with an AGC target of 1e6. Each full scan was followed by the selection of the 12 most intense ions were isolated by the quadrupole and fragmented by HCD by a normalized colision energy of 25. The product ions were analysed by the orbitrap at a resolution of 17500 at m/z 200 with an AGC target of 5e5. Dynamic exclusion was set to 60 seconds.

4.5 Final Discovery Proteomics using 1μM of CYN

4.5.1 Sample preparation for LC-MS^2 analysis using the Rapigest protocol

Cells were detached from 6 well plates using 300 μL of 2,5 g/L trypsin solution for approx. 30 seconds. Trypsin was inactivated with DMEM medium (containing 10% FBS), and centrifuged 250 g, 10 min, 4 °C. Cells were immediately washed twice with ice cold PBS. The pellet was kept at -80 ° C until cell lysis step.

Following the protocol, the pellet was dissolved in 60 μL of triethylammonium bicarbonate (TEAB) buffer and the cells lysed with 0.2 % RapiGest™ reagent. The proteins were measured using the BCA protein quantitation kit (Pierce, Thermo®). 25 μg of H sample were mixed with the respective 25 μg of L sample, in order to have H/L mixed lysates for every replicate of the experiment.Then, using the final 50 μg of H/L protein from each replicate we proceeded to do reduction with dithiothreitol, alkylation with Iodoacetamide and trypsin digestion. After digestion with trypsin, 5% TFA (trifluoroacetic acid) was added to the samples and the reaction was incubated at 37 ° C for 90 minutes. Finally the samples were centrifuged and the supernatant was

lyophilized. To resuspend the lyophilized peptides, 100 µL of 0.1 M TEAB pH 8.5 buffer was added.

4.5.2 Sample fractionantion by HPLC

We separated the peptides of every sample in 3 fractions employing reversed-phase HPLC at pH 9.8. For the off-line fractionation we employed a Acquity UPLC I-Class system equipped with photodiode array and fluorescence detectors (Waters, Manchester, UK), using a Gemini NX 3 µm 50 × 2.0 mm column. Mobile phase: ammonium formate in water, 20 mM, pH 9.8 and acetonitrile. Nine fractions per sample (1 min each) were automatically collected and concatenated in 3 final vials per sample. The vials were evaporated and fractions solubilized in 3% ACN at 0.1% FA .

4.5.3 Nanoscale LC-MS^2

Nano LC-MS2 experiments were conducted using a nanoACQUITY UPLC (Waters®) system coupled with a hybrid Quadrupole-Orbitrap mass spectrometer (Thermo Fisher Scientific®) property of Grupo Fleury, São Paulo. For every run 4.5 µL of each fraction was loaded onto a PicoChip® proteopep III C18 column (1.8 µm 80 Å, 15 µm diameter × 105 mm). A two-step linear gradient was used starting from 2% (vol/vol) dimethyl sulfoxide (DMSO) and 0.1% (vol/vol) FA. Gradient increased to 5% (vol/vol) DMSO, 25% (vol/vol) acetonitrile, and 0.1% (vol/vol) FA over 90 minutes; followed by a 30-minute gradient of 5% (vol/vol) DMSO, 40% (vol/vol) acetonitrile, and 0.1% (vol/vol) FA. A nano-electrospray was used at positive mode as ionization source, and the Quadrupole-Orbitrap was used as hybrid mass analyzer. For MS2 detection, experiments of the data-dependent acquisition method were performed, in a top 14 strategy. For each cycle, one full MS scan (m/z 390–1,650) was acquired in the Orbitrap at a resolution of 70,000 at m/z 200 with an automatic gain control target of 3e6. Each full scan was followed by the quadrupole selection and isolation of the 14 most intense ions at a window m/z 4, which were dissociated through higher-energy collisional dissociation, using normalized collision energy of 26 (MS2). The product ions were analyzed by the Orbitrap at a resolution of 17,500 at m/z 200 with an automatic gain control target of 5e4. Ions with an unassigned, +1, and >+8 charge were rejected, and dynamic exclusion was set to 30 seconds.

4.6 Discovery proteomics data analysis

4.6.1 Quantitation of peptides and proteins by MaxQuant

The resulting MS/MS data were searched against UniProt Human database (downloaded August 10, 2016) using MaxQuant software (v1.5.5.1) with an overall false discovery rate (FDR) for peptides of less than 1%. Peptide sequences were searched using trypsin specificity and allowing a maximum of two missed cleavages. Oxidation of methionine and acetylation on protein N-terminal were fixed as variable modifications. Carbamidomethylation on Cys was specified as fixed modification.
R6 and K4 (medium AA), and R10 and K8 (heavy AA) were choosen as stable isotope labels depending on the experiment. Mass tolerances were set at ±6 ppm for precursor ions and ±0.5 Da for MS/MS. A minimum of seven amino acids was required as peptide length. Minimum unique peptides for identification was set to 1. Quantification was performed on all unique and razor peptides for a given protein, allowing for unmodified, oxidized (M), and acetylated (Protein N-term) peptides. The quantification of proteins was based on the normalized M/L and H/L ratios, as determined by MaxQuant.

4.7 Validation of the shotgun proteomics data

4.7.1 Western blot of selected proteins

Proteins were separated by NuPAGE® BisTris mini gels (Invitrogen) under reducing conditions and then electrophoretically transferred onto nitrocellulose membranes (iBlot 2™ Invitrogen). After protein transfer, the membranes were treated with the blocking buffer (1% BSA) followed by the desired primary AB; monoclonal antibodies for each of the selected proteins were aquired from Thermo. After washing steps, followed an incubation with horse radish peroxidase (HRP) conjugated goat anti-human IgG. Then, the bands were visualized using Clarity™ ECL peroxidase substrate (Bio-Rad).

4.7.2 JC-1 probe for mitochondrial membrane potential

Mitochondrial membrane potential was determined using the The MitoProbe™ JC-1 Assay Kit (Life Technologies). JC-1 (5',6,6'-tetrachloro-1,1',3,3'-tetraethylbenzimidazolylcarbocyanine iodide), reagent accumulates in the inside of intact mitochondria and forms red fluorescent aggregates. JC-1 dissociates into green fluorescent monomers as the membrane potential decreases due to a stimulus. We followed the MitoProbe kit instructions for sample processing using CCCP (carbonyl cyanide 3-chlorophenylhydrazone) as a positive control reagent. Samples were analyzed on a LSR Fortessa X-20 (BD), λ_{EX} 488 nm and λ_{EM} 530 & 590 nm.

5.0 RESULTS AND DISCUSSION

5.1 Purification of CYN and analogs from lab strain

According to previous analysis from prof. Ernani's group the *C. raciborskii* 11K strain produces high quantities of CYN and 7-deoxy-CYN, and secretes approximately 50% of the synthesized toxins to the culture medium (data not shown). There was also evidence of production of a third less polar CYN analog in small amounts. For the selective isolation of these metabolites, our initial approach was to separate the analytes from a simple liquid matrix as culture medium (broth) using SPE cartridges and activated carbon. Next, we tested the sorbents' performance on cyanobacteria biomass, which is a more complex matrix.

At this point, it is important to make clear that our main goal in the current project is to investigate the molecular mechanisms of toxicity of CYN. However, the standardization of a reliable protocol for the isolation of other CYN analogs is relevant to our group interests. It is for this reason that efforts were made to implement a broad protocol suitable for the isolatation of several CYN structural variants.

5.1.1 Tests on sample size and cartridge handling

Before testing the extraction of toxins from large amounts of biological material, we did preliminary tests in small and intermediate-scale. We used broth samples with a high density of cyanobacteria ($1x10^8$ cells mL^{-1}). For our purposes, we will refer to "small-scale" when using a broth sample with a volume of less than 100 mL. We refer to "intermediate-scale", when using volumes of culture medium between 100 -1000 mL. Finally, we refer to "large-scale" everytime we intend to extract toxins from volumes higher than 1 L of culture medium.

Small scale tests with culture broth

In this stage we used an HPLC-DAD (λ= 262 nm), and the retention times for CYN and 7-Deoxy-CYN were 13.4 and 25.5 minutes, respectively. The SPE's adsorption capacity for the analytes is shown on figure 5. In this figure, we see an overlay of the

chromatograms of the samples before and after they have seeped through the SPE cartridges by vacuum.

In most of this chromatogram overlays (fig. 5, A-C), a breakthrough of one or both analytes in the recovered fraction was detected. This shows a poor retention of the analytes by the SPE sorvent. Only the Sep-Pack C18 cartridge (fig. 5D) adsorved the analytes strong enough to avoid breakthrough on the recovered medium fraction.

On the other hand, the powdered activated carbon (PAC) effectiveness for adsorving the analytes was estimated. Figure 6 shows no breakthrough of CYN nor 7-deoxy-CYN. Several assays were made to try to elute the analytes from the PAC with different eluent solutions described in material and methods item 4.2.2. Preliminary results showed little or no elution at all of CYN and its analog from the PAC sorvent. This shows a great binding interaction with the sorvent that might be usefull in large-scale extractions.

Figure 5 - Overlay of the of the chromatograms (λ= 262 nm) obtained from culture medium sample before* and after** permeating through 0,5 g SPE cartridges: A) Supra-clean C18 Perkin Elmer, B) Oasis HLB Waters, C) Strata C18 Phenomenex and D) Sep-Pack C18 Oasis.

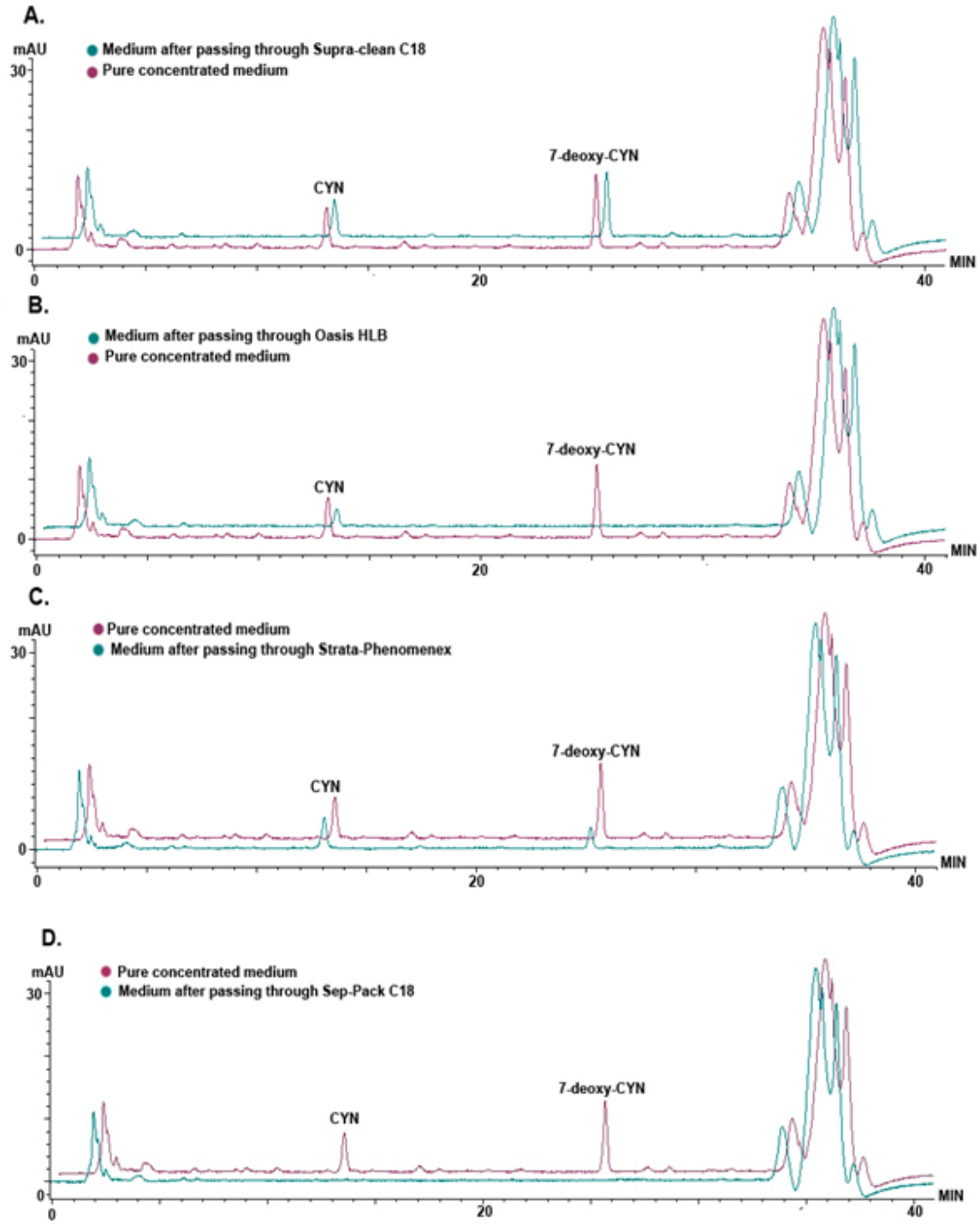

For each SPE cartridge test, n=3.
*10 mL of *C. raciborskii* 11K medium samples were centrifuged, dried and reconstituted in 200 µL of water before HPLC injection.
**10 mL of *C. raciborskii* 11K medium samples from the recovered fraction (after passing medium through the SPE) were dried and reconstituted in 200 µL of water before injection.

Figure 6 - Overlay of the of the chromatograms (λ= 262 nm) obtained from culture medium sample before* and after** contact with PAC on a tube.

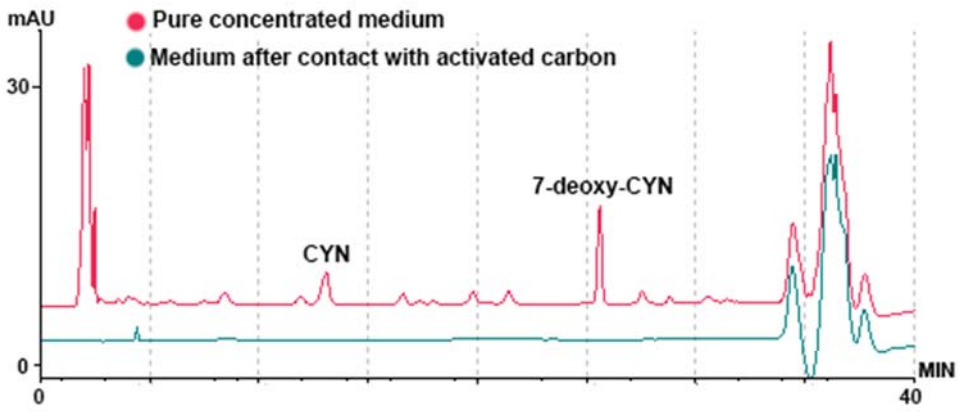

For PAC tests, n=3.
*10 mL of *C. raciborskii* 11K culture medium samples were dried and reconstituted in 200 µL of water before injection.
** 10 mL of *C. raciborskii* 11K recovered culture medium fractions (after contact with PAC) were dried and reconstituted in 200 µL of MeOH before injection.

Intermediate scale tests with culture broth

When extracting larger quantities (100 – 1000 mL) of culture cell broth we came across with a less polar CYN analog. Confirmation on LC-MS showed a precursor ion of 320 m/z that has been reported in the literature as a desulfated deoxy-CYN. The name given in the literature for this molecule is 7-deoxy-desulfo-cylindrospermopsin (7D-desulfo-CYN), and no information has been reported yet on the toxicity of this CYN analog. Figure 7 shows the structure and calculated mass of the 3 CYN variants present on the toxic strain.

Figure 7 - Cylindrospermopsin and analogs produced by the *C. raciborskii 11K* strain .

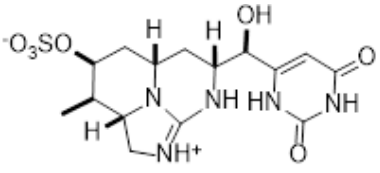

Cylindrospermopsin
Average mass: 415.4215

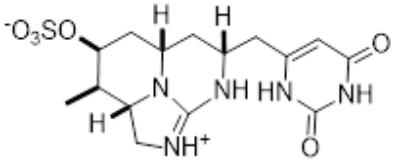

7-deoxy-Cylindrospermopsin
Average mass: 399.4221

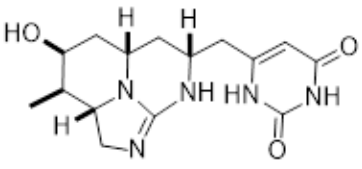

7-deoxy-desulfo-Cylindrospermopsin
Average mass: 319.3589

Choice SPE columns: C18 vs graphitized non-porous carbon

In this qualitative medium-scale experiment we tested the adsorption of the analytes in two different SPE columns: 1g Sep-Pak C18 and 1g Envi-carb graphitized non-porous carbon (GNPC). On each cartridge we passed 300 mL of centrifuged cell culture broth. The adsorbed analytes were eluted using 5 mL of each of the following aqueous solutions: 10%, 50%, 75% and 100% MeOH (fig. 8). The GNPC cartridges were eluted in back-flush mode (or reverse mode) due to the high affinity to the stationary phase observed in preliminary tests. The recovered volumes were dryed and concentrated in 200 µL MeOH before HPLC analysis. All tests were performed in duplicates.

Figure 8 - Overlap of HPLC-DAD chromatograms (λ= 262 nm) obtained after sample* elution with 5 mL of 10% MeOH from a C18 (red chromatogram) or from a GNPC (green chromatogram) cartridge.

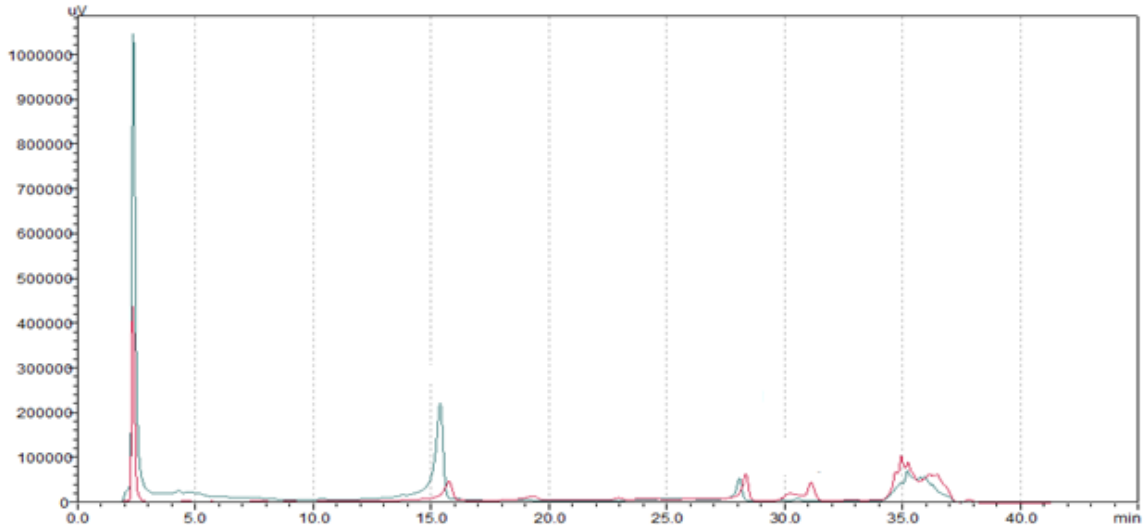

Retention times for the main analytes: CYN 15 min, 7D-CYN 28 min, 7D-desulfo-CYN 30-31 min.
*We used 300 mL of centrifuged *C. raciborskii 11K* strain culture broth as sample. For every condition n=2.

Figure 9 - Overlap of HPLC-DAD chromatograms (λ= 262 nm) obtained after sample* elution with 5 mL of 50% MeOH from a C18 (red chromatogram) or from a GNPC (green chromatogram) cartridge.

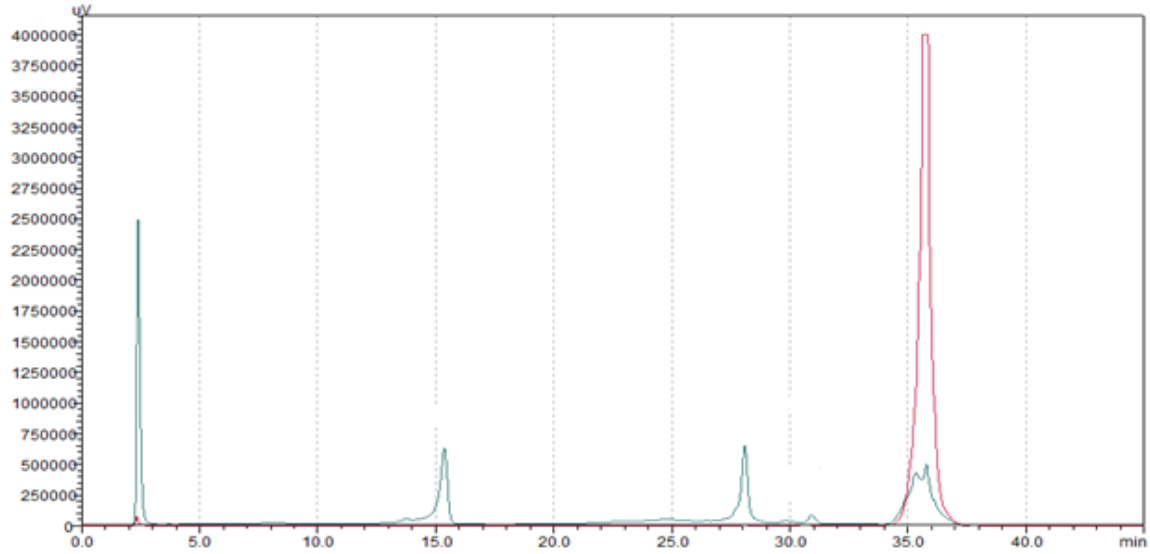

Retention times for the main analytes: CYN 15 min, 7D-CYN 28 min, 7D-desulfo-CYN 30-31 min.
*We used 300 mL of centrifuged *C. raciborskii 11K* strain culture broth as sample. For every condition n=2.

Figure 10 - Overlap of HPLC-DAD chromatograms (λ= 262 nm) obtained after sample* elution with 5 mL of 75% MeOH from a C18 (red chromatogram) or from a GNPC (green chromatogram) cartridge.

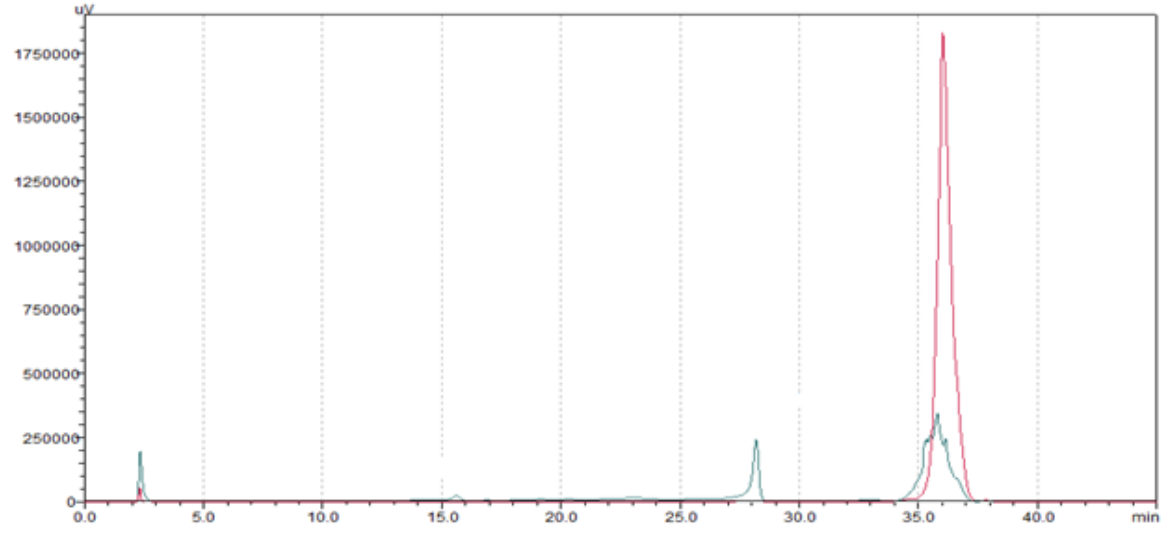

Retention times for the main analytes: CYN 15 min, 7D-CYN 28 min, 7D-desulfo-CYN 30-31 min.
*We used 300 mL of centrifuged *C. raciborskii 11K* strain culture broth as sample. For every condition n=2.

Figure 11 - Overlap of HPLC-DAD chromatograms (λ= 262 nm) obtained after sample* elution with 5 mL of 100% MeOH from a C18 (red chromatogram) or from a GNPC (green chromatogram) cartridge.

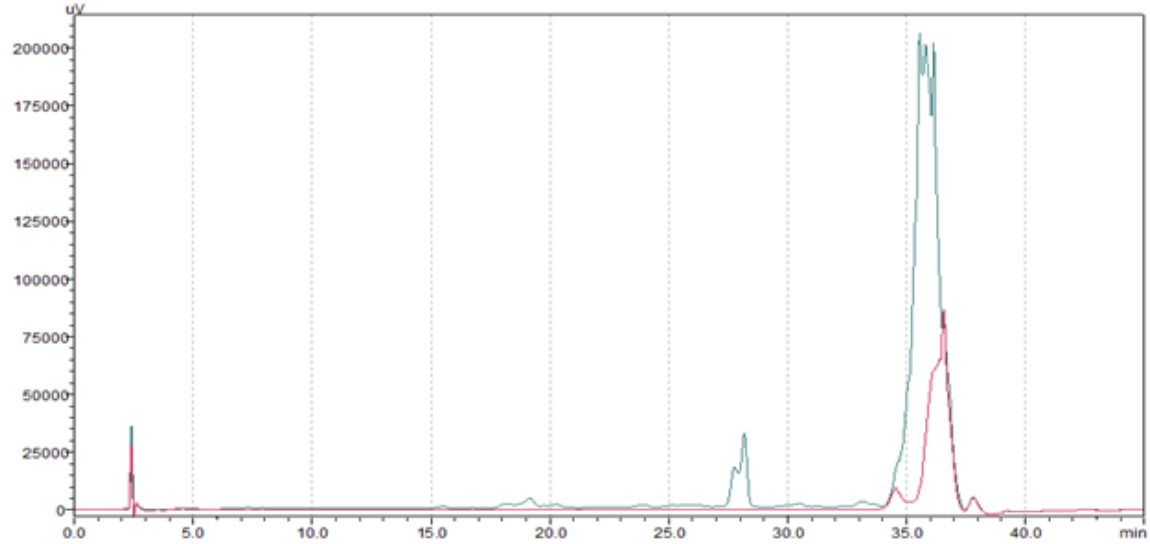

Retention times for the main analytes: CYN 15 min, 7D-CYN 28 min, 7D-desulfo-CYN 30-31 min.
*We used 300 mL of centrifuged *C. raciborskii 11K* strain culture broth as sample. For every condition n=2.

Figure 12 - Overlap of HPLC-PDA chromatograms (λ= 262 nm) obtained from recovered sample* after passing through a C18 (red chromatogram) or a GNPC (green chromatogram) cartridge.

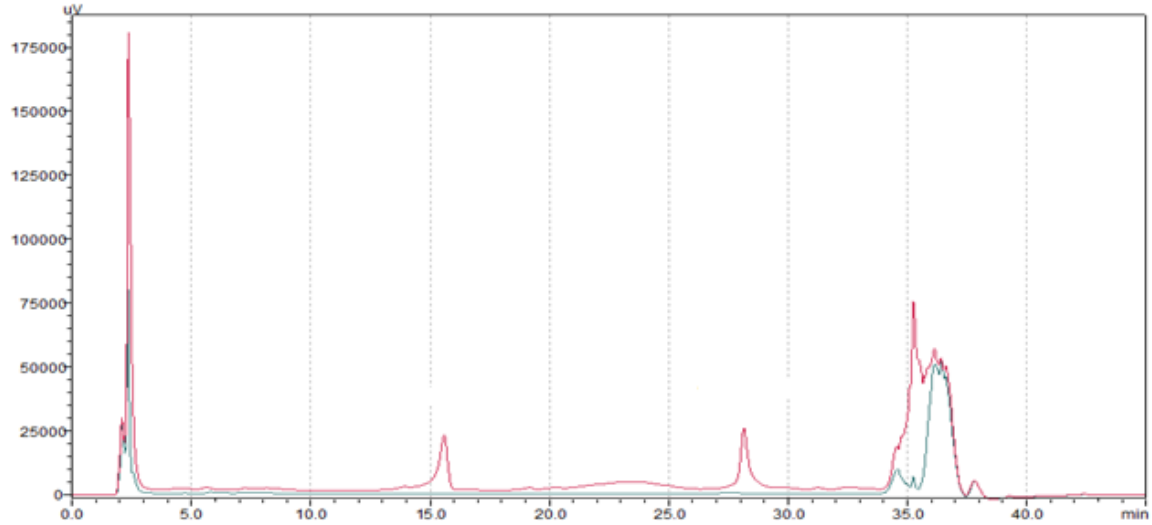

Retention times for the main analytes: CYN 15 min, 7D-CYN 28 min, 7D-desulfo-CYN 30-31 min.
*We used 300 mL of centrifuged *C. raciborskii 11K* strain culture broth as sample. For every condition n=2.

According to these qualitative results the GNPC cartridge had a greater affinity for the three analytes. Figure 12 shows breakthrough of the toxins in the recovered sample after passing through the C18 SPE column. This evidences a limited capacity

of the C18 cartridges to adsorb CYN and 7D-CYN at the tested conditions. In contrast, no toxins were detected on the sample recovered from the GNPC columns (figure 12).

Evaluation of two SPE elution techniques for GNPC

Once it was defined that the graphitized carbon cartridges were the best option, we did an extra test to optimize the elution of CYN and its analogs. On the previous test we eluted the graphitized carbon cartridge using several MeOH solutions with the cartridge in backflush mode. This creates a difficulty because this SPE columns are not particularly designed for backflush mode, although it can be improvised. For this reason, we tested another elution technique used in the literature (MeOH:CH_2Cl_2 4:1 with 5% formic acid), to elute the analytes without the need for backflushing the cartridge. All of the tests were done in duplicates.

We also used this data to calculate the percent recovery for these two kinds of elution techniques (see figure 13). As can be seen in figure 13, elution using MeOH:CH_2Cl_2 4:1 (v/v) with 5% formic acid (FA) had the best performance at eluting CYN from the carbon cartridge. On the other hand, for the other analytes the backflush technique shows a slightly better percent recovery. Since MeOH:CH_2Cl_2 4:1 with 5% FA eluted easier (no backflush mode) and more efficiently our main analyte (CYN), it was choosen as the elution method for the next isolation experiments.

Figure 13 - Percent recovery for CYN, 7D-CYN and 7D-desulfo-CYN from GNPC using two elution techniques: MeOH:CH_2CL_2 (4:1) 5% FA (3 fractions of 5 mL) and 10%, 50%, 100% MeOH on backflush mode (3 fractions of 5 mL). For every elution n=2.

Elution method used on the graphitized carbon cartridge	Recovered Fraction from cartridge	Percent recovery (%)											
		CYN				Deoxy-CYN				Desulfo-deoxy-CYN			
		Replicate 1	Replicate 2	SD	RSD	Replicate 1	Replicate 2	SD	RSD	Replicate 1	Replicate 2	SD	RSD
Methanol-Dichloromethane 4:1, 5% Formic Acid	1st Fraction	100.52	98.02	1.77	1.18	34.39	28.32	4.29	8.83	72.75	75.45	1.91	1.73
	2nd Fraction	1.12	0.79	0.23	15.35	40.93	54.25	9.42	13.84	0.00	2.54	1.80	141.42
	3rd Fraction	0.00	0.00	0.00	NaN	3.91	0.00	2.76	70.71	0.00	0.00	0.00	NaN
	Total	101.64	98.81	2.00	1.32	79.22	82.57	2.37	1.97	72.75	77.99	3.71	3.32
10%, 50%, 100% MeOH-Water (Cartridge on Backflush)	1st Fraction (10% MeOH)	40.65	36.12	3.20	5.46	22.44	24.13	1.19	3.46	12.00	9.01	2.11	12.81
	2nd Fraction (50% MeOH)	46.61	49.51	2.05	2.88	52.90	61.70	6.23	7.43	81.78	79.84	1.37	1.13
	3rd Fraction (100% MeOH)	0.89	1.03	0.10	6.78	8.39	0.74	5.41	61.75	0.00	2.45	1.73	141.42
	Total	88.15	86.66	1.06	0.80	83.73	86.57	2.01	1.58	93.78	91.30	1.75	1.26

NaN= not a number

Large scale tests with culture broth

Finally we performed extractions to test the affinity of the analytes to the SPE column when using large samples. We used 1.5 and 4 liters of centrifuged cell culture broth obtained from a 16 L lot of dense toxic cyanobacterial culture ($1x10^9$ cells mL^{-1}). For this experiment the estimated concentration of the toxins on the medium was: 182.8 µg/L of cylindrospermopsin, 282.3 µg/L of deoxy-CYN and 8.4 µg/L of desoxy-desulfo-CYN. For this estimation, a 100 mL broth sample of the same lot was centrifuged, filtered, liofilized and resontituted in 200 uL of MeOH.

Figure 14 shows no breakthrough of any of the 3 main analytes after we permeated the sample through the GNPC column. This shows a complete adsorption of the analytes to the SPE column. A succesful elution of all the analytes from the carbon cartridge was achieved by eluting with 10 mL of MeOH:CH_2Cl_2 4:1 with 5% FA. All extraction tests were performed in duplicates.

Figure 14 - HPLC chromatogram measured at wavelenght detection of 262 nm (grey chromatogram) showing the absence of the three CYN analogs in a 4 L broth sample* recovered** after passing through a graphitized carbon cartridge. No $M+H^+$ precursor ions corresponding to the masses of the toxins were detected on this run (purple chromatogram).

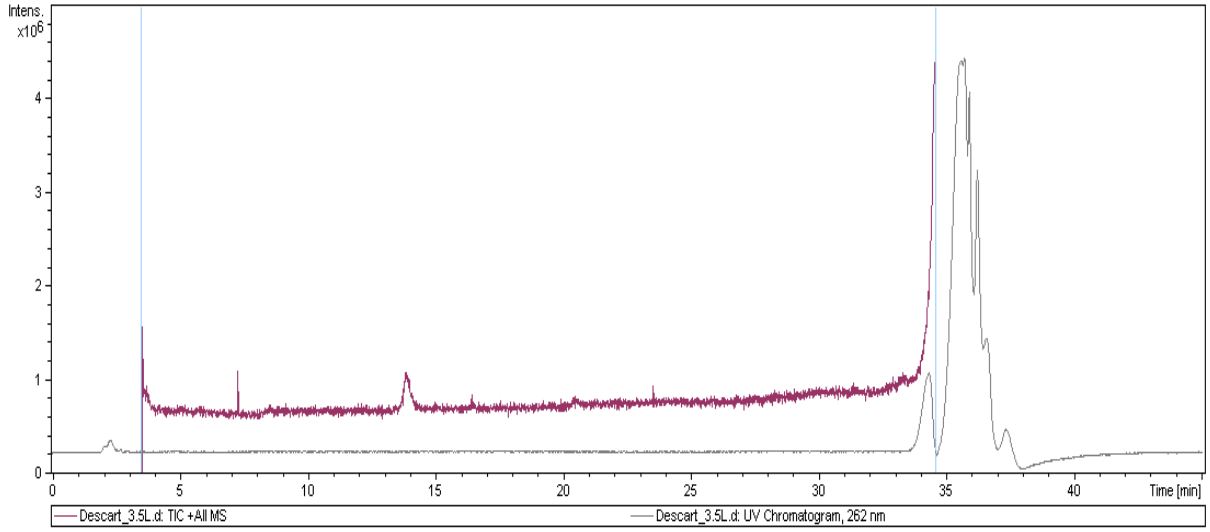

* We used 4 L of centrifuged and filtered *C. raciborskii 11K* culture broth as sample.
** 100 mL from the total 4L recovered medium (after passing medium through the SPE) was dried and reconstituted in 200 µL of MeOH before injection.

Tests with cyanobacterial biomass

CYN and 7-deoxy-CYN are heavily excreted by the cells and are available in great quantities in the medium-supernatant of *C. racibosrkii* 11k cultures. The other metabolite, 7D-desulfo-CYN is more hydrophobic due to the lack of a sulfate group in its structure. Thus, it is scarce in the aqueos culture medium. Therefore, we extracted the remaining biomass from the past experiments and we tested the affinity of 7D-desulfo-CYN on 0.5 g SepPack C18 and 0.5 g HLB cartridges. Additionally we did extractions at pH 7 and 10 to compare retention of 7D-desulfo-CYN on the SPE columns (fig. 15).

After permeating the sample through the C18 or HLB cartridges, a single wash with 6 mL of 15% MeOH was effective at eliminating all CYN and 7D-CYN from the solid phases. Figure 16 shows the absence of CYN on the chromatograms and a small remaining peak of 7D-CYN on fig. 16 C,D. Figure 17 shows another experiment using samples at pH 7. The discarded fraction and the 15% MeOH eluted fraction containing CYN and 7D-CYN were collected, dried, reconstituted in 200 uL MeOH and analyzed by LC-DAD-MS.

Figure 15 - Stacked EIC (extracted ion chromatogram) and UV (λ 262 nm) chromatograms showing performance of HLB and SepPak cartridges on the retention of CYN (red) and 7D -CYN (blue) from biomass samples*. After permeating through the columns, we eluted samples at pH 10 with 10% MeOH from HLB (A) and SepPak (B). Similarly we eluted samples at pH 7 with 10% MeOH from HLB (C) and SepPak (D).

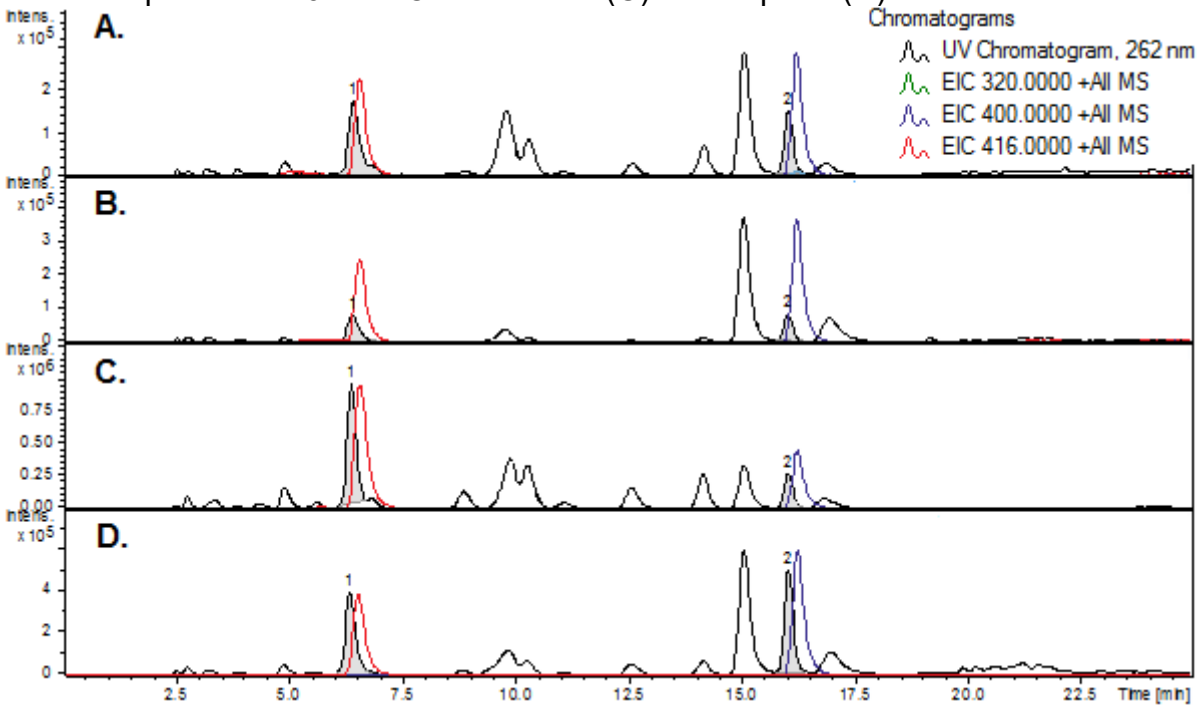

*Samples of 0,1 g of *Cylindrospermopsis sp*. dry biomass were extracted with 50% MeOH, centrifuged, filtered, diluted to 1% MeOH and adjusted to the desired pH.

Figure 16 - Stacked EIC and UV (λ 262 nm) chromatograms showing performance of HLB and SepPak cartridges on the retention of 7D-desulfo-CYN (green) from biomass samples. First we permeated all the samples through the columns and eluted them with 10% MeOH. Next, we eluted samples at pH 10 with 100% MeOH from HLB (A) and SepPak (B). In the same manner, we eluted samples at pH 7 with 100% MeOH from HLB (C) and SepPak (D).

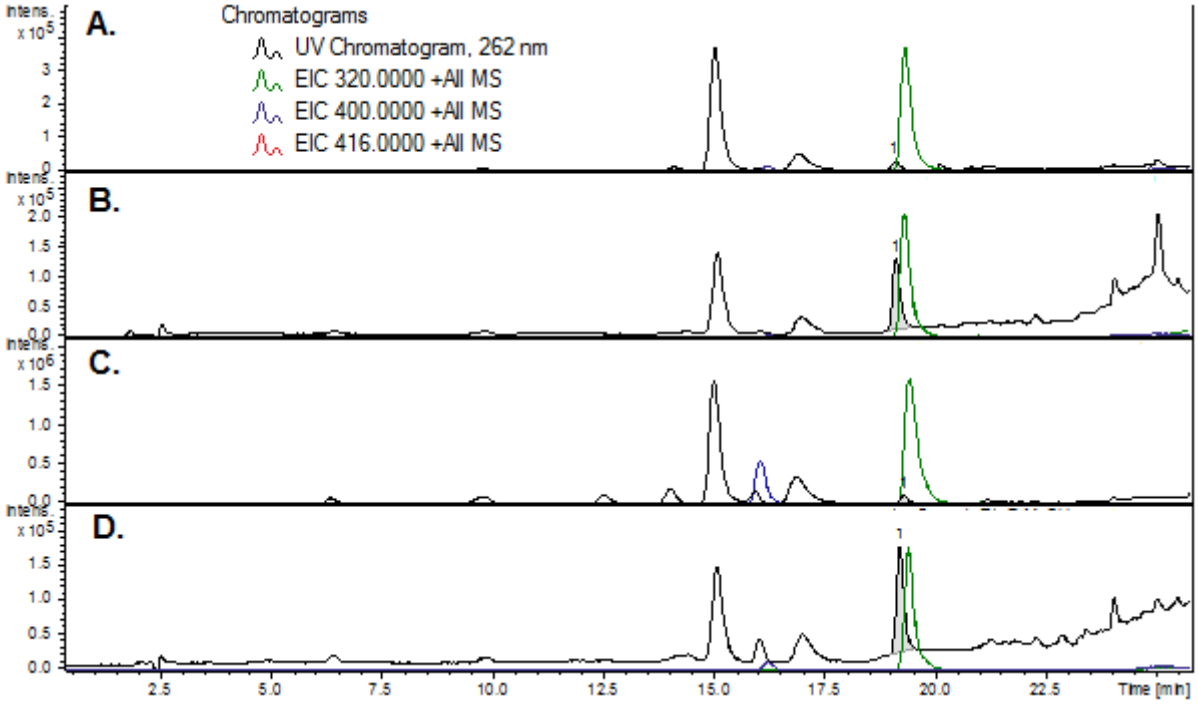

*Samples of 0,1 g of *Cylindrospermopsis sp*. dry biomass were extracted with 50% MeOH, centrifuged, filtered, diluted to 1% MeOH and adjusted to the desired pH.

Figure 16 shows similar performance on the retention of 7D-desulfo-CYN by HLB and SepPak cartridges, athough SepPak cartridges eluted less contaminants after the 100% MeOH final elution.

Figure 17 - Stacked EIC and UV (λ 262 nm) chromatograms showing performance of SepPak cartridges on the retention of CYN (red), 7D -CYN (blue) and 7D-desulfo-CYN (green) from biomass samples*. Samples at pH 7 were permeated through the cartridges and the resulting liquid after passing through the column was collected (C). Cartridges were then eluted with 15% MeOH (A) and pure MeOH (B).

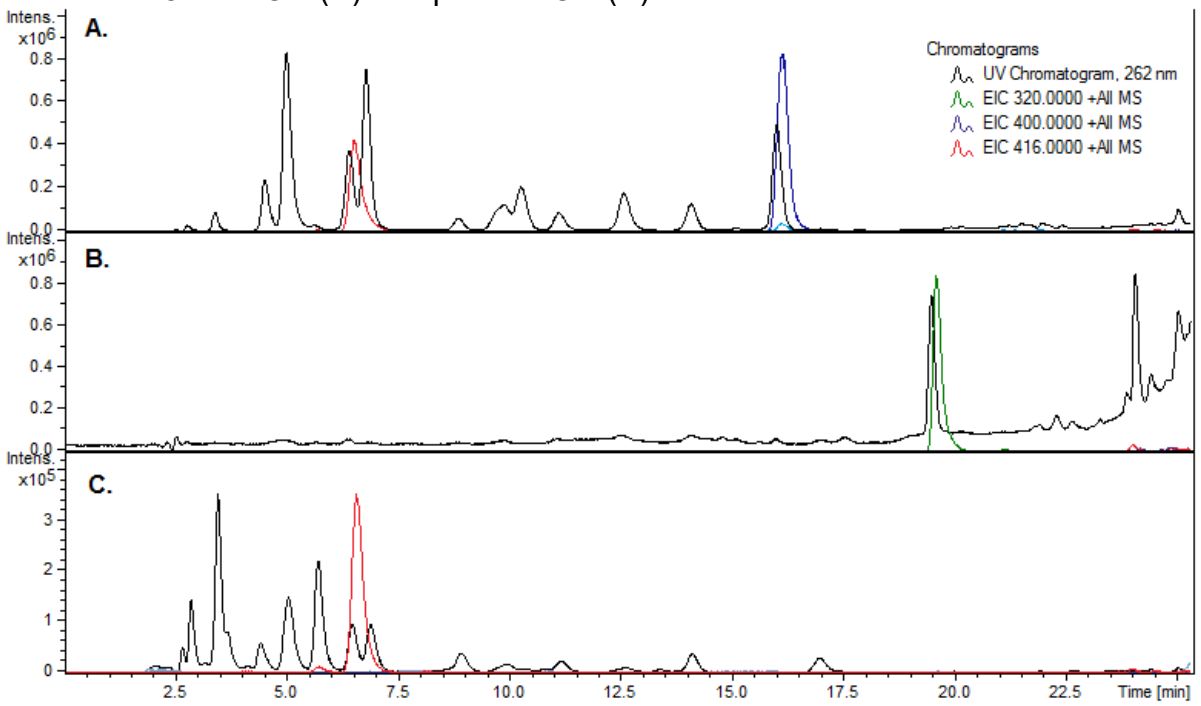

*Samples of 0,1 g of *Cylindrospermopsis sp*. dry biomass were extracted with 50% MeOH, centrifuged, filtered, diluted to 1% MeOH and adjusted to the desired pH.

Elution of C18 cartridge with 10 mL 15% MeOH (fig. 17) yielded a purer 7D-desulfo-CYN. Almost no contaminants were left after this elution (fig. 17 B).

In this manner, the aqueous extract from liofilized biomass requires a C18 cartridge step to retain 7D-desulfo-CYN and an elution with 15% MeOH to eliminate the CYN zwitterions and other metabolites from the C18. We propose to intall the GNPC cartridge in series to the C18 column in order to recover all of the CYN and 7D-CYN in the biomass.

Tests using acyclovir as internal standard (IS) showed great affinity for the GNPC cartridge and good affinity for the C18 column. The final total recovery proposed protocol is shown on figure 18. Next we will calculate some validation parameters of the proposed SPE-HPLC-DAD method.

Figure 18 - Total recovery isolation workflow for the purification of hydrophilic and hydrophobic CYNs from either solid (steps 1a – 10a) or aqueous (steps 1b – 6b) matrixes. Optional steps (9a and 6b) include adding of IS at the SPE stage, whenever the goal of the analysis is to quantitate CYNs in an unknown sample.

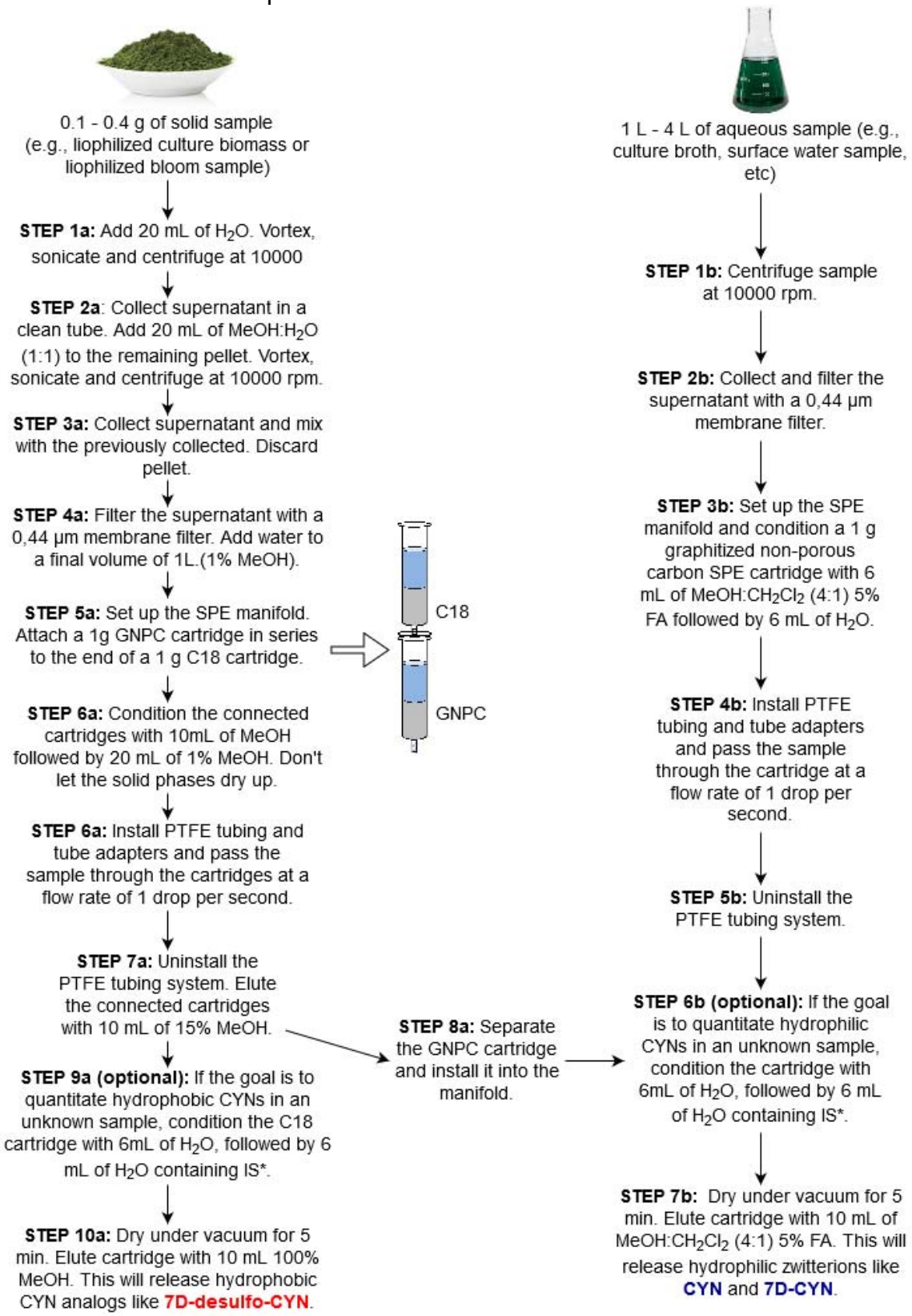

*IS: We used 4 µg of acyclovir as internal standard.

5.1.2 Quality control and purity of the isolated toxins

The following figures show the quality of the purified toxin extracts. All CYN structural variants extracted by SPE underwent an HPLC-DAD isolation step using a C18 preprative column and a chromatographic method similar to the one described in section 4.2.4.

Figure 19 - EIC* and UV (λ 262 nm) chromatograms (A), UV spectrum (B), MS1(C) and MS2 (D) spectrum for the purified 7D-desulfo-CYN (lot 2017.01.01). For this lot a purity of 91% was calculated.

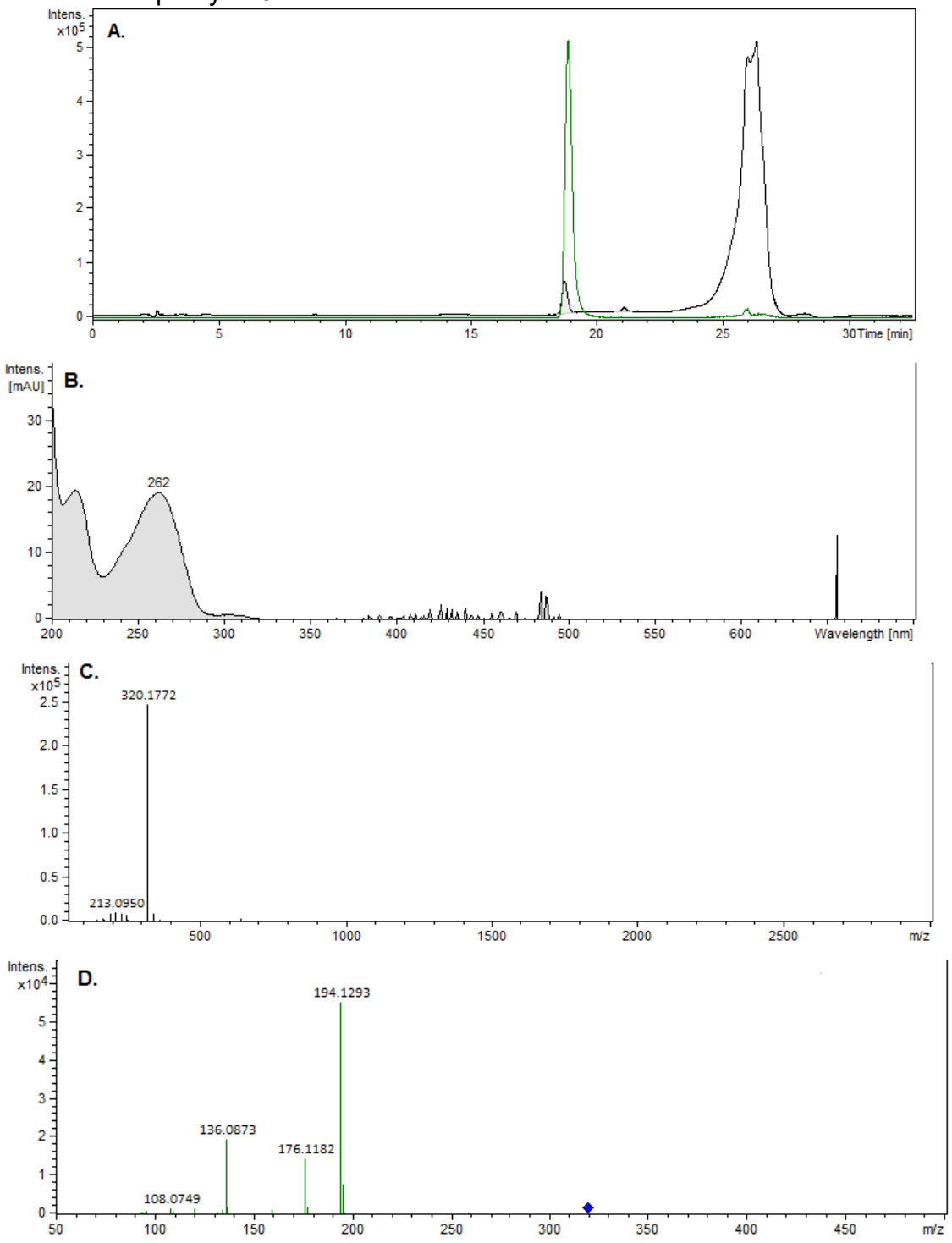

* The green chromatogram corresponds to the MS1 EIC at 320 m/z.

Figure 20 - EIC* and UV (λ 262 nm) chromatograms (A), UV spectrum (B), MS1 (C) and MS2 spectrum (D) for the purified CYN (lot 2016.07.28). For this lot a purity of ≥99% was calculated.

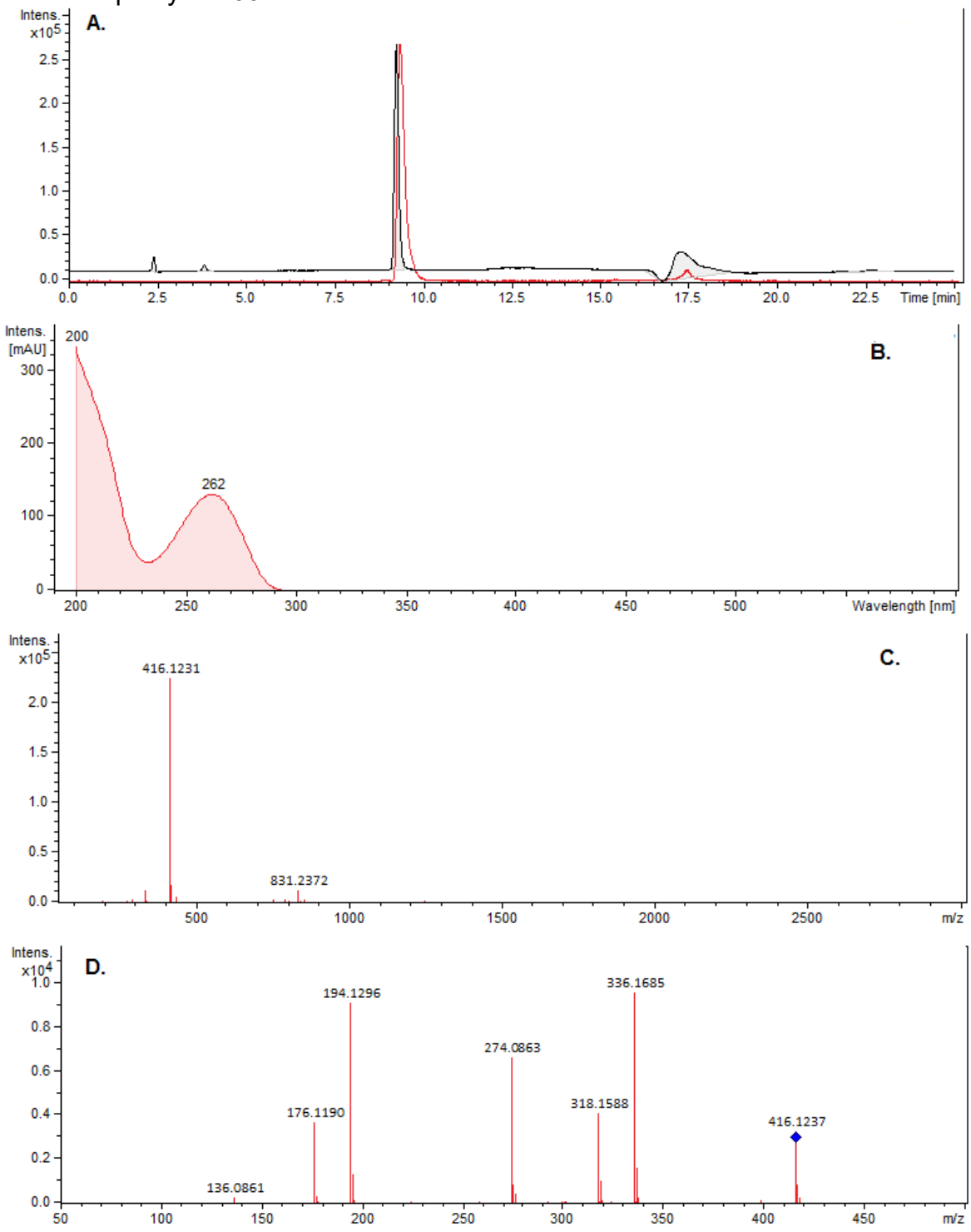

* The red chromatogram corresponds to the MS1 EIC at 416 m/z.

Figure 21 - EIC* and UV (λ 262 nm) chromatograms (A), UV spectrum (B), MS1 (C) and MS2 spectrum (D) for the purified 7D-CYN (lot 2016.12.05). For this lot a purity of ≥99% was calculated.

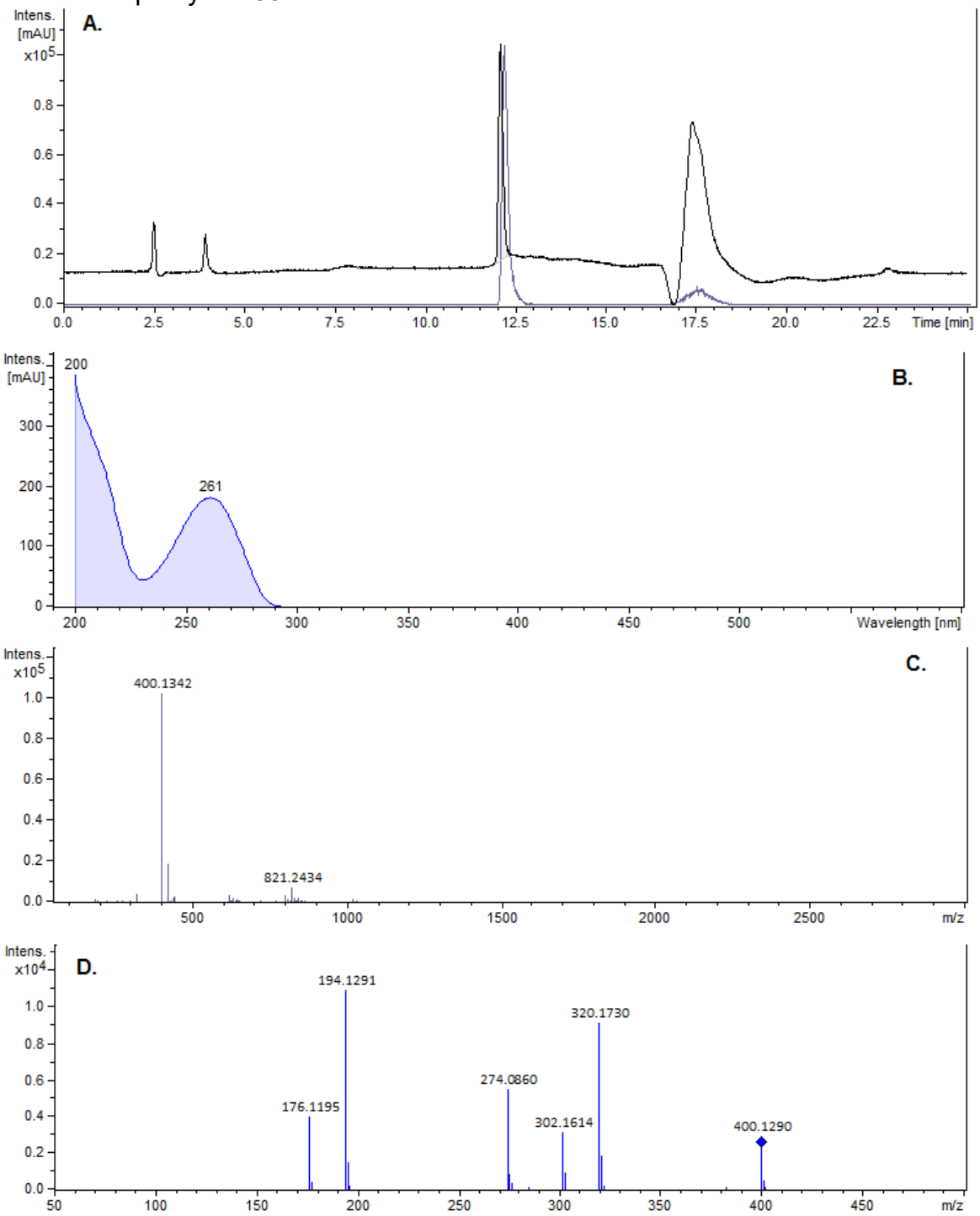

* The blue chromatogram corresponds to the MS1 EIC at 400 m/z.

Figure 22 - Mean and calculated monoisotopic m/z values, and mean errors from QTOF for CYN and analogs.

Ions Measured	Mean measured (m/z) n=3	Calculated (m/z)	Mean error (ppm)
CYN	416.1235	416.1240	1,2
7D-CYN	400.1288	400.1291	0,87
7D-desulfo-CYN	320.1728	320.1723	1,6

5.1.3 Analytical performance parameters of the quantitative LC-DAD method

The final HPLC-DAD method is described on item 4.2.3. All of the following analytical parameters were calculated using this assay.

Linearity, precision and bias

Figure 23 - Calibration curve for CYN quantitation by HPLC-DAD. As matrixes we used 500 mL broth samples from a non-CYN producing strain (*C. raciborskii* ITEP 18) spiked with 6 concentrations of CYN analytical standard (Abraxis) and 4 µg of acyclovir as IS. For every point n=3. Error bars indicate RSD multiplied by 10 for visualization.

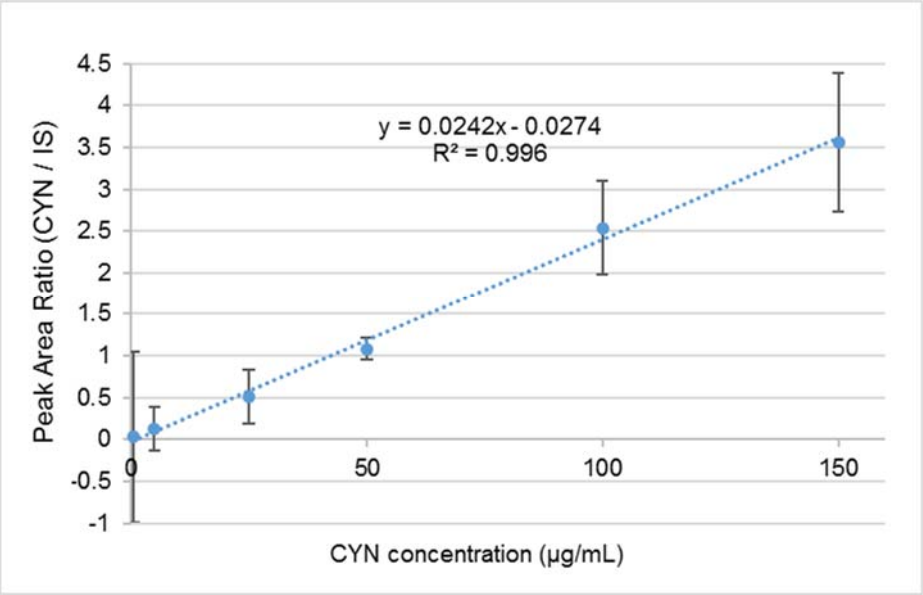

As an extraction protocol we used figure 18 steps 1b to 7b. The extract was dried and reconstituted in 200 µL of MilliQ grade water.
RSD= relative standard deviation

Figure 24 - Selected analytical performance parameters, criteria and experimental results for the final method. Limits of detection and quantitation were calculated by spiked sample dilution.

Parameters	**Criteria**	**Experimental data**
Linearity	r ≥ 0.990	r = 0.996
Calibration curve data deviation	RSD% ≤ 15 *	RSD % = 1.3 – 10.2
Lower limit of quantitation	1 µg/L [α]	0.2 µg/L
Limit of detection	N.A.	0.04 µg/L

RSD%= percent relative standard deviation, r= correlation coefficient
* Ministry of Health, National Agency for Sanitary Vigilance, regulatory guidelines RDC No. 27, Brazil 2012.
[α] Ministry of Health regulatory guidelines No. 2.914, Brazil 2011.

Figure 25 - Criteria, experimental data and status for precision and within-day bias for 5 levels of quality control samples. As matrixes we used 500 mL broth samples from a non-CYN producing strain (*C. raciborskii* ITEP 18) spiked with 5 concentrations of CYN analytical standard (Abraxis) and 4 µg of acyclovir as IS. For every point n=5.

Quality Control Sample (µg/mL)	Within-day Precision (RSD%)			Within-day Bias/Trueness (RB%)		
	Criteria*	Experimental	Status	Criteria*	Experimental	Status
0.5	≤ 20	7.5	Accepted	80 – 120	115	Accepted
1.5	≤ 15	1.9	Accepted	85 – 115	98	Accepted
75	≤ 15	1.6	Accepted	85 – 115	100	Accepted
120	≤ 15	1.2	Accepted	85 – 115	95	Accepted
250	≤ 15	6.2	Accepted	85 – 115	90	Accepted

As an extraction protocol we used figure 18 steps 1b to 7b. The extract was dried and reconstituted in 200 µL of MilliQ grade water.
RB%= percent relative bias
* Ministry of Health, National Agency for Sanitary Vigilance, regulatory guidelines RDC No. 27, Brazil 2012.

Selectivity

Finally figure 26 shows good resolution between the peaks in the λ 262 nm chromatogram. Desulfo-CYN a degradation product of CYN synthesized by acid hydrolisis and heat was added to the mix in order to assess peaks resolution.

Figure 26 - UV (λ 262 nm) and MS1 EIC for a mix of five analytes obtained on scan mode on a LC-DAD-QTOF. The retention times (min) for the 5 compounds are: CYN 9.1 (blue), acyclovir 10.0 (red), desulfo-CYN* 11.3 (orange), 7D-CYN 11.7 (purple) and 7D-desulfo-CYN 12.7 (green).

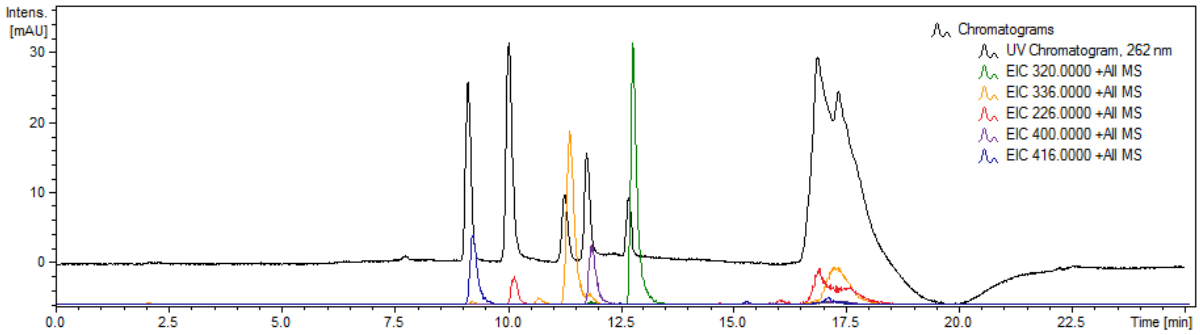

*Desulfo-CYN is a in-house synthesized degradation product of CYN.

5.2 Defining sub-lethal CYN working ranges for HepG2 cells

On the following section, we first describe the flow citometry experiments done to evaluate the cytotoxicity of the analytical standard of CYN on HepG2 cells. Toxic levels of CYN on HepG2 cells have been described by different methods in the literature. Nevertheless, we treated HepG2 cells with the the isolated CYN analogs in order to compare their toxicity with the commercial CYN standard.

5.2.1 Standardization of a flow citometry test to measure necrosis and apoptosis

Apoptosis was assessed by detecting the externalization of phosphatidylserine on the cell membrane by labeling it with Annexin V binded to allophycocyanin, APC (excitation / emission= 650 / 660 nm). Necrosis was measured by the change in permeability of the cell membrane. The intact cell normally does not allow the entry of dyes, like propidium iodide, PI (excitation / emission= 552 / 588 nm). However, when membrane injury occurs, PI can enter and bind to the DNA of the cell.

Initially, we tested various reagents as positive control for the apoptosis assays in HepG2 cells. Cisplatin (32 mg/mL) is considered as a “gold standard for apoptosis induction”. Along with cisplatin we tested DMSO 10% and MeOH 20%, which also cause a degree of necrosis in HepG2 cells. We also tested the correct amount of Annexin V to be used in the assays (2.5 or 5 µL). Furthermore, we added 2 µL of PI

(as recommended in the literature) to the samples and evaluated the data using the FlowJo software.

Figure 27 shows the results of apoptosis induction using three candidate positive controls. We concluded that any of these regents would act as an effective positive control for apoptosis. The PI reagent easily stained the DNA of the necrotic mammalian cells using 2 µL. On further experiments we preferred the use of 20% MeOH as a “double” positive control due to the fact that it produces a fare amount of necrosis too.

Figure 27 - Cell counts of apoptotic HepG2 cells after 24 and 48 hour treatment with cisplatin 32 µg/mL, 10% DMSO and 20% MeOH. Apoptosis induction was measured by flow citometry using annexin V stain in two concentrations (2.5 µL and 5 µL). n=2

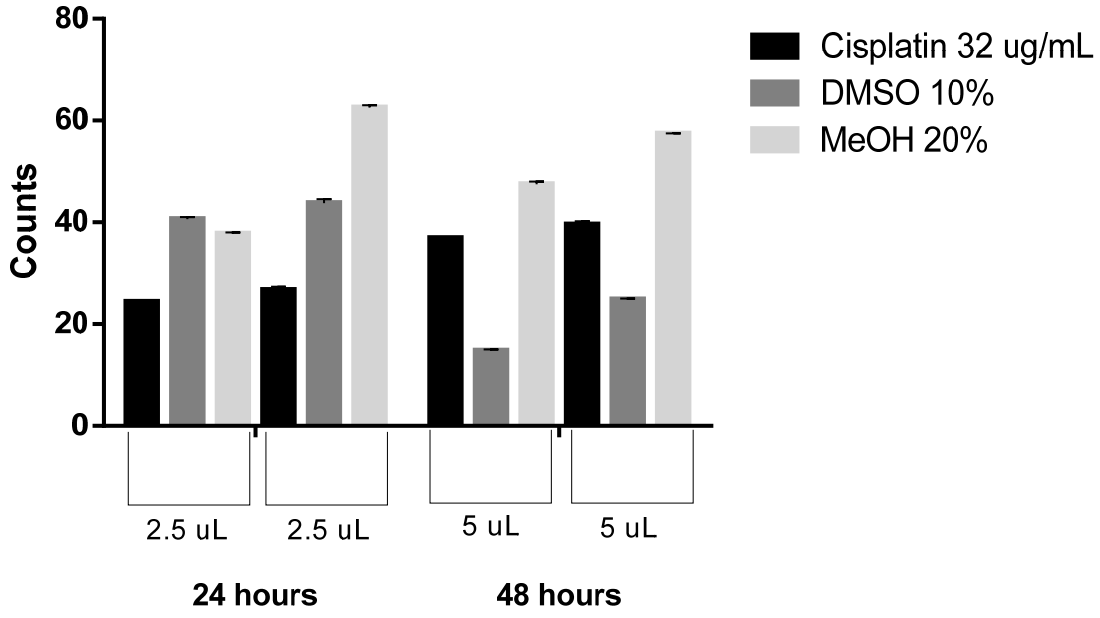

Figure 26 is a typical scatterplot from a replicate showing significant apoptosis and necrosis signals in HepG2 cells treated with 20% MeOH. The lower left square shows the viable cells (57%), or unstained with Annexin and PI. Apoptotic cells (stained with Annexin V only are located at upper left square, necrotic cells stained with PI only are located at lower right square and from cells with late apoptosis (double stained with Annexin V and PI) are located at upper right square.

Figure 28 - Example of a flow citometry scatterplot created by the FlowJo software (v10.2) showing porcentages of apoptosis, late apoptosis, necrosis and viable HepG2 cells after a 24 hour treatment with 20% MeOH.

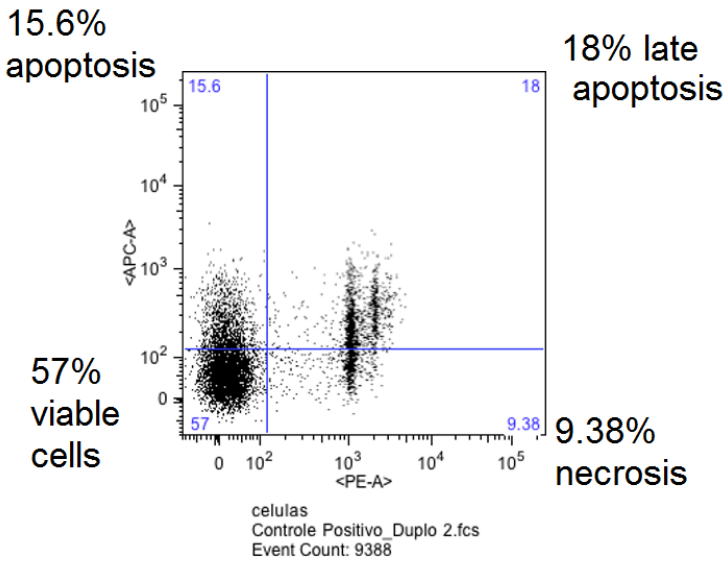

APC-A: allophycocyanin signal, PE: phycoerythrin / PI signal

Once the positive controls, the amount of Annexin and the amount of PI were defined, we studied the induction of necrosis and apoptosis on HepG2 cells using different concentrations of the CYN commercially available standard.

Although many concentrations of CYN were tested before arriving to a useful spectrum, the most relevant concentrations are shown on figure 27. The goal of this experiment was to define razor CYN concentrations which could cause apoptosis or/and necrosis on HepG2 cells in relevant time intervals. For this purpose, HepG2 cells were estimulated with different concentrations of CYN analytical standard (Abraxis) for up to 48h (fig. 27). In summary these results show that the treatment of HepG2 cells with 1 µM of CYN during 24 hours (fig. 27), did not produce apoptotic-necrotic effects. On a 48 hour treatment, the use of up to 0.5 µM of CYN did not induce apoptotic-necrotic effects. Furthermore, an aggressive 2 hours treatment with 381 µM of CYN showed no no cell injury (data not shown). This was the higher concentration we could prepare with the available CYN standard. Even though it is not a practical working concentration, the results with 381 µM of CYN served as evidence of the delayed toxicity of this cyanotoxin. In other words the negative effects of the toxin on the cells are not inmediate even at high concentrations.

Figure 29 - Viability of HepG2 cells treated with 0.5, 1, and 5 µM of a CYN analytical standard for 12, 24 and 48 hrs. PI and Anexin V stained cells were analysed by flow citometry. n= 4

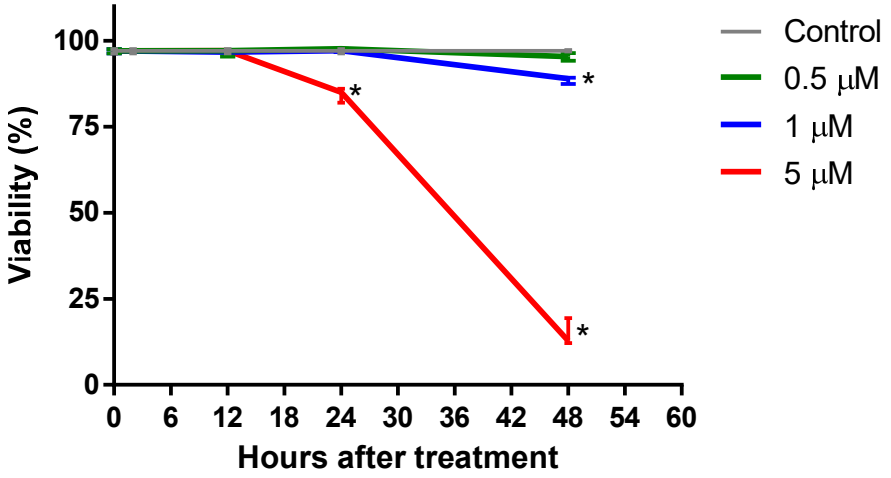

* p < 0.05, Mann-Whitney test between time point vs time zero.

Figure 30 - Viability of HepG2 cells after a 48 hrs treatment with (A) 1 µM CYN, 1 µM 7D-CYN, 5 µM 7D-CYN and (B) 1 µM 7D-desulfo-CYN and 5 µM 7D-desulfo-CYN. All CYN variants were purified from C. raciborskii 11K. PI and Anexin V stained cells were analysed by flow citometry. n= 4

A.

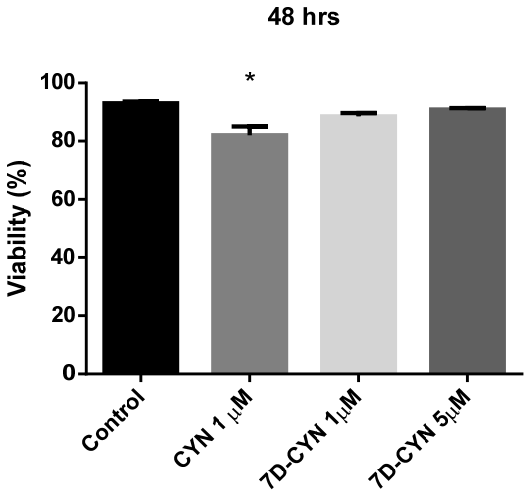

B.

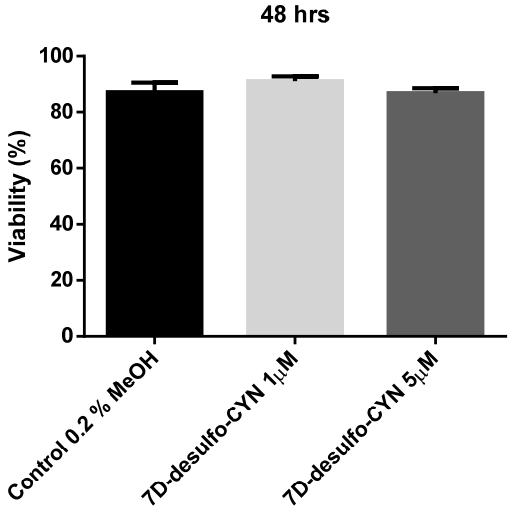

* p < 0.05, Mann-Whitney test between time point vs time zero.

In the same manner we treated HepG2 cells with the in-house purified CYN and analogs (isolated and quantified according to section 5.1) to compare their potency against the commercial CYN standard. We prepared the CYN and 7D-CYN standards in MilliQ water. 7D-desulfo-CYN was solubilized in 50% MeOH diluted in DMEM medium to a final MeOH concentration of 0.2%. Controls cells for 7D-desulfo-CYN were grown in DMEM medium supplemented with 0.2% MeOH.

7D-CYN and 7D-desulfo-CYN stimulated cells showed no difference in viability compared to their respective controls at the tested concentrations (fig. 28). On the

other hand the isolated CYN standard (lot 2016.07.03) showed after a 48 hrs treatment a lethality compared to the CYN commercially available standard.

5.3. Preliminary Discovery Proteomics: cell stimulation using 0.1 – 1 µM of CYN

The toxin used on this preliminary experiments was a 0,5 mg CYN standard solubilized in Milli-Q water (Abraxis, Inc.). In order to detect small changes in protein abundance we used SILAC as a quantitative proteomics approach.

Several toxin treatments with concentrations < 1 µM CYN were done on the HepG2 cells. For these low concentration experiments we used a triple SILAC approach: CYN treated cells on H (heavy labeled) and M (medium labeled) medium, and control cells on L (light labeled) medium. Two biological replicates and one control were plated for every timepoint. Samples were not fractionated and were processed according to section 4.4.3. The objective of these experiments was to test if at this low concentrations we could get constant biological responses through the timepoints. We tested outliers using a two-tailed significance A test, using Benjamini-Hochberg FDR threshold value of 0.001. Results showed little to none alterations on concentrations < 1 µM CYN after a maximum 6 hour treatment.

Following these experiments we started using 1 µM of CYN on the cell stimulations. Figures 31 – 34 show results of one of these preliminary experiments using 1 µM of CYN. We used a double SILAC approach: CYN treated cells on H (heavy labeled) and control cells on L (light labeled) medium. One biological replicate and one control were plated for every timepoint. Samples were fractionated and processed according to section 4.4.3. The objective of these experiments was to test if at this concentration we could detect constant biological responses through 11 timepoints (maximum treatment time was 12 hrs). We identified regulated proteins using a two-tailed significance A test, using Benjamini-Hochberg FDR threshold value of 0.01.

Figure 31 - Histograms showing distribution of the log_2 transformed protein ratios of the samples at time zero and after 0.5, 1, 1.5, 2, 2.5, 3, 3.5, 4, 8, 10, 12 hrs treatment with CYN.

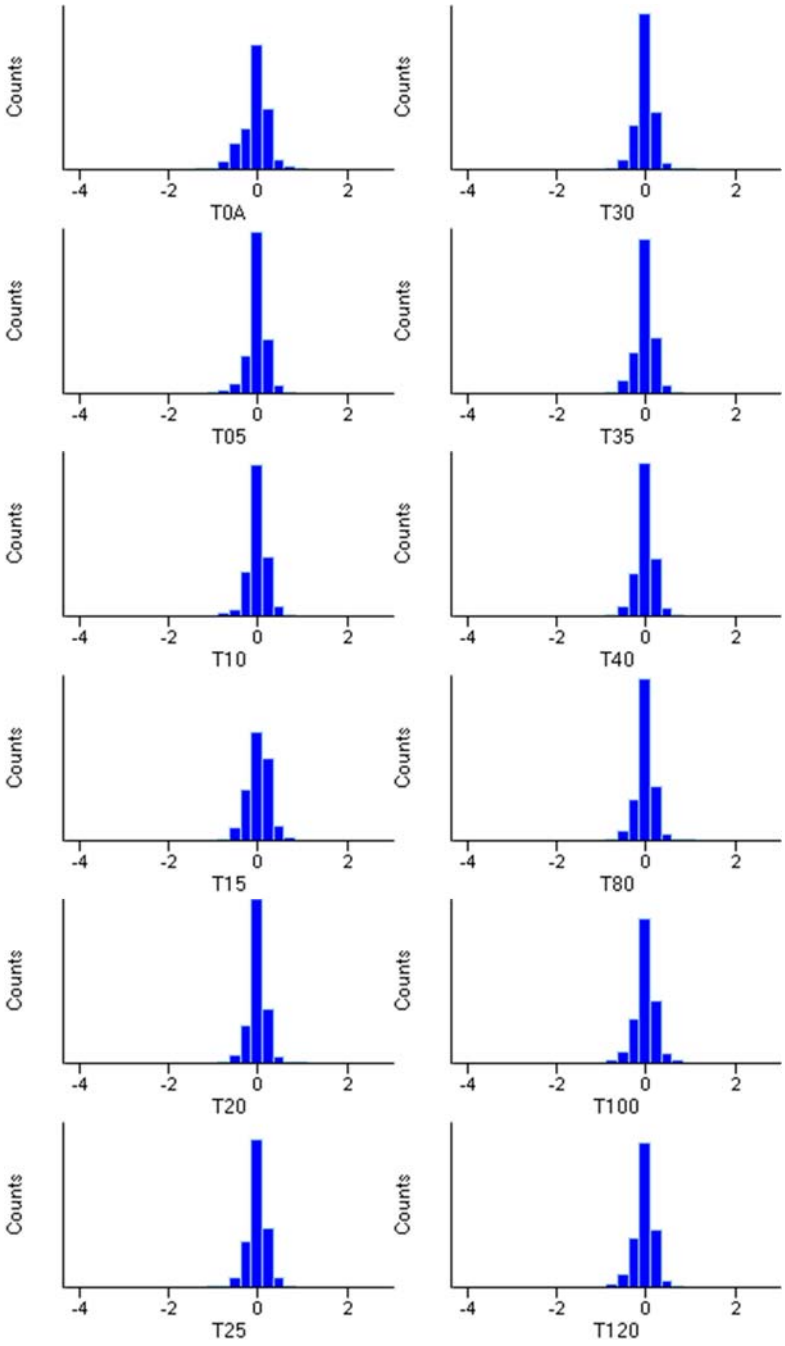

Figure 32 - Boxplot of the H/L log_2 transformed ratios of the samples at time zero and after 0.5, 1, 1.5, 2, 2.5, 3, 3.5, 4, 8, 10, 12 hrs treatment with CYN.

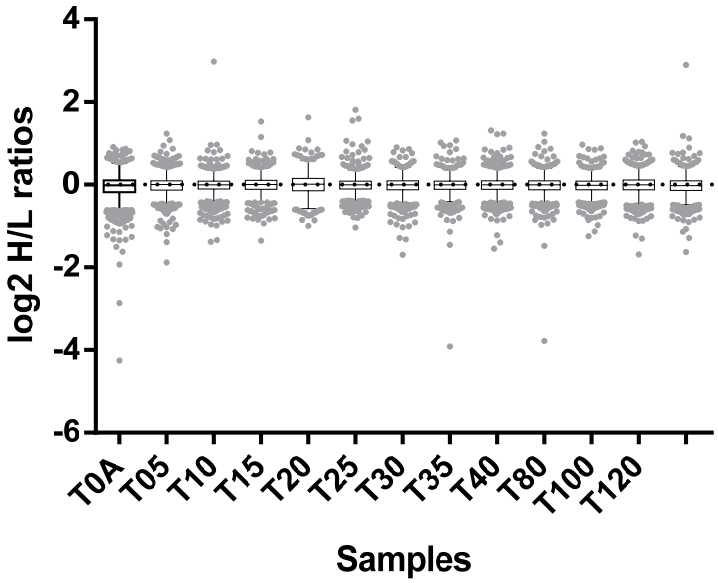

Figure 33 - Two-dimensional principal component analysis (PCA) plot of the preliminary CYN stimulation experiments on HepG2. Samples are represented by dots. The elipses (red, blue and green) represent sample clusters.

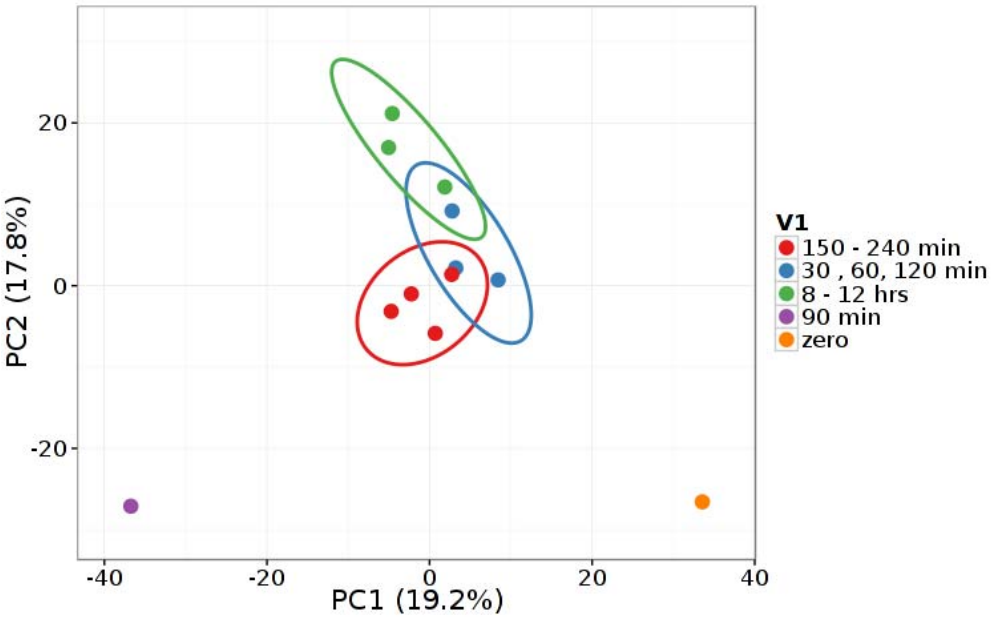

Figure 34 – Protein name, gene name and rank* of all significant proteins after 0.5, 1, 1.5, 2, 2.5, 3, 3.5, 4, 8, 10, 12 hrs treatment with CYN.

Protein names	Gene names	Rank*
DNA topoisomerase 2-alpha	TOP2A	5
Gelsolin	GSN	3
Utrophin	UTRN	3
DnaJ homolog subfamily C member 3	DNAJC3	3
Sister chromatid cohesion protein PDS5 homolog A	PDS5A	3
La-related protein 1	LARP1	3
Up-regulated during skeletal muscle growth protein 5	USMG5	3
Paternally-expressed gene 3 protein	PEG3	3
Drebrin	DBN1	2
Protein LSM14 homolog A	LSM14A	2
Serum albumin	ALB	2
Zinc finger CCCH domain-containing protein 18	ZC3H18	2
2-oxoglutarate dehydrogenase, mitochondrial	OGDH	2
Translin	TSN	2
Density-regulated protein	DENR	2
Formimidoyltransferase-cyclodeaminase;Glutamate formimidoyltransferase;Formimidoyltetrahydrofolate cyclodeaminase	FTCD	2
Transgelin	TAGLN	2
Tubulin beta-2A chain;Tubulin beta-2B chain	TUBB2A;TUBB2B	2
Cytoskeleton-associated protein 5	CKAP5	2
Early endosome antigen 1	EEA1	2
Succinate dehydrogenase cytochrome b560 subunit, mitochondrial	SDHC	2
Protein FAM49B	FAM49B	2
RNA-binding protein 8A	RBM8A	2
ADP-sugar pyrophosphatase	NUDT5	1
HLA class I histocompatibility antigen, A-2 alpha chain;HLA class I histocompatibility antigen, A-69 alpha chain;HLA class I histocompatibility antigen, A-68 alpha chain	HLA-A	1
Thioredoxin reductase 1, cytoplasmic	TXNRD1	1
AP-1 complex subunit gamma-1	AP1G1	1
SRSF protein kinase 1	SRPK1	1
Epithelial cell adhesion molecule	EPCAM	1
Long-chain-fatty-acid--CoA ligase 1	ACSL1	1
Tumor protein D52	TPD52;PrLZ	1
Phosphoacetylglucosamine mutase	PGM3	1
Nicastrin	NCSTN	1
Tetratricopeptide repeat protein 38	TTC38	1
Heat shock 70 kDa protein 4L	HSPA4L	1
Vitamin K-dependent gamma-carboxylase	GGCX	1
Lanosterol synthase	LSS	1

Importin subunit alpha;Importin subunit alpha-7;Importin subunit alpha-6	KPNA6;KPNA5	1
Translocation protein SEC62	SEC62	1
Dynamin-1-like protein	DNM1L	1
26S proteasome non-ATPase regulatory subunit 12	PSMD12	1
U3 small nucleolar ribonucleoprotein protein MPP10	MPHOSPH10	1
Exportin-1	XPO1	1
ATP-dependent Clp protease ATP-binding subunit clpX-like, mitochondrial	CLPX	1
Protein transport protein Sec24A	SEC24A	1
Complement C3;Complement C3 beta chain;Complement C3 alpha chain;C3a anaphylatoxin;Acylation stimulating protein;Complement C3b alpha chain;Complement C3c alpha chain fragment 1;Complement C3dg fragment;Complement C3g fragment;Complement C3d fragment;Complement C3f fragment;Complement C3c alpha chain fragment 2	C3	1
Prolyl 4-hydroxylase subunit alpha-1	P4HA1	1
Arylsulfatase B	ARSB	1
Beta-galactosidase	GLB1	1
Cytoplasmic aconitate hydratase	ACO1;IRP1	1
Proteasome subunit beta type-6	PSMB6	1
Glycylpeptide N-tetradecanoyltransferase 1	NMT1	1
S-adenosylmethionine synthase isoform type-2;S-adenosylmethionine synthase	MAT2A	1
Replication factor C subunit 1	RFC1	1
Flap endonuclease 1	FEN1	1
60S ribosomal protein L13a	RPL13A	1
Cytosolic Fe-S cluster assembly factor NUBP1	NUBP1	1
Signal recognition particle 54 kDa protein	SRP54	1
ADP-ribosylation factor 1;ADP-ribosylation factor 3	ARF1;ARF3	1
WD repeat-containing protein 5	WDR5	1
U6 snRNA-associated Sm-like protein LSm6	LSM6	1
AP-2 complex subunit beta	AP2B1	1
60S ribosomal protein L38	RPL38	1
Nucleobindin-1	NUCB1	1
28 kDa heat- and acid-stable phosphoprotein	PDAP1	1
Mannosyl-oligosaccharide glucosidase	MOGS	1
DNA replication licensing factor MCM6	MCM6	1
LDLR chaperone MESD	MESDC2	1
Nucleolar protein 9	NOP9	1
Beta-catenin-like protein 1	CTNNBL1	1
Isochorismatase domain-containing protein 1	ISOC1	1
AT-rich interactive domain-containing protein 3A	ARID3A	1
Methylosome protein 50	WDR77	1
Partner of Y14 and mago	WIBG	1
Kinesin light chain 4	KLC4	1

Hematological and neurological expressed 1 protein	HN1	1
Ras GTPase-activating protein-binding protein 2	G3BP2	1
YTH domain family protein 2	YTHDF2	1
CD2-associated protein	CD2AP	1

* Total number of time points during the experiment in which the protein was significantly regulated

On this experiment 1090 proteins were shared along the 11 timepoints, but only few significant proteins along the timepoints show a constant regulation pattern.

Based on these preliminary data we decided to continue using 1 µM of CYN, but with less time points, and using at least 6 biological replicates on the final experiments. In order to improve our chances to detect significant changes, a 6 hour treatment was considered as the minimum stimulation time with the toxin.

5.4 Final Discovery Proteomics: cell stimulation using 1 µM of CYN

For these experiments we used a concentration of 1 µM CYN purified from *C. raciborskii* 11K (lot 2016.07.03). We used a double SILAC approach: CYN treated cells on H medium and control cells on L medium. HepG2 cells plated on 6 well plates ($1x10^6$ cell/well) were collected at time zero and after 6, 12 and 24 hours treatment with CYN. Six biological replicates and controls were plated for every timepoint.

We followed the Rapigest® digestion protocol detailed at section 4.5.1 and the fractionation protocol detailed on section 4.5.2.

5.4.1 General data visualization and quality control

Figures 35 – 40 show the distribution and variability of the H/L log_2 transformed ratios of the replicates through the experiment. The replicates shown on figures 35 – 40 were used for further statistical analyses.

Ratios H/L from 06 - 10 correspond to Time point: 0, ratios 11 – 16 correspond to Time point : 6 hrs, ratios 18 – 22 correspond to Time point: 12 hrs, and ratios 23 – 28 correspond to Time point: 24 hrs.

Figure 35 – Scatter plots showing Pearson correlation coefficients (A) and Histogram (B) of the H/L log_2 transformed ratios of the time zero replicates selected for statistical analysis.

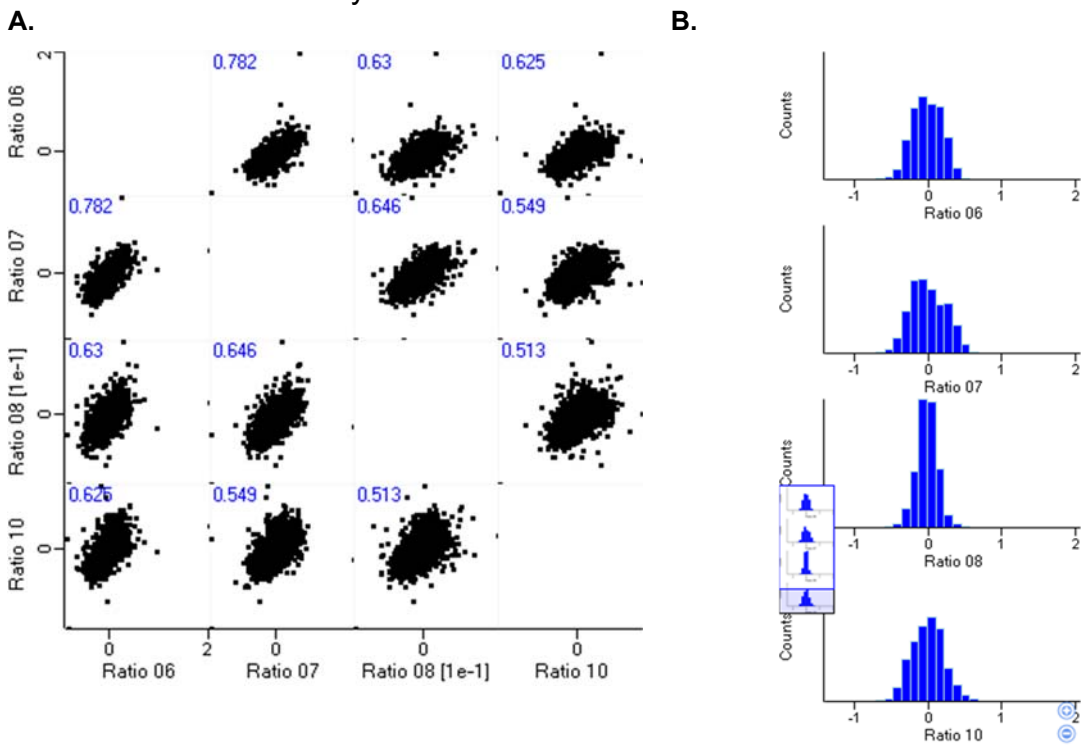

Figure 36 – Scatter plots showing Pearson correlation coefficients (A) and Histogram (B) of the H/L log_2 transformed ratios corresponding to CYN stimulation for 6 hrs. The displayed data shows the replicates selected for statistical analysis.

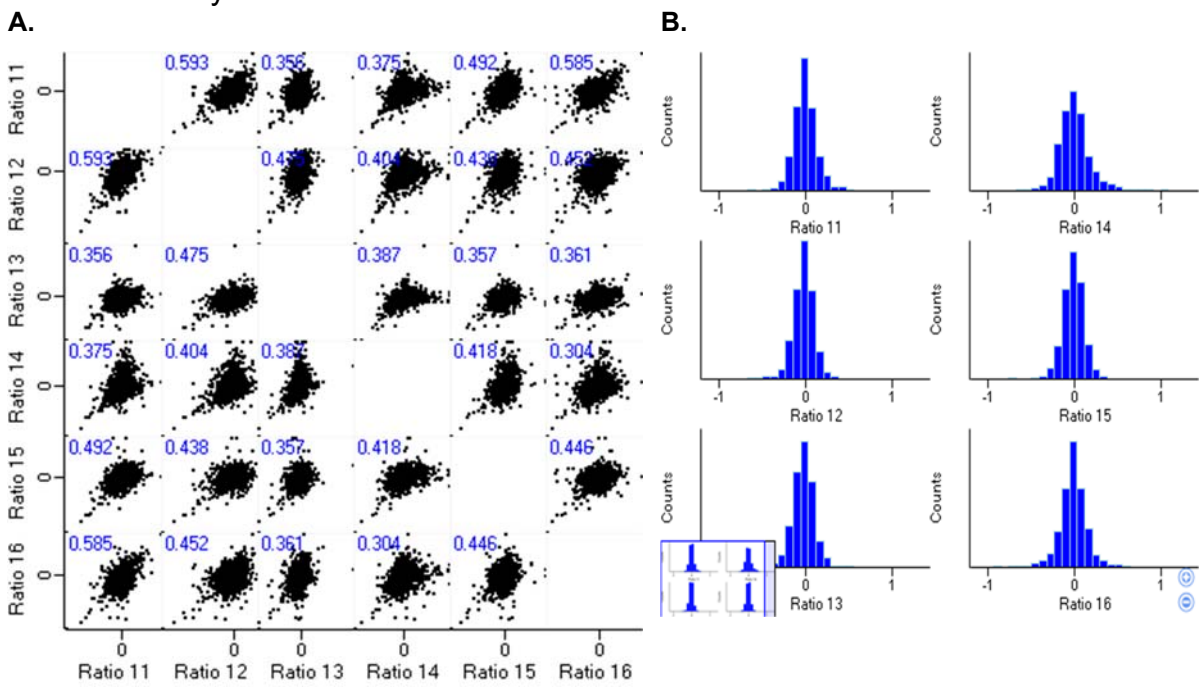

Figure 37 – Scatter plots showing Pearson correlation coefficients (A) and Histogram (B) of the H/L log_2 transformed ratios corresponding to CYN stimulation for 12 hrs. The displayed data shows the replicates selected for statistical analysis.

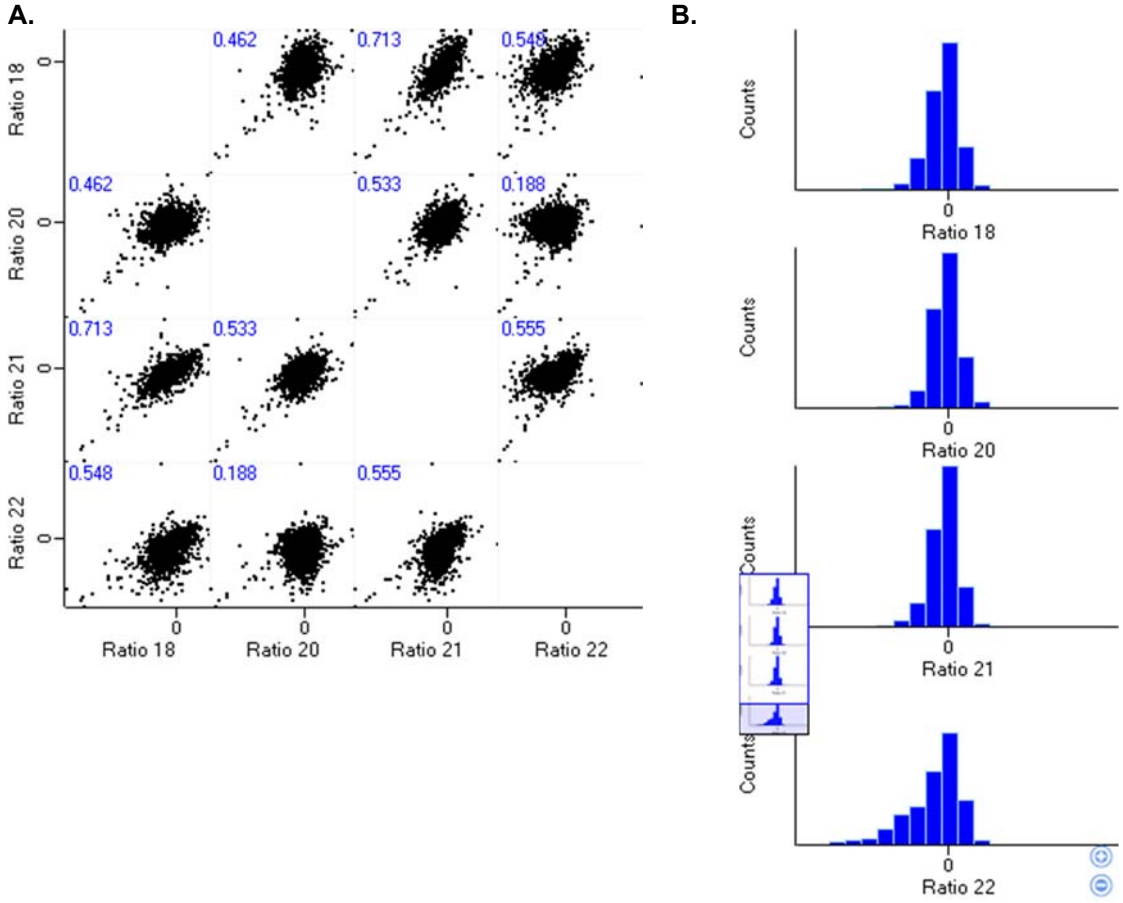

As seen on the scatter plots (figs. 35 – 37) some of the replicates have low correlation within the groups. Figure 37-B shows a skewed distribution for some of the replicates. On the other hand, Figure 38 shows a good correlation of the replicates within the 24 hrs group.

Simple normalization protocols were implemented on the data shown on figures 35 – 37. Z-score normalization on the separate H and L intensities, mean substraction and median substraction of the log_2 ratios were some of the tested strategies. No improvement on the Pearson correlation coeficient was observed after the normalizations. On a parallel experiment the same original cell samples were processed according to the SDC protocol (section 4.4.3), by mixing 25 µg of H with 25 µg of the respective L lysate for each replicate. Tryptic digests were fractioned according to section 4.5.2. After fractionation, nano LC-MS^2 analysis and data processing we found that the 0 hrs, 6 hrs, 12 hrs and 24 hrs had similar H/L ratio distributions (as seen on figures 35 – 38). In conclusion, a change in the sample processing did not improve the quality of the data.

Figure 38 – Scatter plots showing Pearson correlation coefficients (A) and Histogram (B) of the H/L log_2 transformed ratios corresponding to CYN stimulation for 24 hrs. The displayed data shows the replicates selected for statistical analysis.

A.

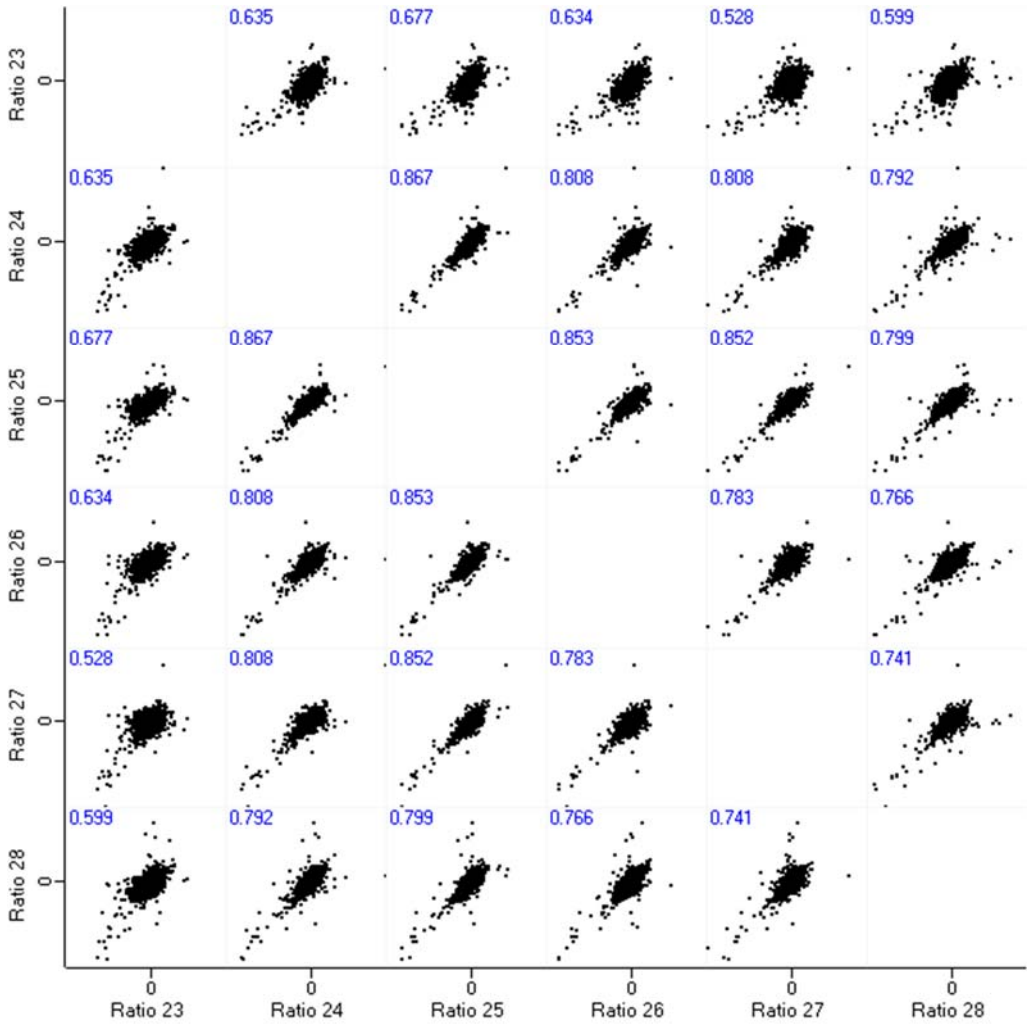

B.

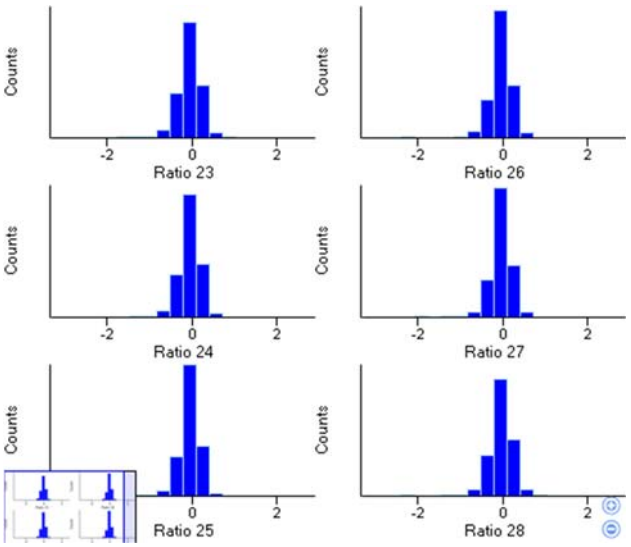

Figure 39 - Tukey`s (A.) and minimum to maximum (B) boxplots of the H/L log_2 transformed ratios* of all the biological replicates selected for further statistical analyses.

A.

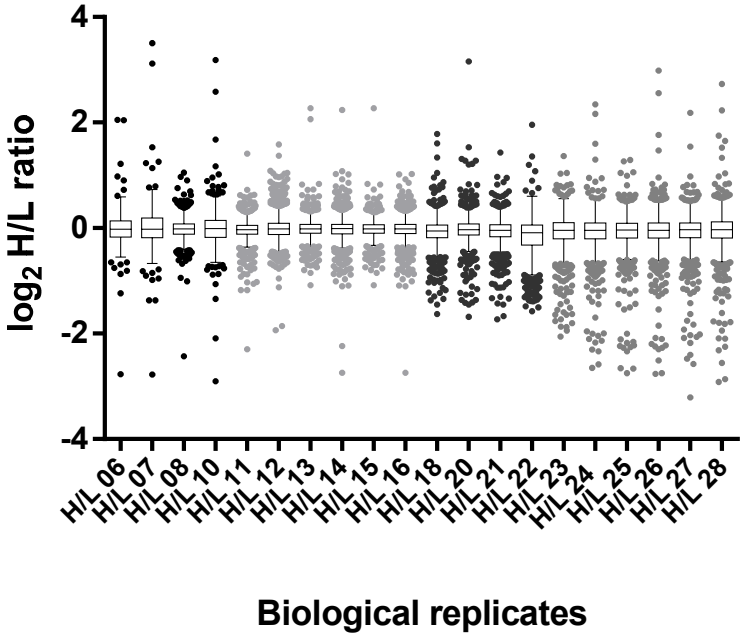

B.

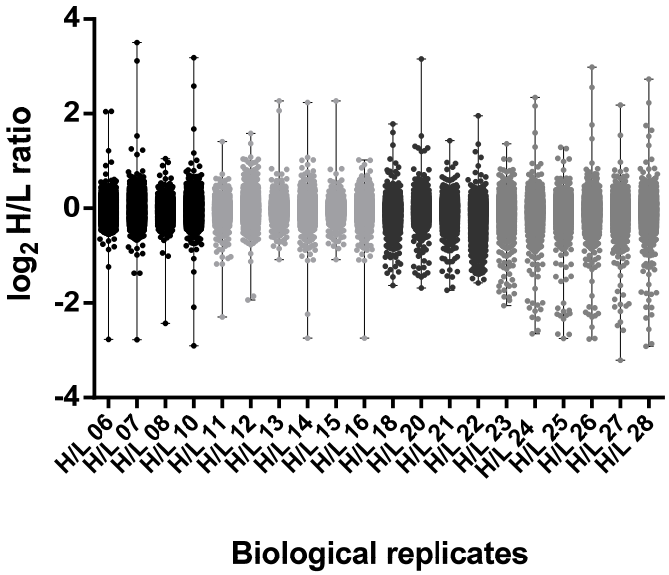

* Ratios H/L: 06 - 10 (0 hrs), 11 – 16 (6hrs), 18 – 22 (12 hrs), 23 – 28 (24 hrs).

Figure 40 - Two dimensional PCA plot of the whole experiment, using all the biological replicates selected for further statistical analyses. Ellipses and shapes show clustering of the samples (dots).

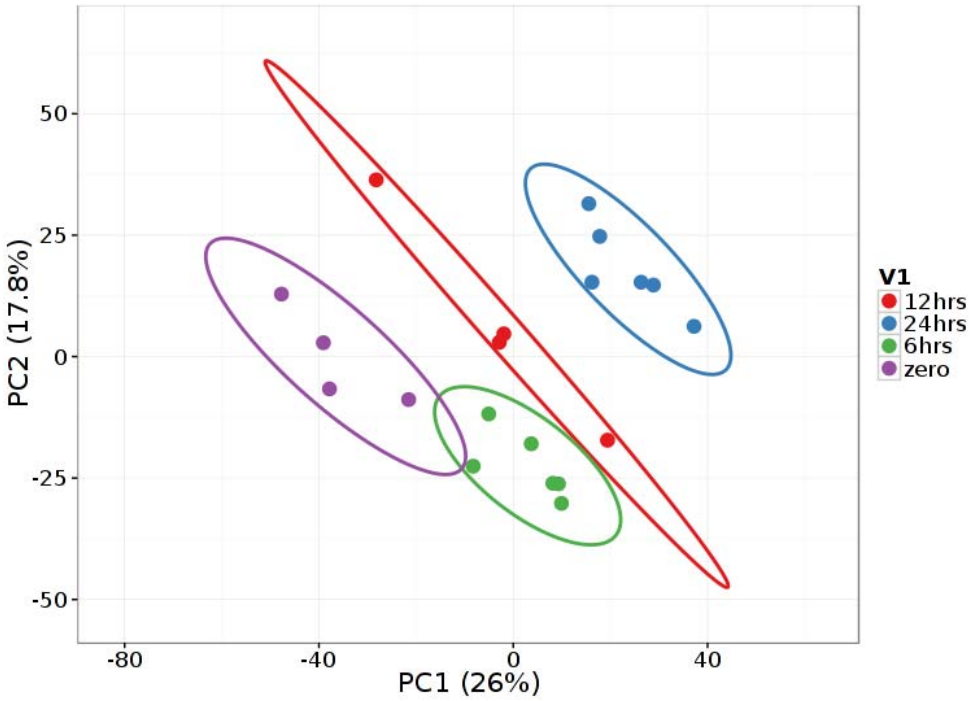

Figures 39 – 45 display more information on the distribution of the data set and on the quality of the acquired MS spectra.

Figure 41 - Summary of protein identification at time zero: (A) General proteome counts, (B) specific identification of proteins and modification sites in all replicates, (C) distribution of unique peptide counts and (D) distribution of all peptide counts.

A.

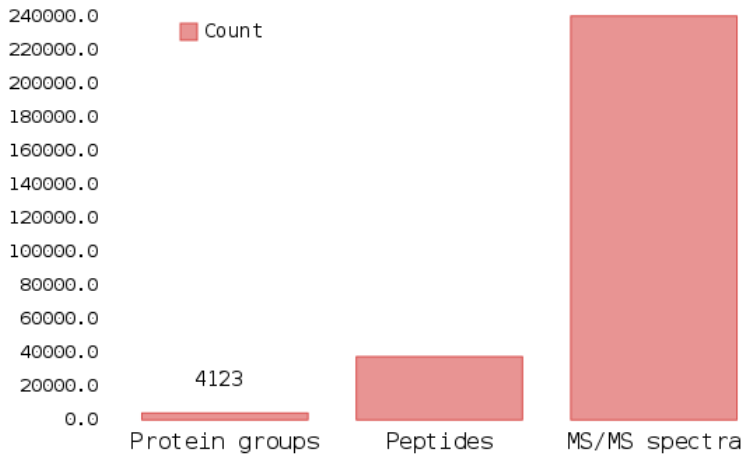

B.

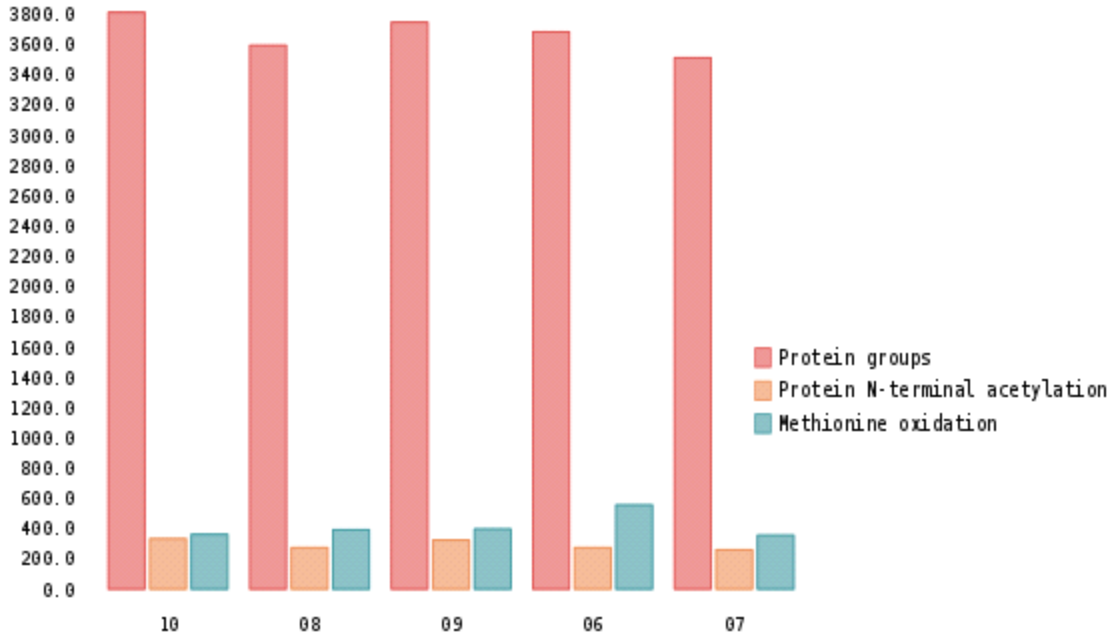

C.

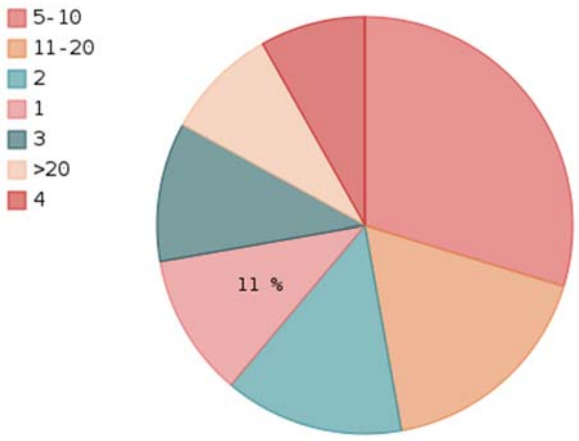

D.

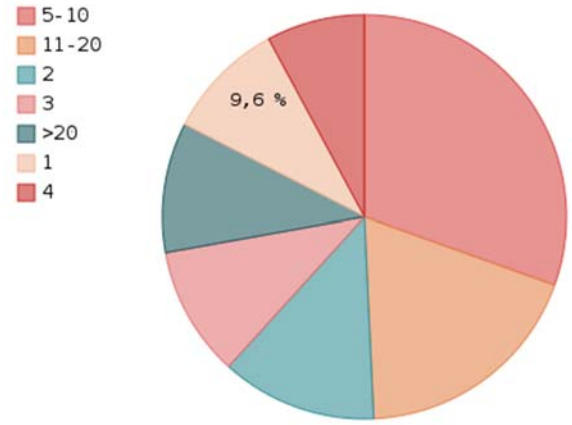

Figure 42 - Summary of protein identification after 6 hrs treatment with CYN: (A) General proteome counts, (B) specific identification of proteins and modification sites in all replicates, (C) distribution of unique peptide counts and (D) distribution of all peptide counts.

A.

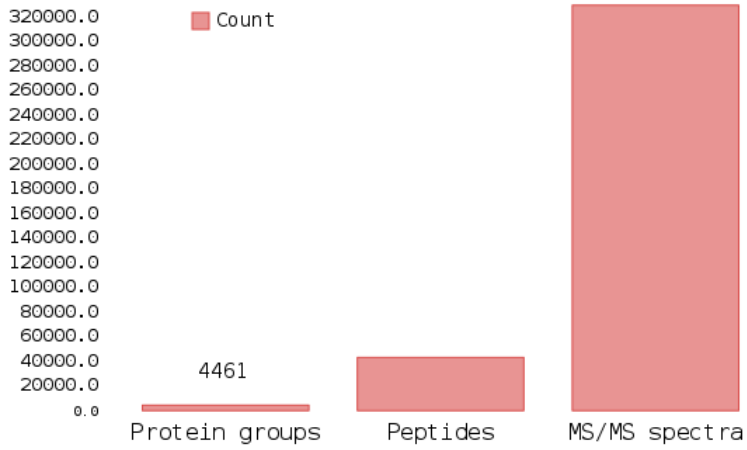

B.

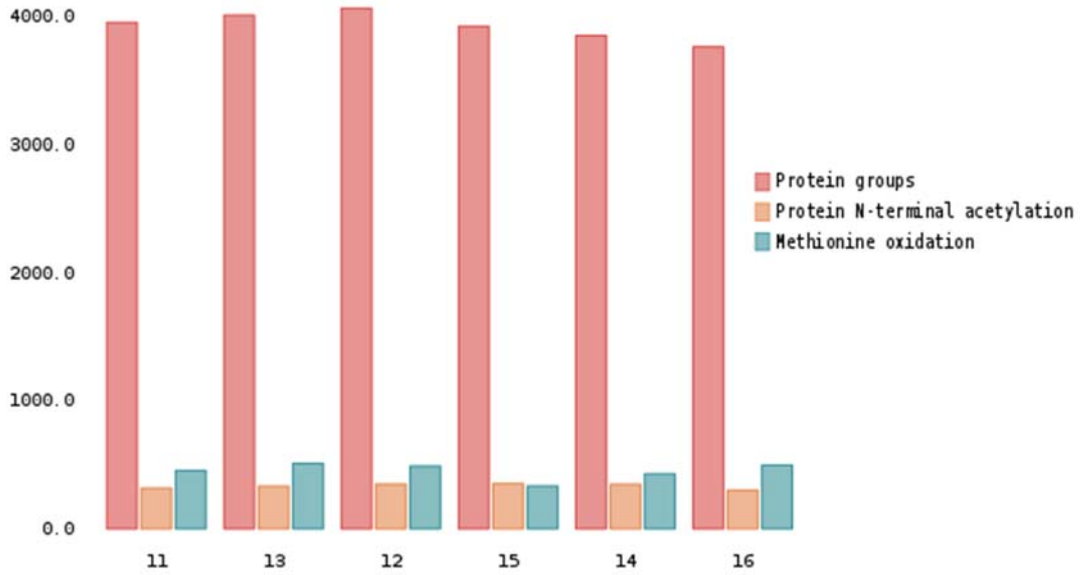

C.

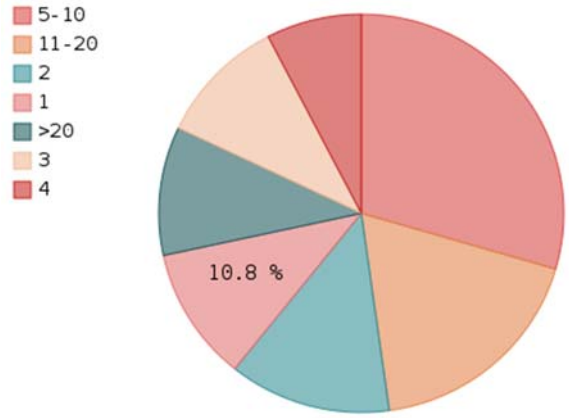

D.

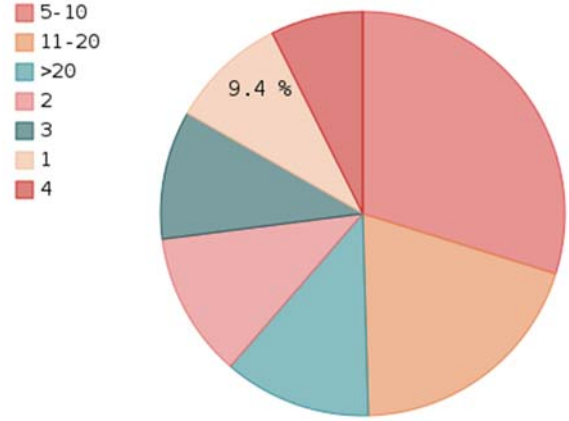

Figure 43 - Summary of protein identification after 12 hrs treatment with CYN: (A) General proteome counts, (B) specific identification of proteins and modification sites in all replicates, (C) distribution of unique peptide counts and (D) distribution of all peptide counts.

A.

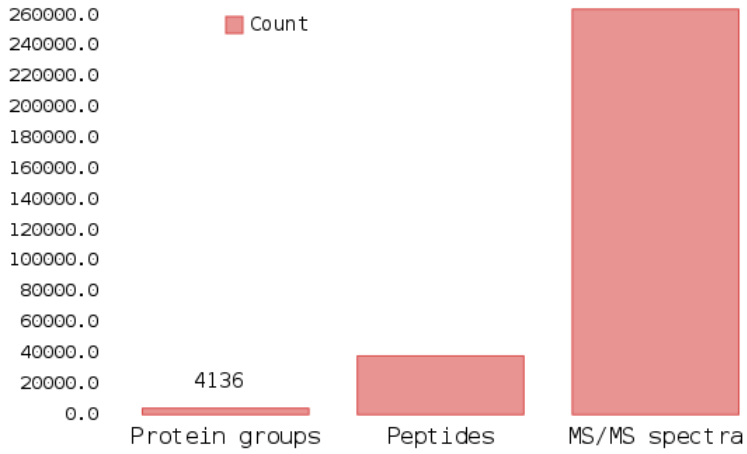

B.

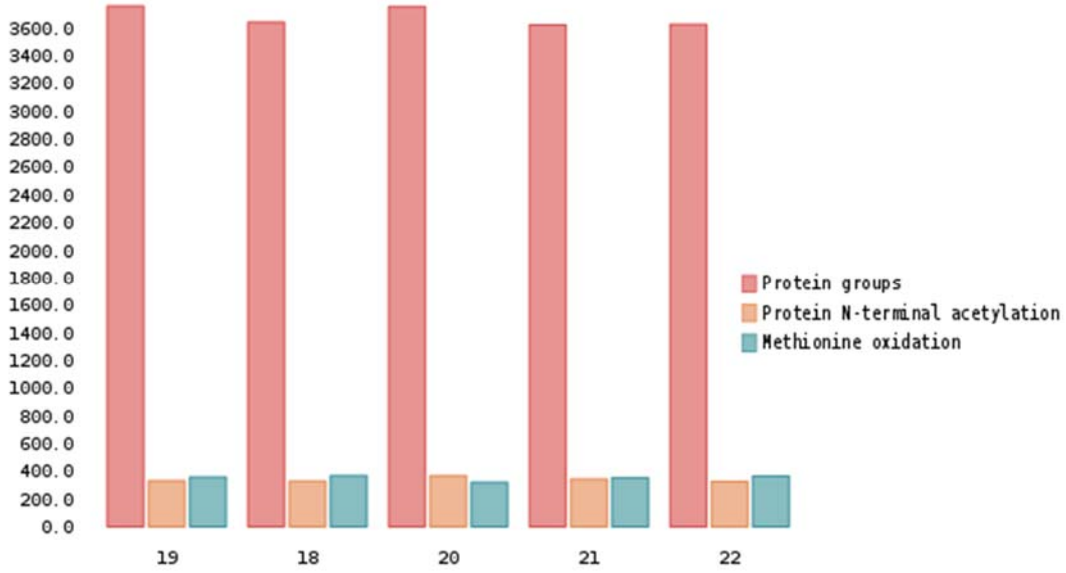

C.

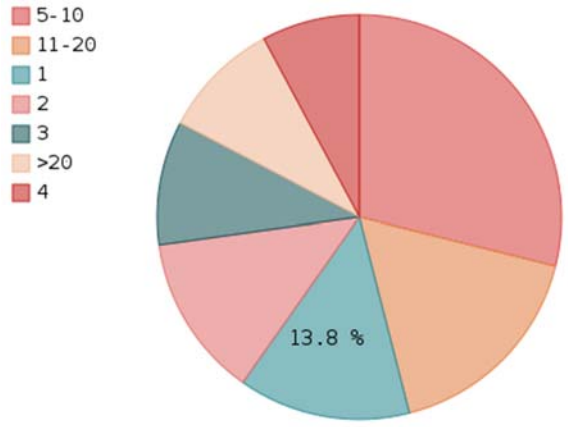

D.

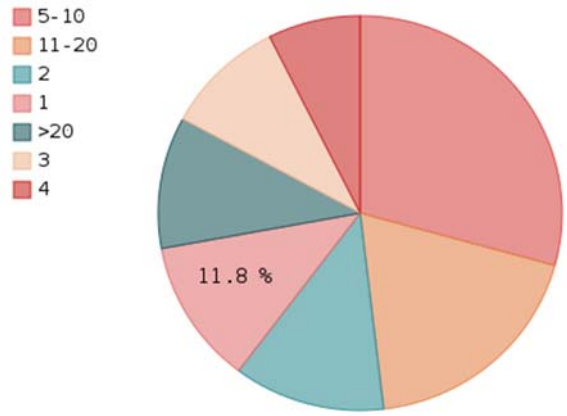

Figure 44 - Summary of protein identification after 24 hrs treatment with CYN: (A) General proteome counts, (B) specific identification of proteins and modification sites in all replicates, (C) distribution of unique peptide counts and (D) distribution of all peptide counts.

A.

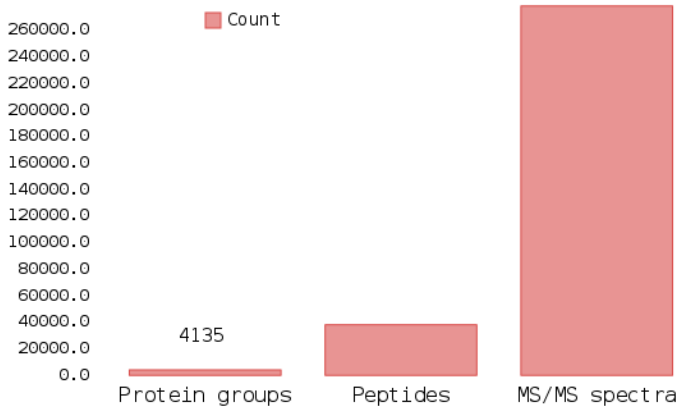

B.

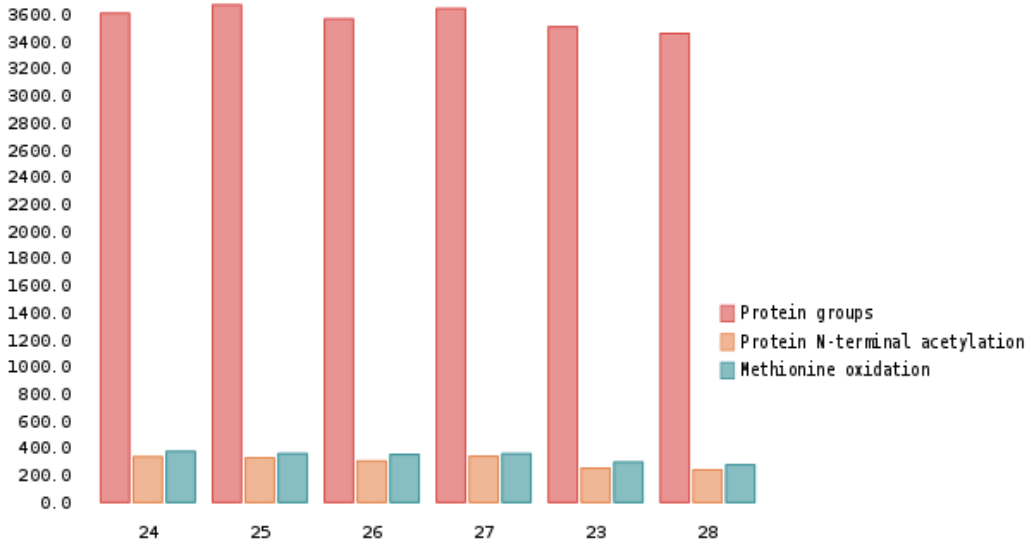

C.

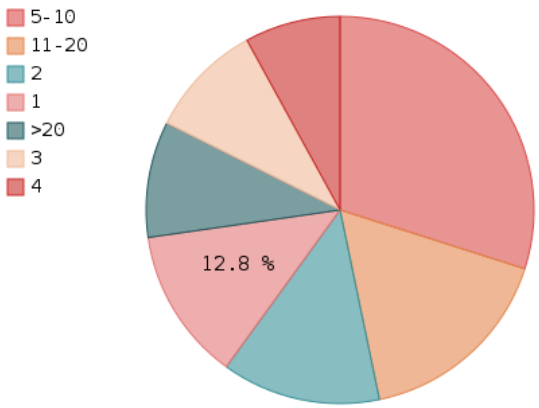

D.

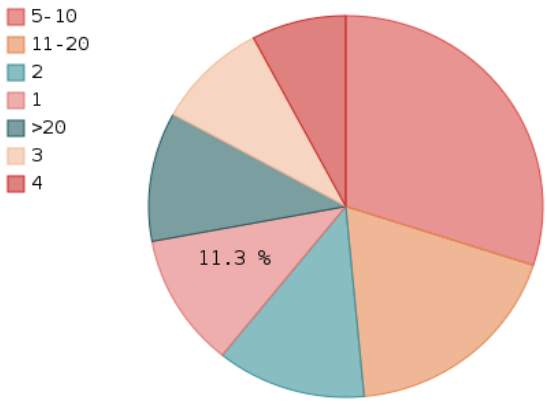

Figure 45 - Venn diagram showing overlap of the total proteins for each time point of the experiment.

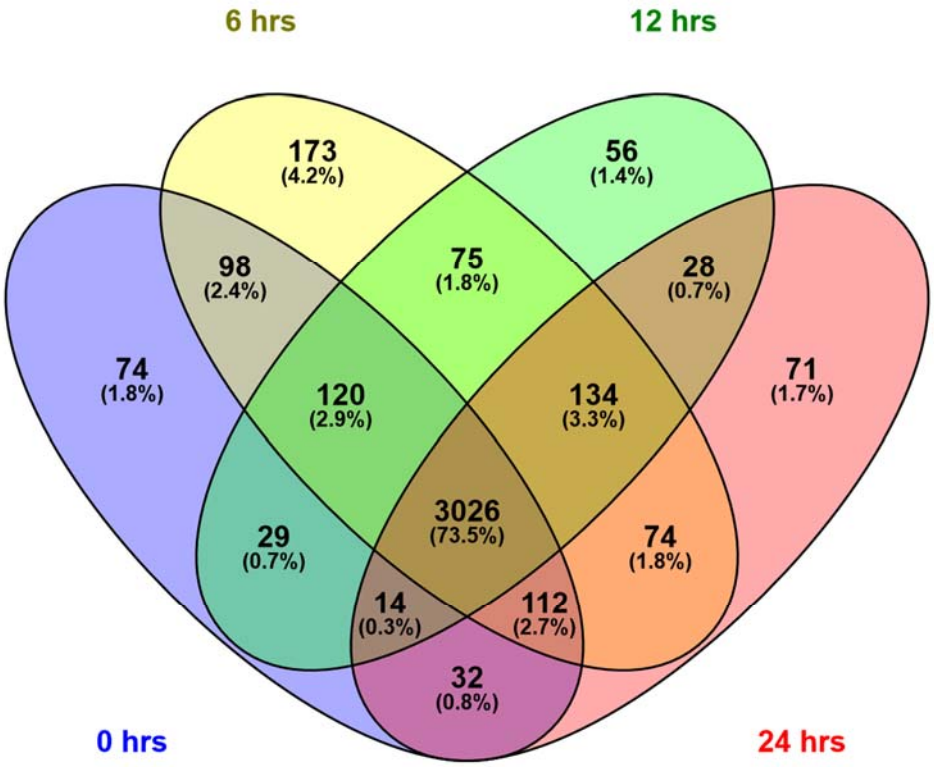

5.4.2 Gene ontologies, processes and metabolic network enrichments

Using the Perseus software (v1.5.5.3) we filtered 2181 quantifiable proteins through the replicates at time zero, 2355 proteins at 6 hrs, 2246 at 12 hrs and 1973 at 24 hrs.

We considered proteins as significantly regulated when their p-values from the One sample t-test scored below 0.05 (or 0.75 for the 12 hrs timepoint). A full list of the regulated proteins for all the timepoints is available in Annex 3.

In greater detail, we used the two-tailed one sample T-test to compare replicates and find outliers within groups; the groups being 6, 12 and 24 hrs treatment with the toxin. Values were $\log_2$ transformed and all p-values below 0,05 were considered significant, adjusting the false discovery rate (FDR) using the Benjamini-Hochberg correction. The test showed a total of 148 and 738 significantly regulated proteins at 6

and 24 hrs respectively. The 12 hr replicates were reanalyzed and p-values below 0,075 were considered significant for the T-test. Figure 46 shows a summary of these results.

Figure 46 - Data display and summary of significant proteins according to the one sample T-test*: Figures show a volcano plot showing regulated proteins after 6 (A), 12 (B) and 24 hrs (C) treatment with CYN. (D) Total numbers of up-regulated (blue) and down-regulated (orange) proteins at each time point.

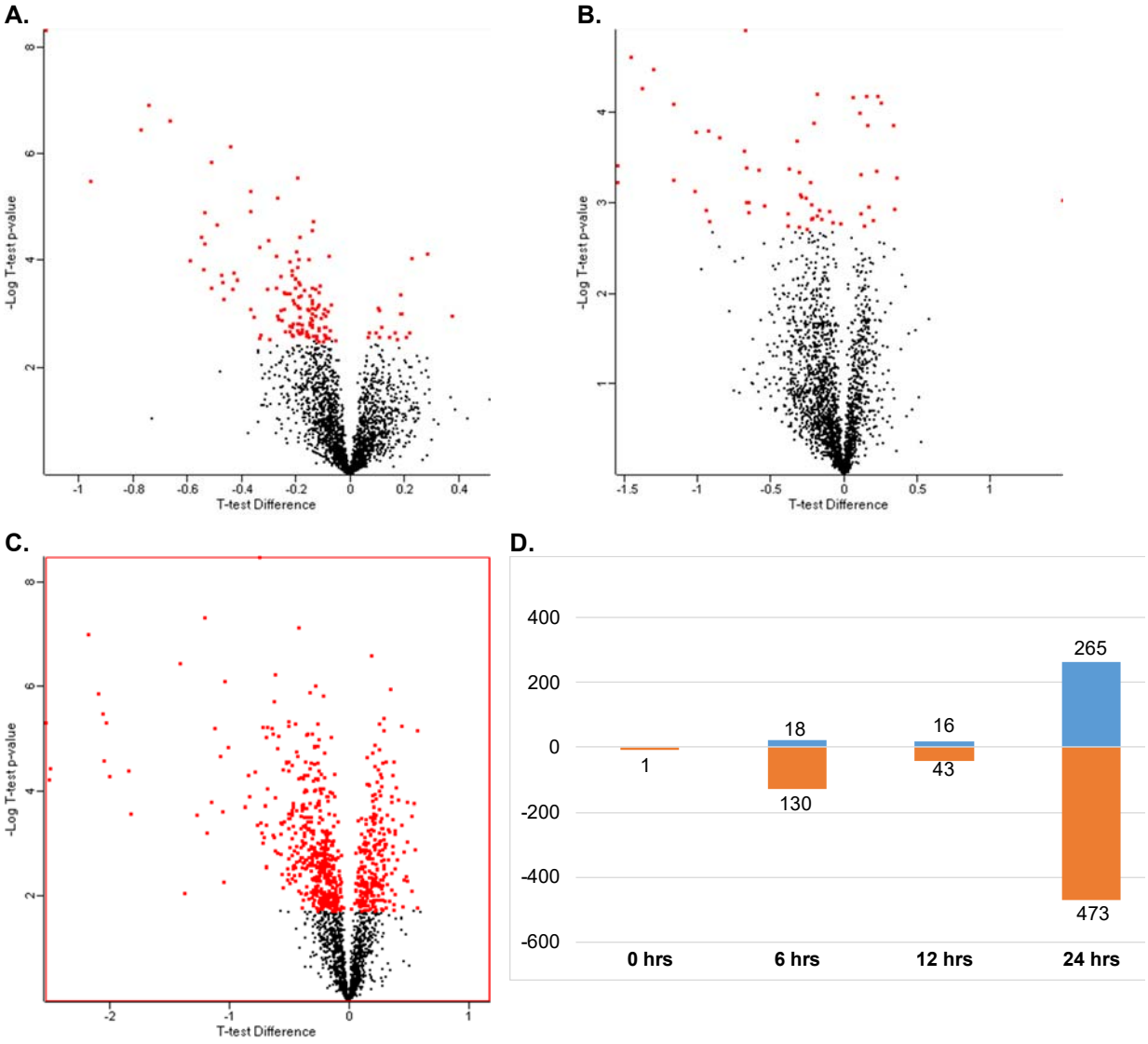

*Red dots show proteins with adjusted p-values less than 0.05 (Benjamini-Hochberg FDR).

The full proteinGrups and other combined data by Maxquant is annexed to this thesis. Also the enriched canonical pathway data of the significant proteins for every time point (exported from Ingenuity Pathway Analisys) is available as an annex.

5.4.2.1 Down-regulated proteins

Figure 47 - Reactome pathway enrichment overview using all down-regulated proteins after 6 (A) 12 (B) and 24 hrs (C) treatment with CYN. Dark grey lines shows relevant pathways.

A.

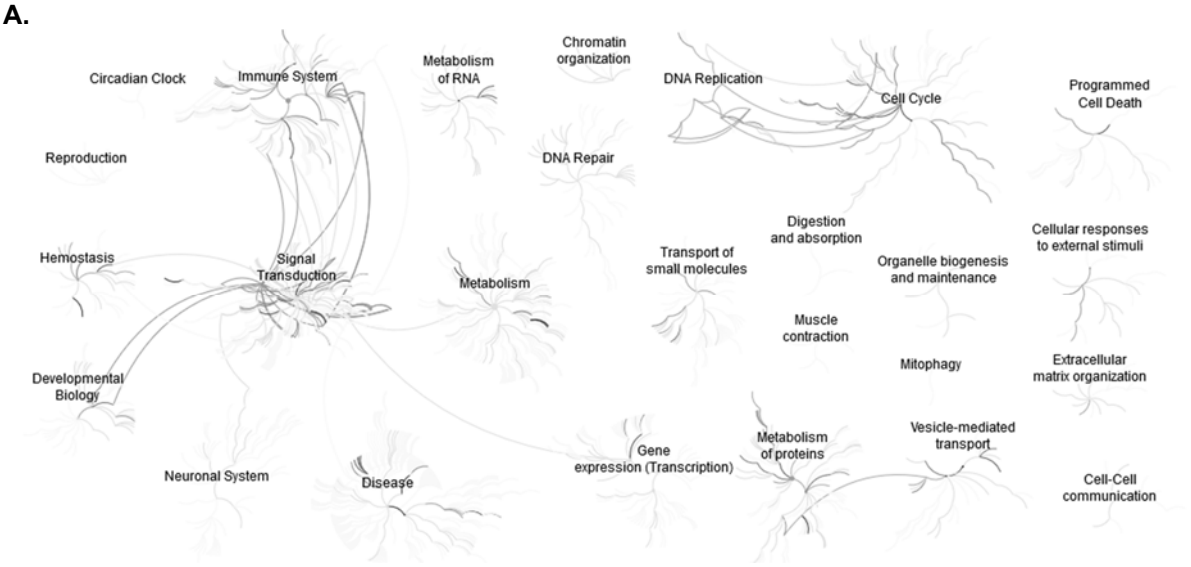

B.

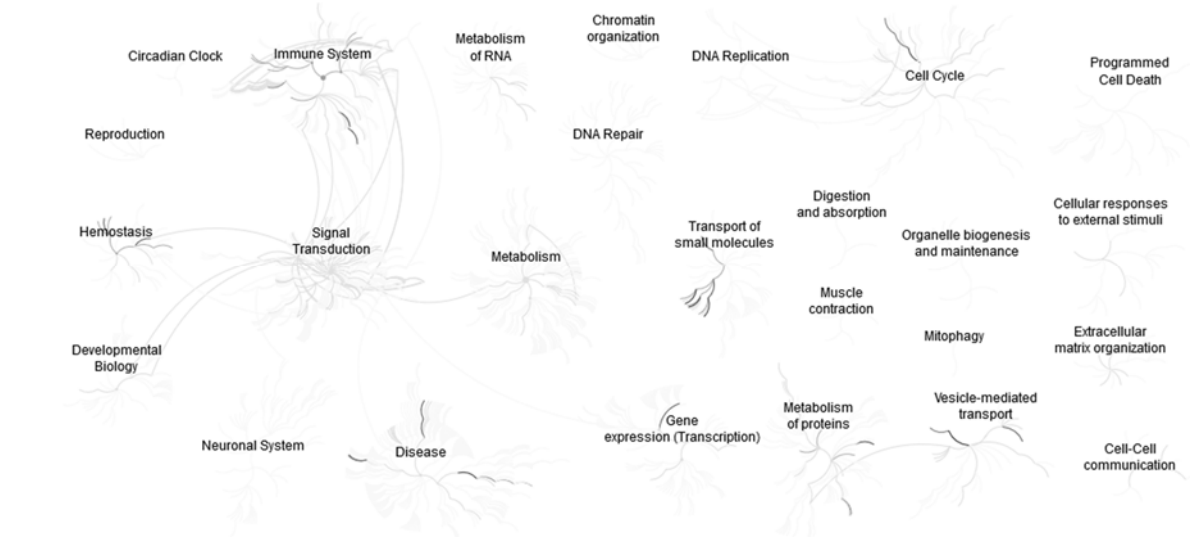

C.

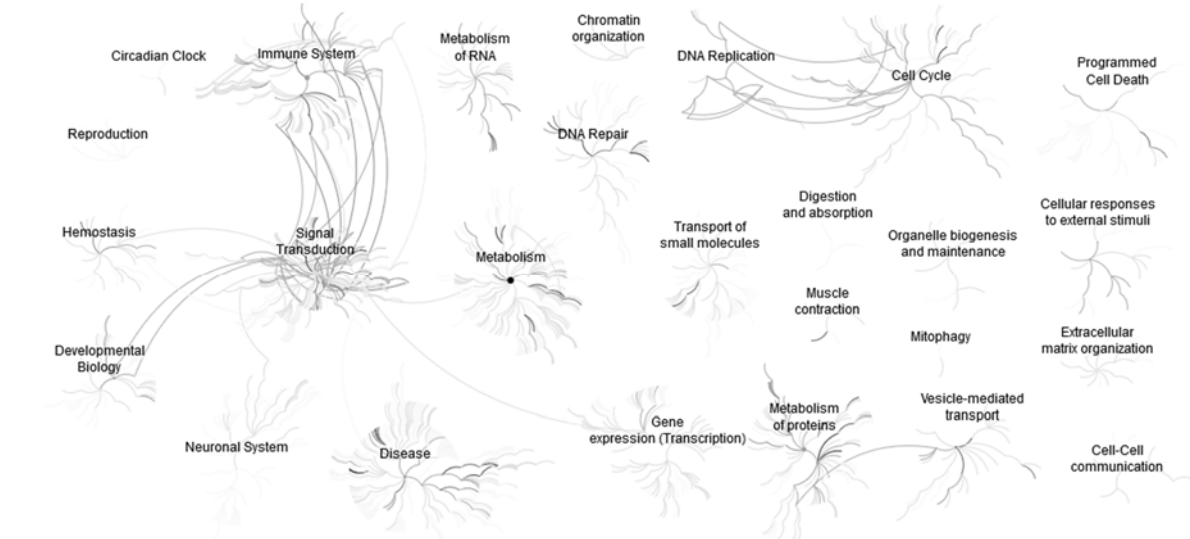

Figure 48 - Bar charts for all unambiguously enriched down-regulated proteins after 6 and 24 hrs treatment with CYN. The charts show absolute number of proteins belonging to the major cathegories of GO biological processes (A), cellular component (B) and molecular function (C).

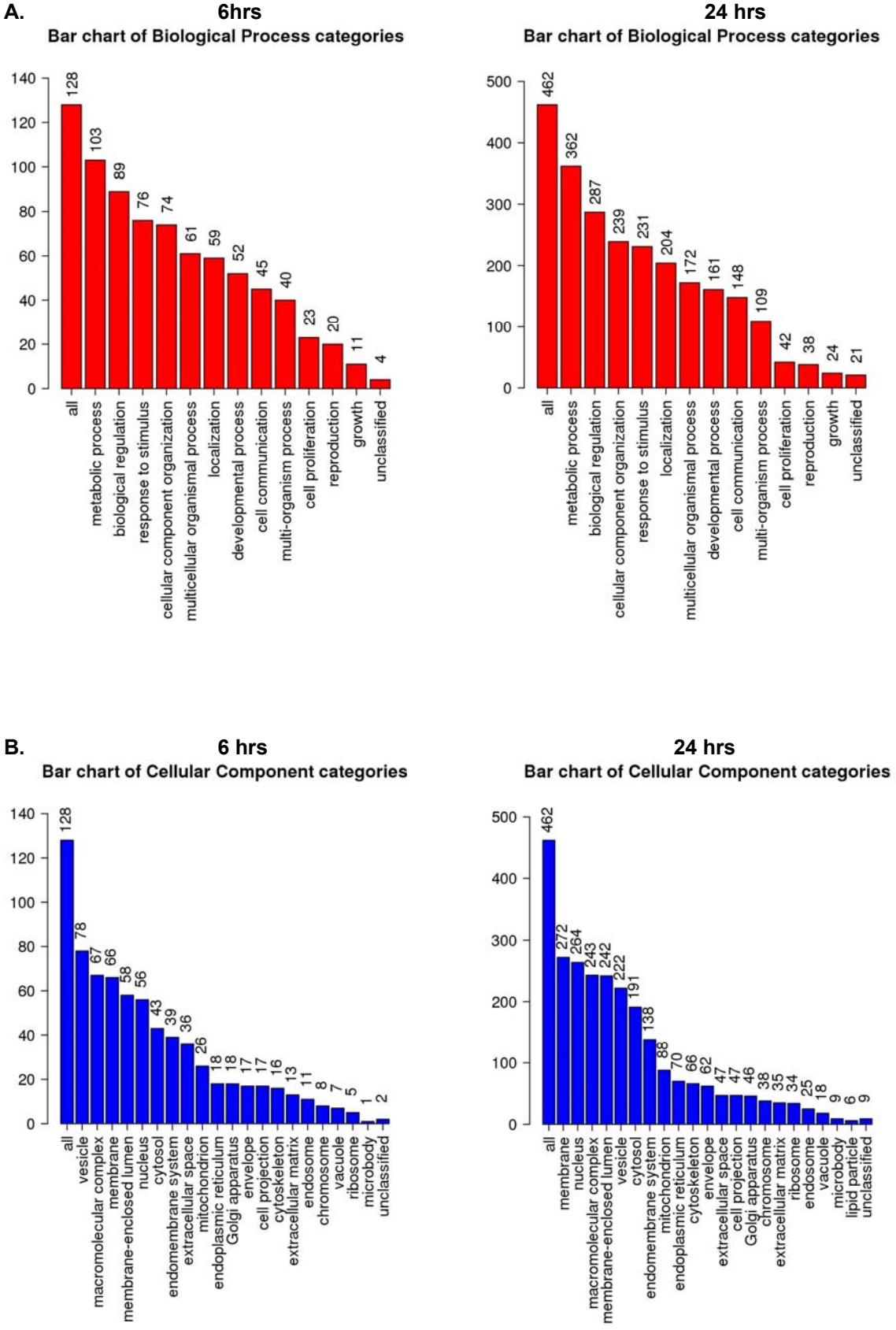

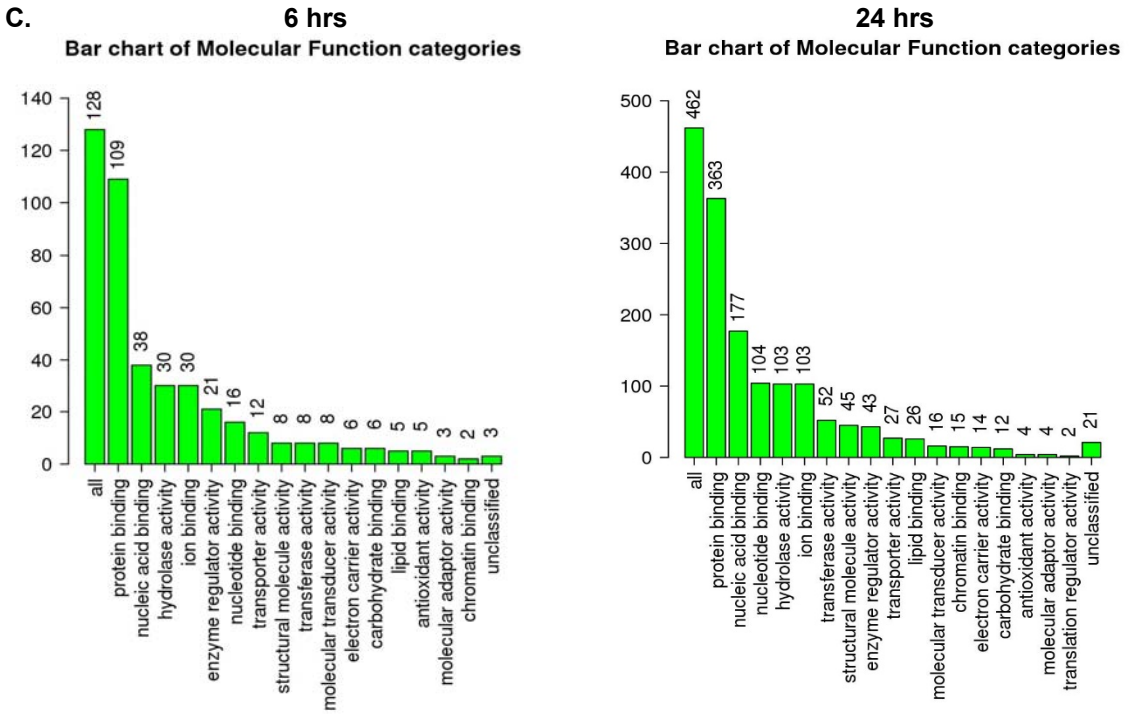

Figures 47 – 50 show results of enrichments using as input only downregulated proteins. Gene ontology enrichment is useful to give a first glance at the data as a whole (Fig. 48). The Reactome pathway enrichment overview is also an important tool to watch global connections between regulated processes and to take a quick look at the toxicodynamics in our model (Fig. 47). More specific enrichments generated by Ingenuity® Pathway Analysis software (fig. 49 – 50) are presented for a comprehensive analysis of the relevant pathways involved in the toxin-proteome interaction.

Figure 49 - Ingenuity® canonical pathway top 25 heat map report. The comparison ranked the enriched networks based on a score, using as input all down-regulated proteins after 6, and 24 hrs treatment with CYN.

Figure 50 - Ingenuity® toxicity lists top 10 report. The comparison ranked the enriched networks using as input all down-regulated proteins after 6, 12 and 24 hrs treatment with CYN.

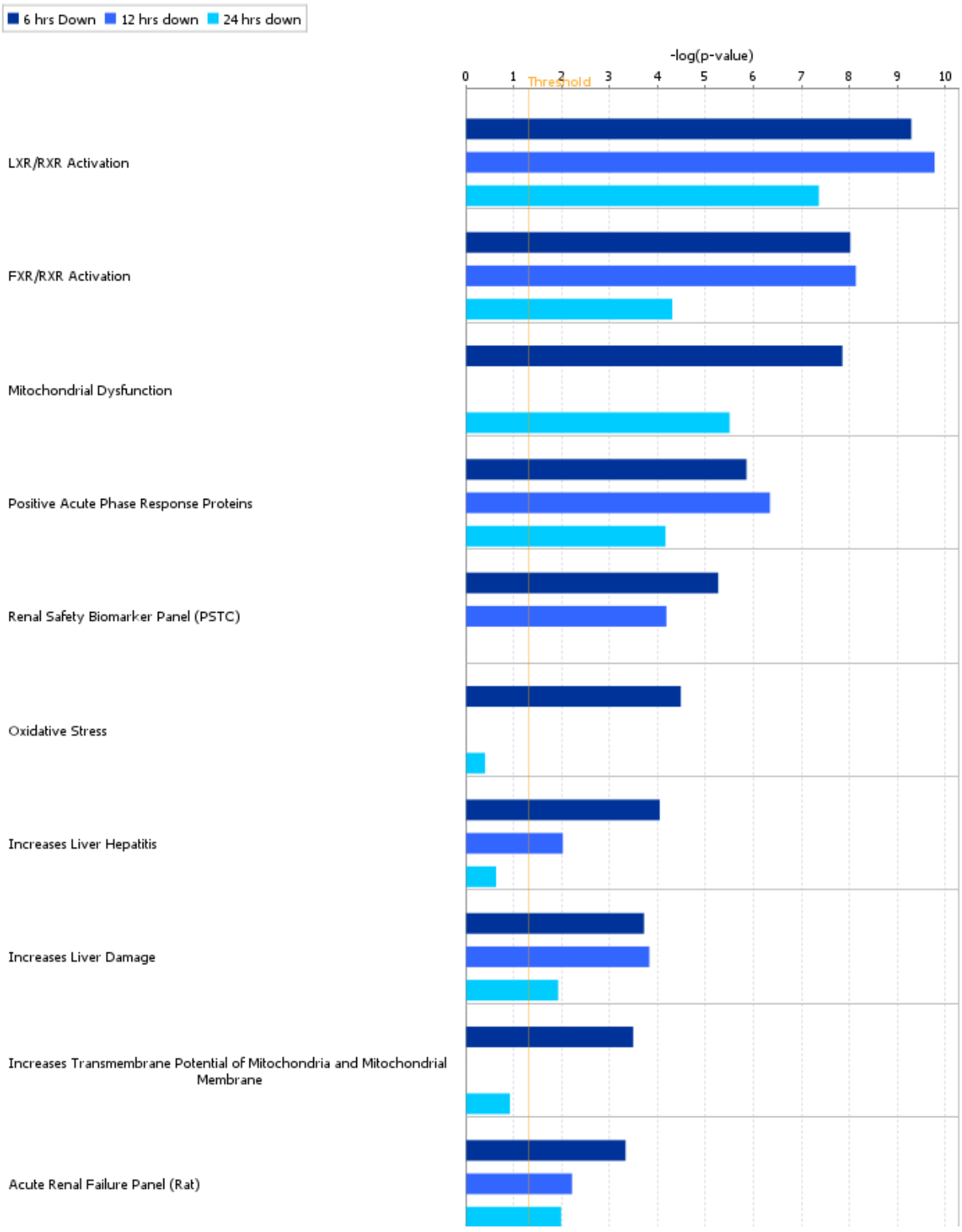

5.4.2.2 Up-regulated proteins

Figures 55 – 59 show results of enrichments using as input only upregulated proteins.

Figure 51 - Reactome pathway enrichment overview using all up-regulated proteins after 6 (A) 12 (B) and 24 hrs (C) treatment with CYN. Dark grey lines show relevant pathways.

A.

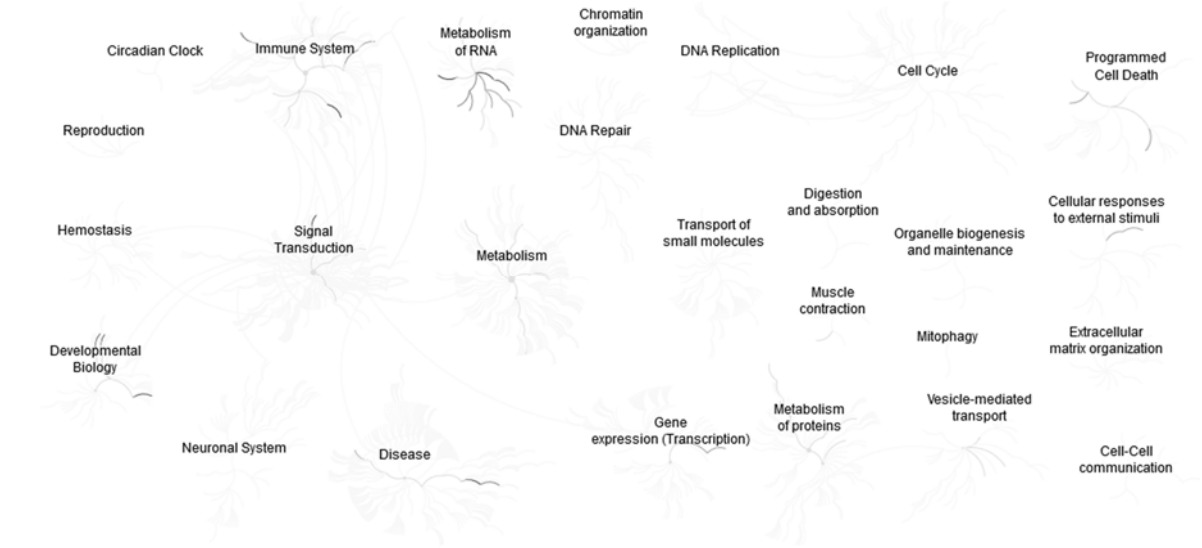

B.

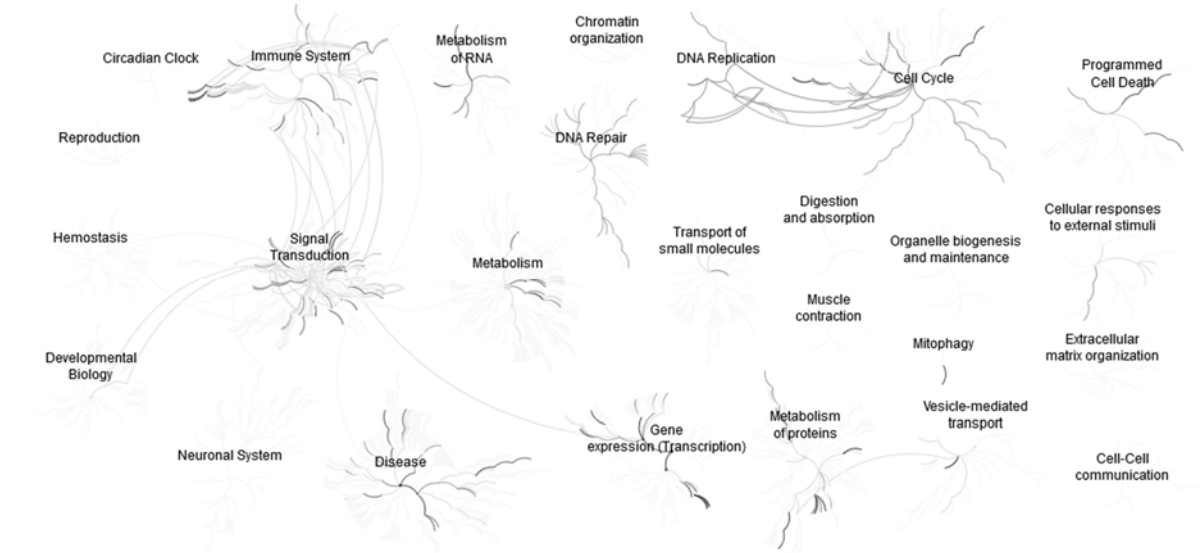

C.

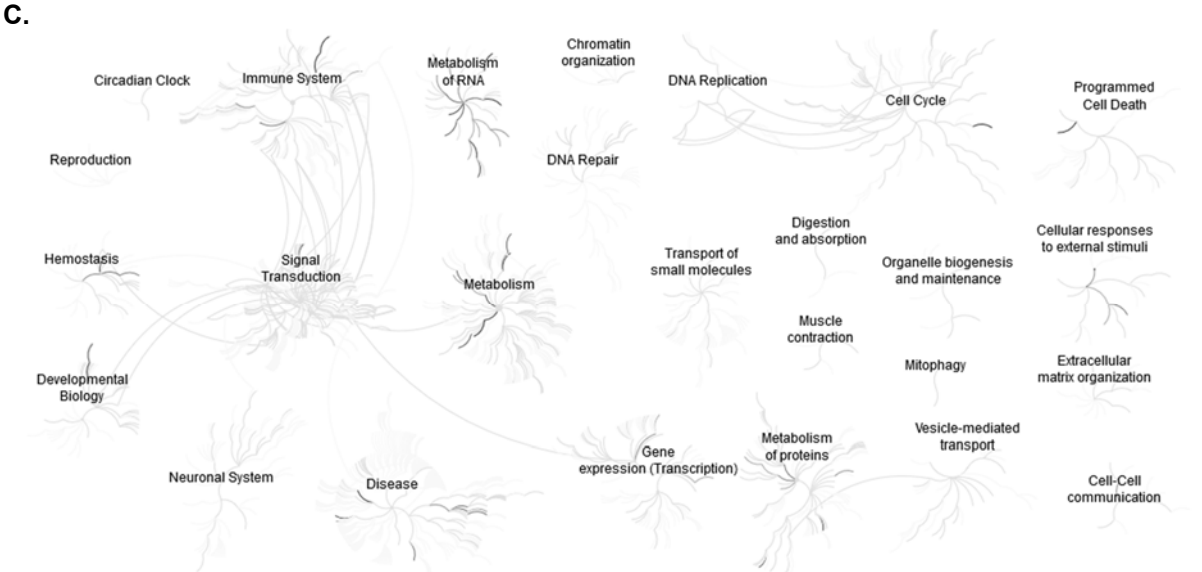

Figure 52 - Bar charts for all unambiguously enriched up-regulated proteins after 6 and 24 hrs treatment with CYN. The charts show absolute number of proteins belonging to the major cathegories of GO biological processes (A), cellular component (B) and molecular function (C).

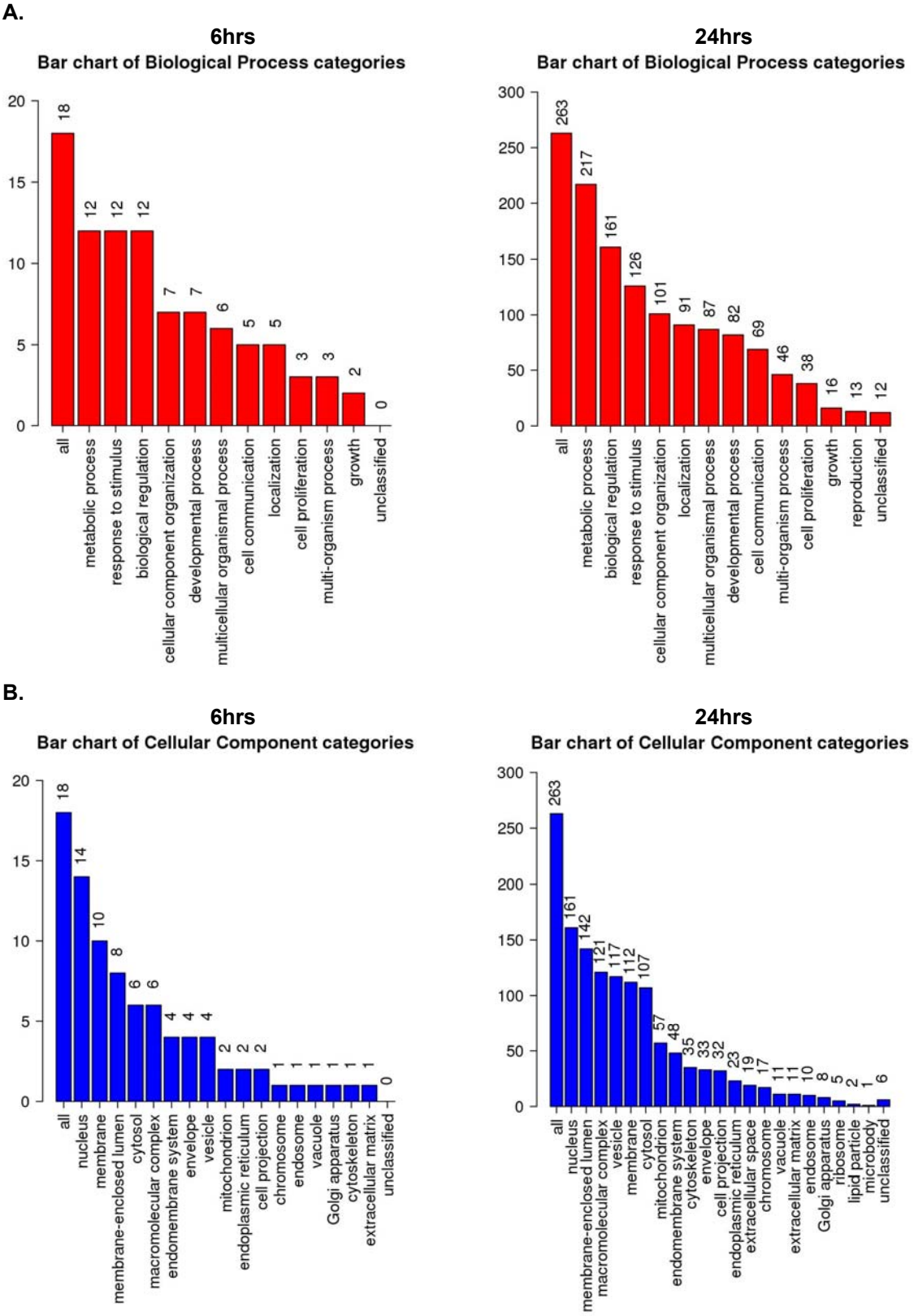

C.

6hrs

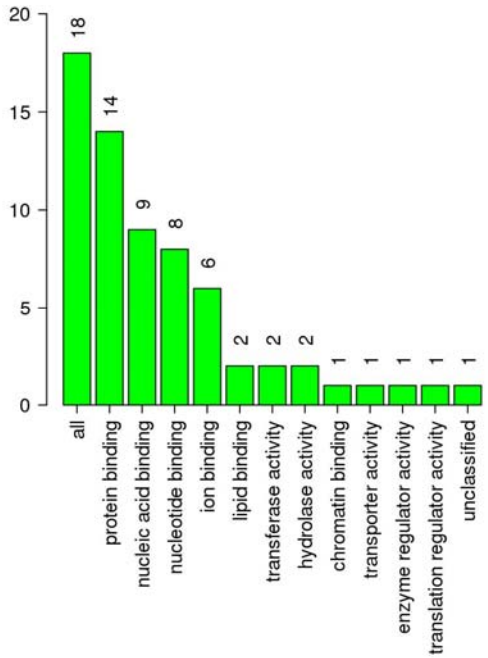
Bar chart of Molecular Function categories
20
15
10
5
0
18
14
9
8
6
2
2
2
1
1
1
1
1
all
protein binding
nucleic acid binding
nucleotide binding
ion binding
lipid binding
transferase activity
hydrolase activity
chromatin binding
transporter activity
enzyme regulator activity
translation regulator activity
unclassified

24hrs

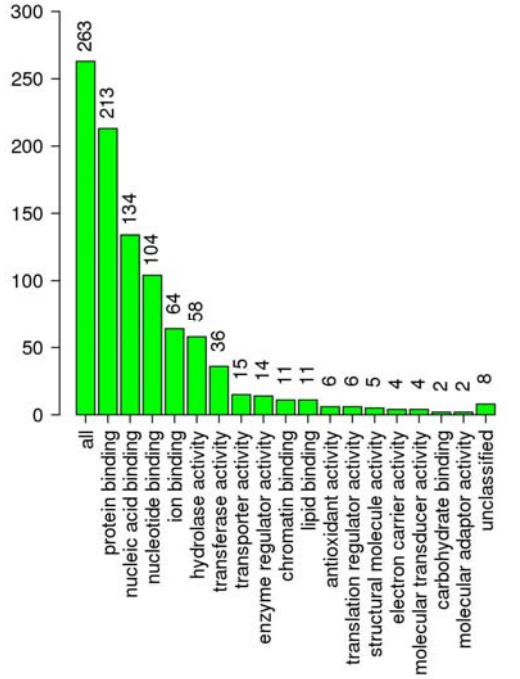
Bar chart of Molecular Function categories
300
250
200
150
100
50
0
263
213
134
104
64
58
36
15
14
11
11
6
6
5
4
4
2
2
8
all
protein binding
nucleic acid binding
nucleotide binding
ion binding
hydrolase activity
transferase activity
transporter activity
enzyme regulator activity
chromatin binding
lipid binding
antioxidant activity
translation regulator activity
structural molecule activity
electron carrier activity
molecular transducer activity
carbohydrate binding
molecular adaptor activity
unclassified

Figure 53 - Ingenuity® canonical pathway top 25 report. The comparison ranked the enriched networks using as input all up-regulated proteins after 6, 12 and 24 hrs treatment with CYN.

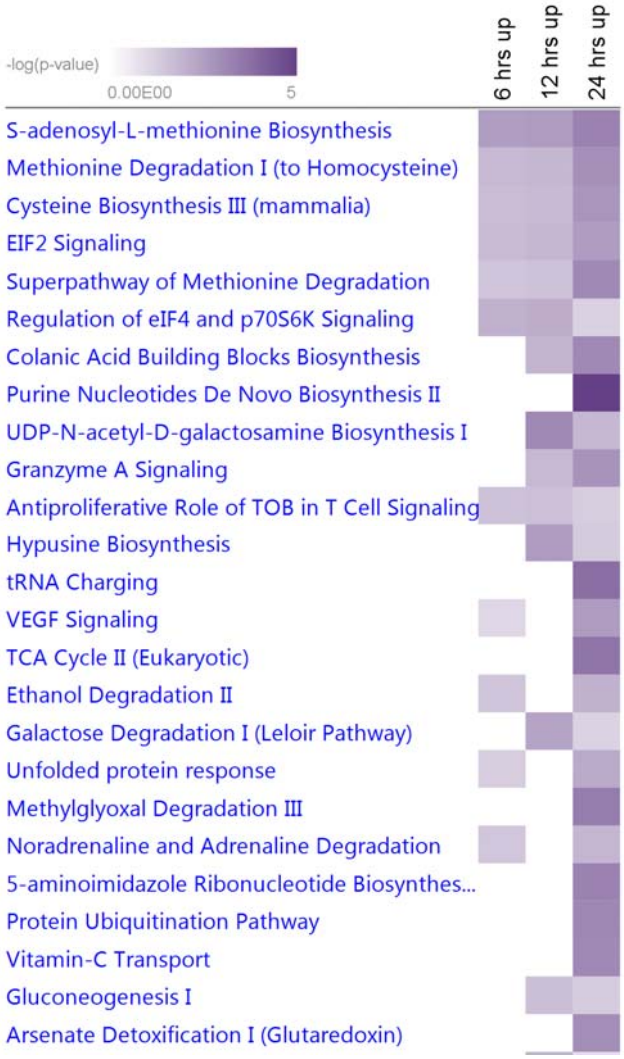

Figure 54 - Ingenuity® toxicity lists top 10 report. The comparison ranked the enriched networks using as input all up-regulated proteins after 6, and 24 hrs treatment with CYN

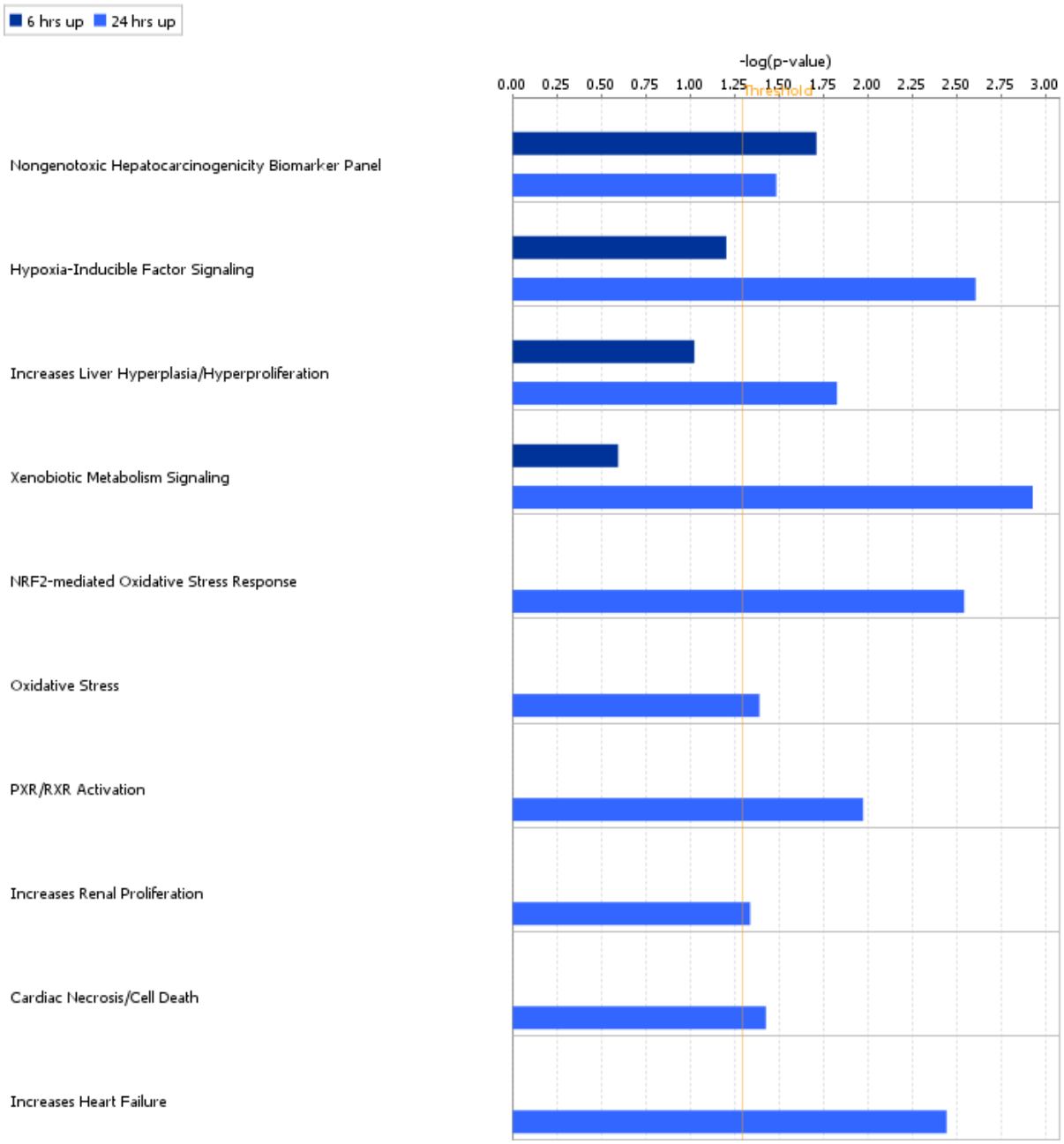

5.4.2.3 Overall results

Figures 55 – 59 show results of enrichments using as input downregulated and upregulated proteins.

Figure 55 - Ingenuity® canonical pathway top 15 report. The comparison ranked the enriched networks using as input all significant proteins after 6 hrs treatment with CYN.

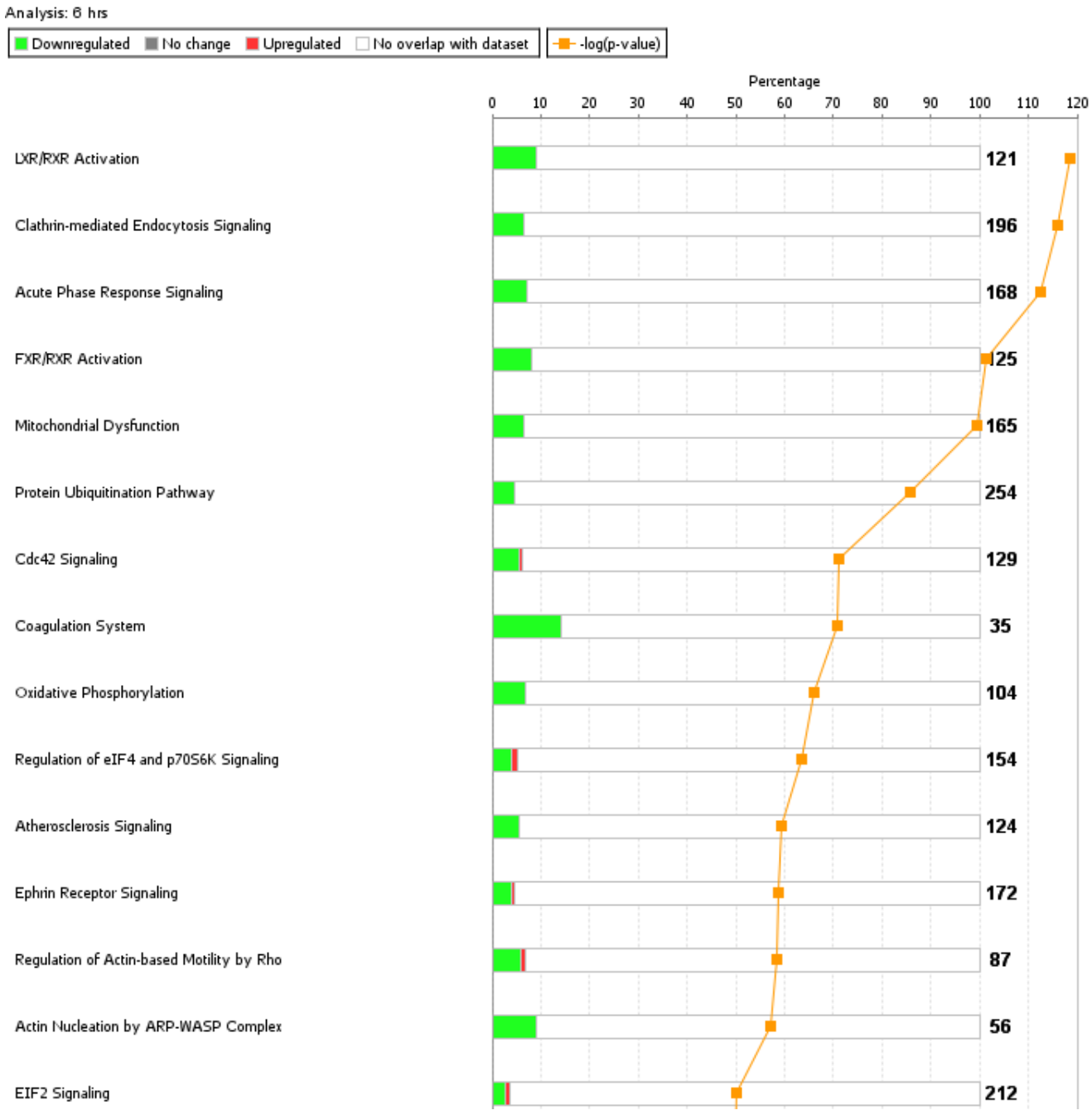

Figure 56 - Ingenuity® canonical pathway top 15 report. The comparison ranked the enriched networks using as input all significant proteins after 12 hrs treatment with CYN.

Figure 57 - Ingenuity® canonical pathway top 15 report. The comparison ranked the enriched networks using as input all significant proteins after 24 hrs treatment with CYN.

Figure 58 - Ingenuity® canonical pathway top 25 report. The comparison ranked the enriched networks using as input all significant proteins after 6, 12 and 24 hrs treatment with CYN.

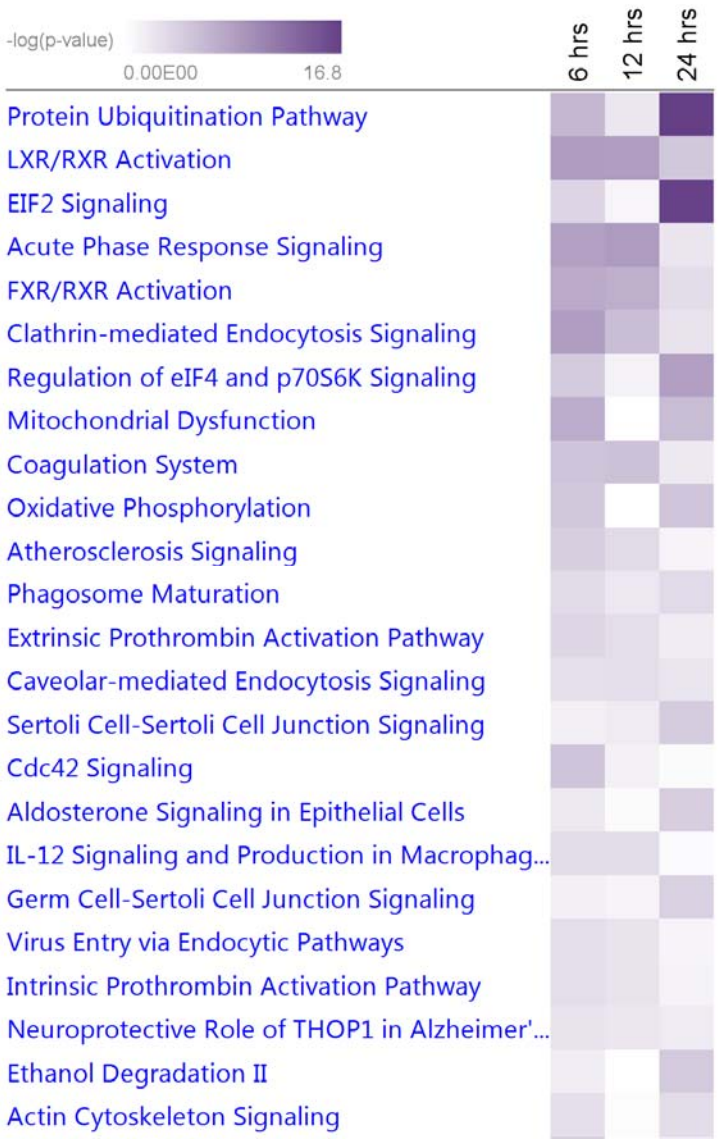

Figure 59 - Ingenuity® toxicity lists top 10 report. The comparison ranked the enriched networks using as input all significant proteins after 6, 12 and 24 hrs treatment with CYN.

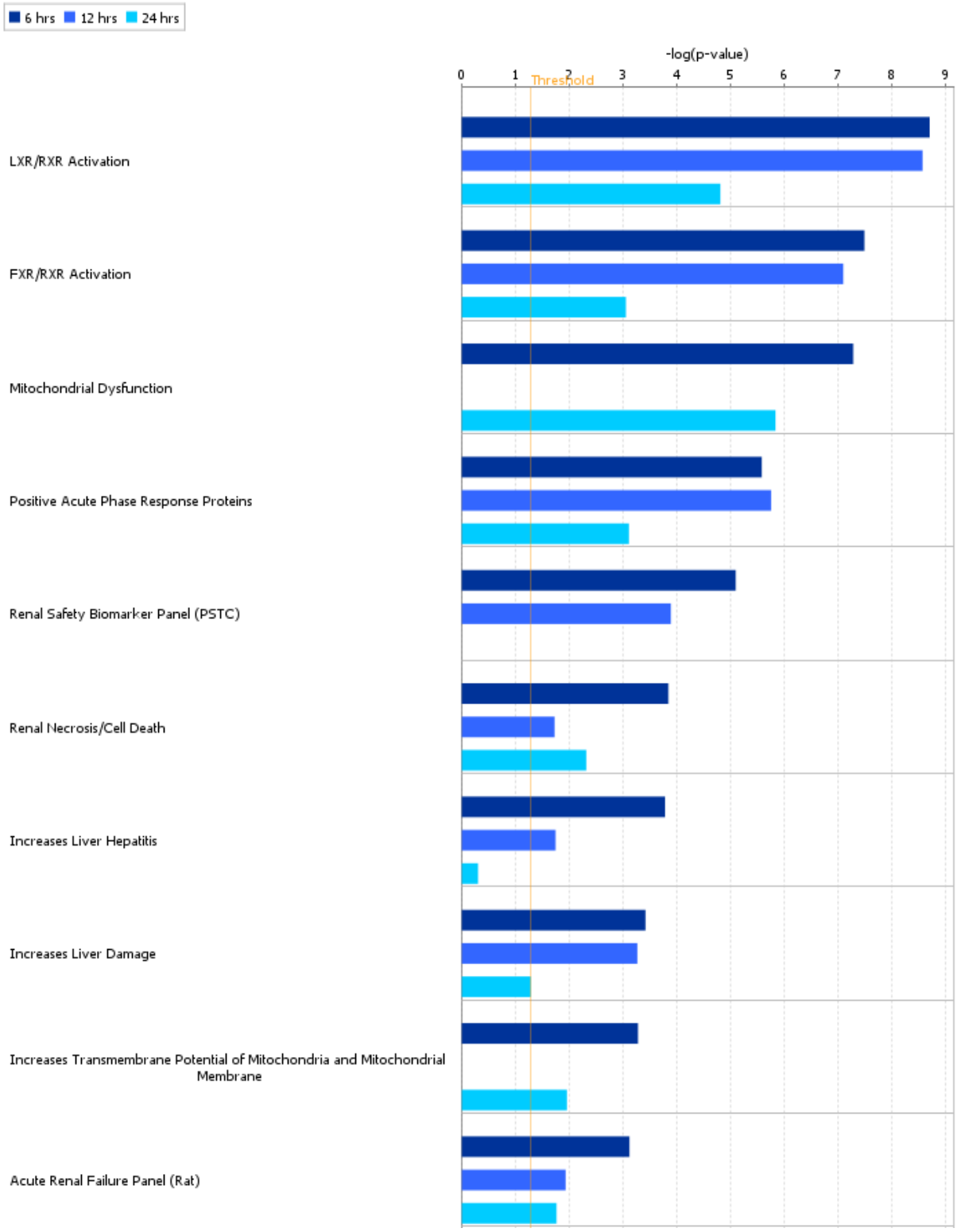

5.5 Validation of selected CYN-regulated proteins by WB

On the final steps of this project, we verified significant changes of selected regulated proteins by western blot (WB). It has been well documented in the literature that stress response caused by xenobiotics launches cellular responses with similar regulation patterns on specific protein families (PETRAK, IVANEK, ET AL., 2008, WANG, BOUWMAN, ET AL., 2009). When chosing targets to validate we selected proteins that were not commonly regulated in comparative proteomics experiments. The final list of candidates and their selection parameters are shown on figure 60.

Figure 60 - List of protein candidates suited for WB validation. The table shows data from regulated HepG2 proteins after a 24 hour treatment using 1 µM of CYN, obtained from the major nano LC-MS^2 untargeted proteomics experiment. Highlighted rows show the proteins selected for WB validation.

Protein	Gene Name	Uniprot name	MW (KDa)	Sequence Coverage* (%)	P-value at 24 hrs	Log ratio difference at 24 hrs	Ingenuity pathway	Metacore Process Network
Ubiquitin-conjugating enzyme E2 N	UBE2N	P61088	17	45, 60, 50, 50	10e-1	-0.13	Protein Ubiquitination	Protein Ubiquitination
Ubiquitin-conjugating enzyme E2 L3	UBE2L3	P68036	18	60, 75, 70, 70	10e-2	-0.3	Protein Ubiquitination	Protein Ubiquitination
Acetyl-CoA acetyltransferase, cytosolic	ACAT2	Q9BWD1	41	63, 60, 63, 63	10e-2	-0.28	Cholesterol, Mevalonate, & Geranylgeranyldiphosphate Biosynthesis	Lipid metabolism, fatty acid B oxidation
Farnesyl pyrophosphate synthase	FDPS	P14324	43	25, 30, 25, 25	10e-3	-0.25	Superpathway of Cholesterol Biosynthesis	Steroid metabolism cholesterol biosynthesis
Eukaryotic translation initiation factor 2A	EIF2A	Q9BY44	65	30, 33, 20, 15	10e-2	-0.33	EIF2 signaling	NA
Proteasome subunit alpha type-2	PSMA2	P25787	26	45, 50, 50, 40	10e-4	-0.29	Protein Ubiquitination	Protein Ubiquitination
Peroxisomal bifunctional enzyme;Enoyl-CoA hydratase/3,2-trans-enoyl-CoA isomerase;3-hydroxyacyl-CoA dehydrogenase	EHHADH / ECHD	Q08426	79	20, 20, 25, 35	10e-4**	0.34**	Fatty Acid β-oxidation I	NA
Proliferating cell nuclear antigen	PCNA	P12004	29	65, 65, 70, 65	10e-2	-0.26	Cell cycle, p53 signaling, Mismatch repair	DNA damage response
Nuclease-sensitive element-binding protein 1	YBX1	P67809	36	40, 35, 40, 40	10e-2**	0.54**	Cancer Drug Resistance By Drug Efflux	Transcription-Translation, DNA damage response

P-values and expression values obtained from a 1 sample t-test: control (L) vs treated (H) at 24 hrs.
MW= molecular weight, N.A. = not available
* Sequence coverage at 0, 6, 12 and 24 hrs respectively
** P-values and expression values obtained from a 2 sample t-test: time zero (H/L) vs 24 hours (H/L)

Figure 61 – CYN regulates the expression of proteins involved with lipid metabolism, cell cycle and protein ubiquitination processes. HepG2 cells were stimulated with 1 µM CYN, and the abundance o the selected proteins was verified by analyzing the resulting Western Blot bands (A – E). Relative expression of ACAT2 (A), ECHD (B), PCNA (C), PSMA2 (D) and UBE2L3 (E), was analyzed by band density under untreated or CYN (1 µM)-stimulated conditions. β-actin is shown as a loading control.

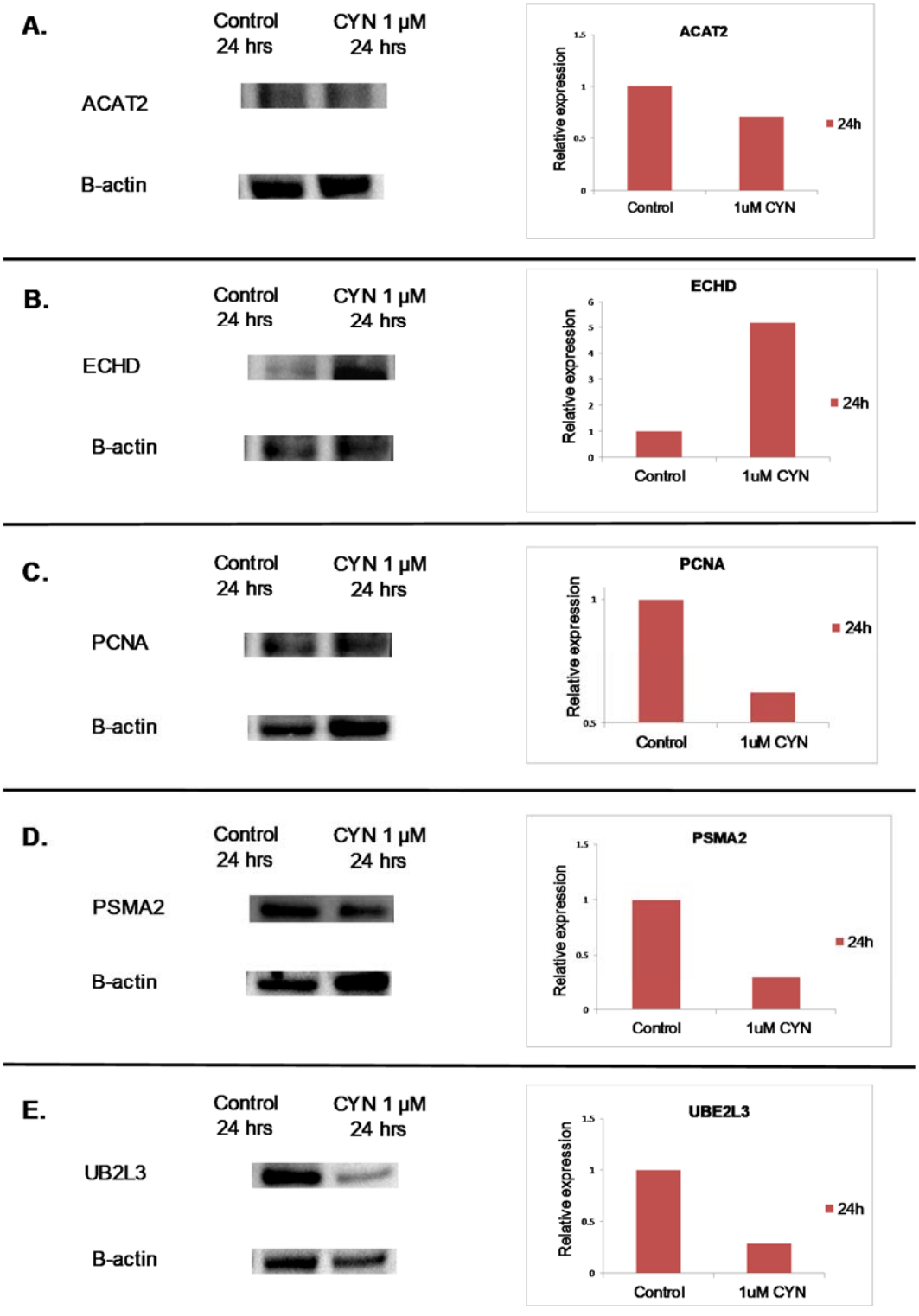

In addition, we chose beta actin (β-actin, ACTB) as a loading control for the WB protocols because it was not regulated by CYN on any of the time points of themajor nano LC-MS^2 experiment, although a sequence coverage of > 80 % was acquired on most of the replicates. Other common loading controls like beta tubulin and GAPDH were regulated by CYN

Figure 60 shows downregulation of the proteins (identified by their gene names) ACAT2, PCNA, PSMA2 and UBE2L3 according to the major LC-MS^2 shotgun proteomics experiment. On the other hand, ECHD was upregulated according to the previously mentioned dataset. These results show correlation with the quantitative WB verification (fig. 61).

These protein targets were chosen because they represent major processes regulated by sublethal doses of CYN, not only at 24 hours but also after 6 and 12 hours treatment. Cholesterol (ACAT2) and fatty acid metabolism (ECHD), DNA replication and damage response (PCNA), cell cycle regulation (PCNA, UBE2L3), ubiquitination and protein degradation (UBE2L3 and PSMA2) may play an important role in CYN`s toxicodynamics. Agreement of the MS2 generated data with the WB validation data, allow us to make further interpretations of the shotgun proteomics MS^2 derived dataset.

5.6 Validation of Mitochondrial toxicity by Flow Citometry

Figure 62 - Mitochondrial membrane potential alterations caused by CYN. HepG2 cells were treated with 1 µM CYN during 6 (B), 12 (D) and 24 hours (F). In a parallel experiment cells were treated with 5 µM CYN during 6 (C), 12 (E) and 24 hours (G).The first plot (A) shows a scatterplot that corresponds to a control sample; HepG2 cells grown without treatment. After the desired treatment cells were stained with JC-1 dye and fluorescence was detected in green and red channels by flow cytometry. Mitochondrial membrane potential was measured by the percentage of green fluorescence (H), and by the ratio of red to green fluorescence (I). n=4

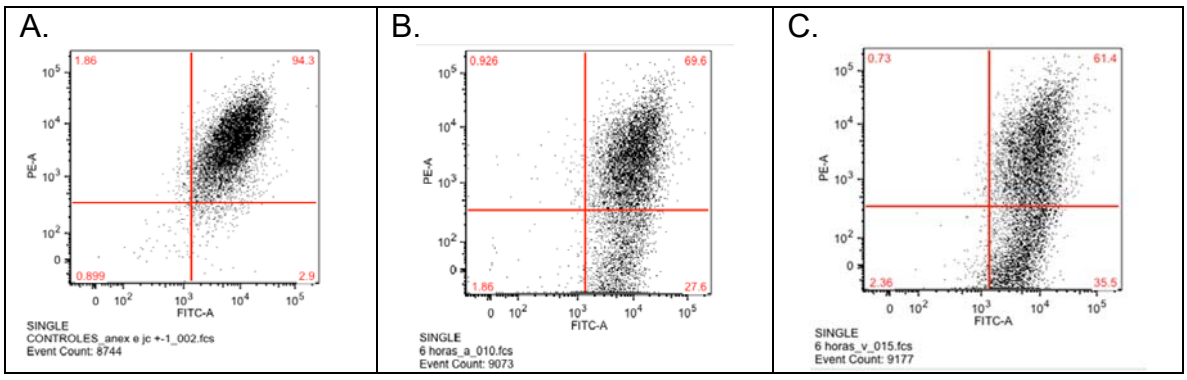

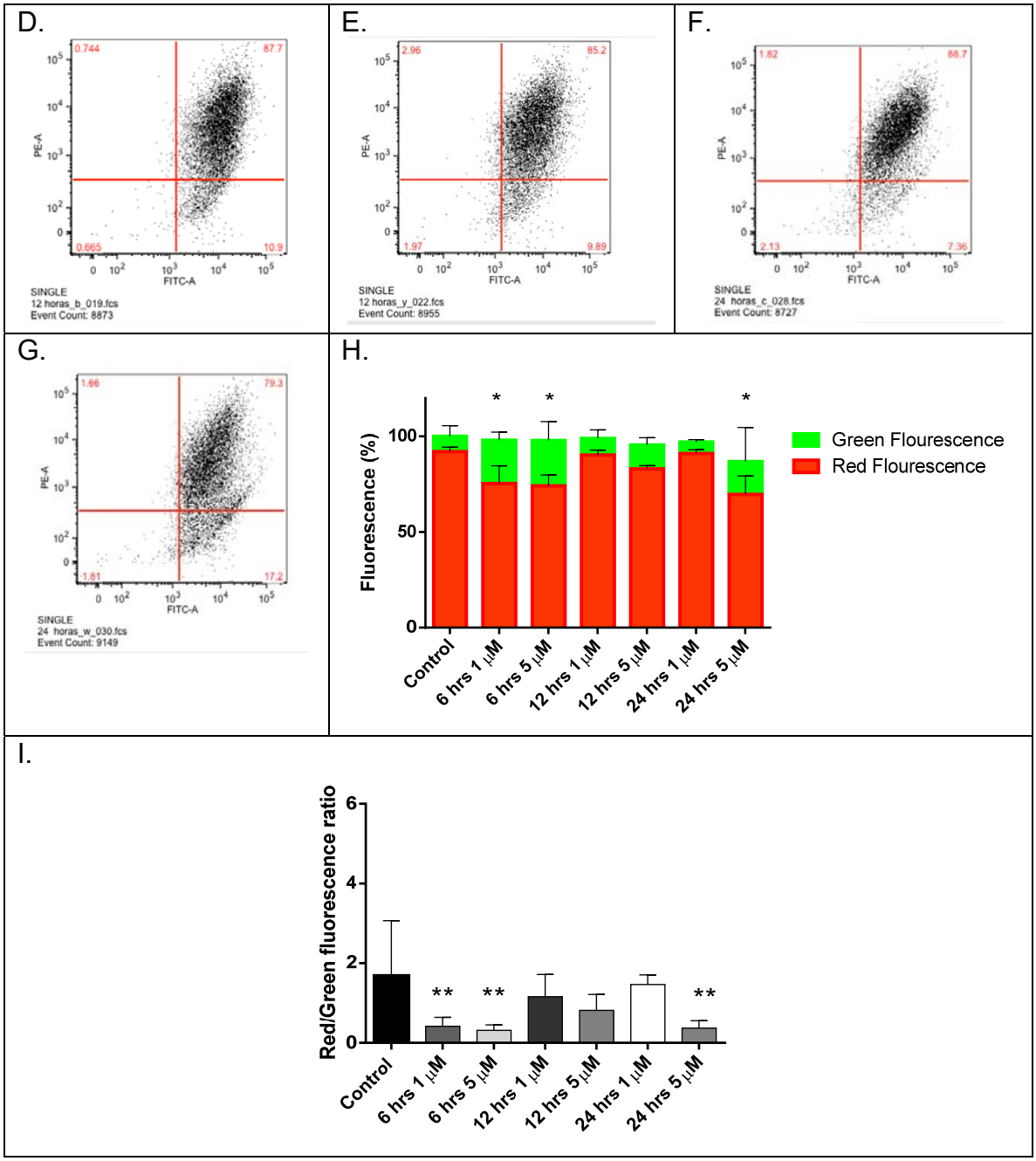

* p < 0.05, One way Anova test between green fluorescence of one time point vs time zero.
** p < 0.05, One way Anova test between red/green ratio of one time point vs time zero.

Mitochondrial membrane potential resistance to stress refers to the capacity of cells to maintain the membrane potential in the presence of a mitochondrial inhibitor, which can depolarize the mitochondrial membrane. JC-1 reagent exhibits potential-dependent accumulation in mitochondria, indicated by a fluorescence emission shift from green (~529 nm) to red (~590 nm). As shown on figure 62, mitochondrial depolarization can be measured by a decrease in the red/green fluorescence ratio.

The JC-1 experiment evidenced damage to the mitochondrial potential on HepG2 cells treated with 1 and 5 μM CYN for 6 hours, and treated with 5 μM CYN during 24 hours. This alteration may be related to the downregulation of transporters and enzymes detected by the shotgun proteomics experiments (fig. 64), at 6 and 24 hours. Downregulation at this level may also trigger the intrinsic apoptotic signaling pathway. According to the WB and proteomics data, the cell suffers stress at mitochondrial membrane level at 6 hours, seems to enter a recovery phase at 12 hours but fails to maintain it's potential at 24 hours (when treated with 5 μM). Downregulation of proteins related to the inner matrix of the mitochondria (fig. 63) appears as one of the earliest (after 6 hr treatment with 1 μM CYN) and most relevant toxicity findings in the present data set.

Figure 63 – Diagram of the oxidative phosphorylation related complexes in the inner membrane of the eukaryotic mitochondria, created by the Ingenuity Pathway Analysis® software. Colorized complexes show downregulation of their comprising proteins after a 6 hour treatment of HepG2 cells with 1 μM of CYN.

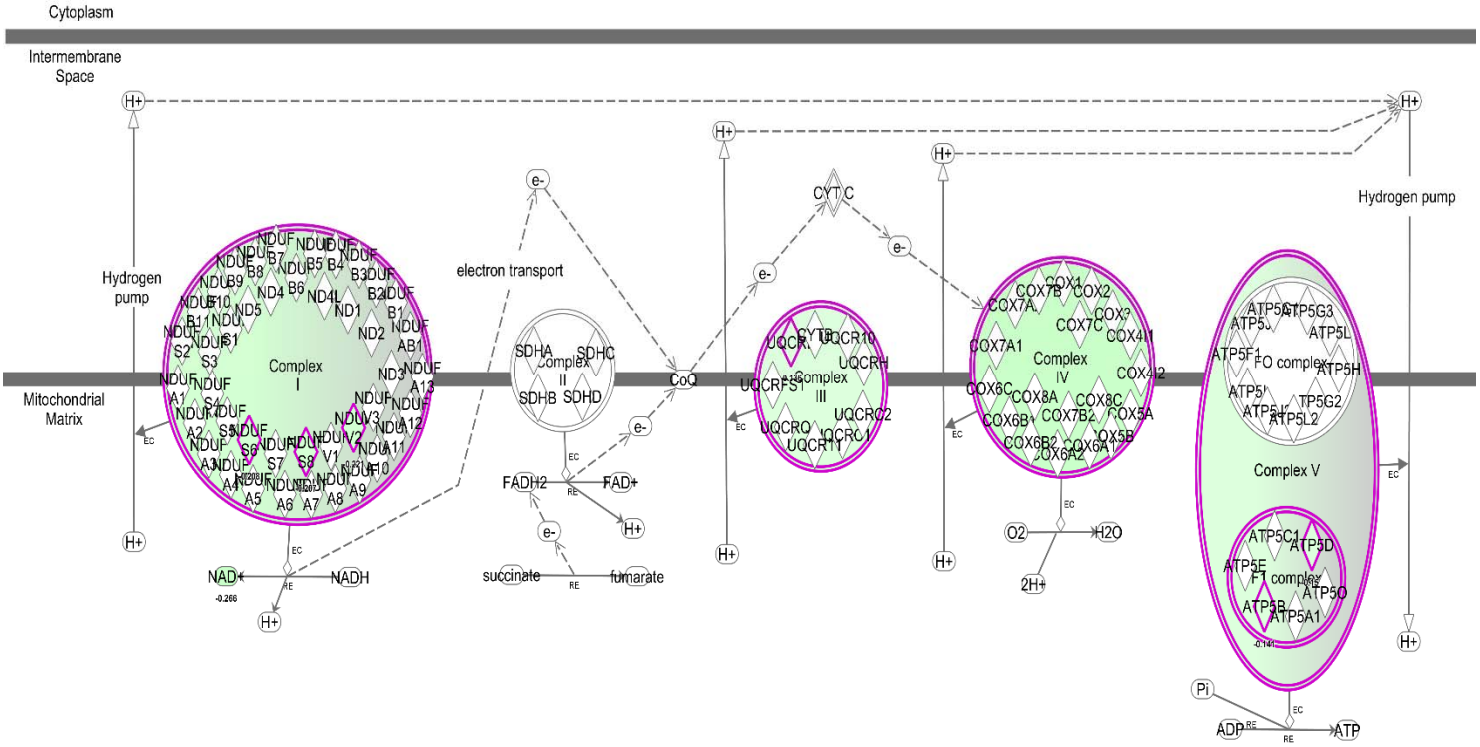

Figure 64 – List of mitochondrial dysfunction related proteins enriched by the Ingenuity Pathway Analysis® software. All proteins were downregulated after a 6 hour treatment of HepG2 cells with 1 µM of CYN.

Entrez Gene Name	Gene symbol	Expr Log Ratio	Location	Family
nicastrin	NCSTN	-0.352997037	Plasma Membrane	peptidase
NADH:ubiquinone oxidoreductase core subunit V2	NDUFV2	-0.220718715	Cytoplasm	enzyme
NADH:ubiquinone oxidoreductase subunit S6	NDUFS6	-0.207719722	Cytoplasm	enzyme
NADH:ubiquinone oxidoreductase core subunit S8	NDUFS8	-0.207388572	Cytoplasm	enzyme
ATP synthase, H+ transporting, mitochondrial F1 complex, delta subunit	ATP5D	-0.153140855	Cytoplasm	transporter
ATP synthase, H+ transporting, mitochondrial F1 complex, beta polypeptide	ATP5B	-0.141401353	Cytoplasm	transporter
ubiquinol-cytochrome c reductase binding protein	UQCRB	-0.135610764	Cytoplasm	enzyme
hydroxysteroid 17-beta dehydrogenase 10	HSD17B10	-0.112984694	Cytoplasm	enzyme
peroxiredoxin 5	PRDX5	-0.098177887	Cytoplasm	enzyme
peroxiredoxin 3	PRDX3	-0.094508012	Cytoplasm	enzyme

5.7 CYN updated toxicity timeline in HepG2 cells

Figure 65 – Updated timeline of CYN-induced toxicity on HepG2 cells, including relevant previously reported toxicity data and current discovery proteomics results.

Time	CYN concentration (μM)		
	0.024 - 0.24	1 (current work)	1.2
0 hrs	Toxin stimulation on HepG2 cells	Toxin stimulation on HepG2 cells	Toxin stimulation on HepG2 cells
0.5 - 2 hrs		Flow citometry using PI + Annexin V did not detect necrosis or apoptosis	
2.5 - 4 hrs		Flow citometry using PI + Annexin V did not detect necrosis or apoptosis	CYP1A1 ↑ *
			CYP1A2 ↑ *
6 hrs		Flow citometry using PI + Annexin V did not detect necrosis or apoptosis	
		Mitochondrial dysfunction ↓	
		Oxidative phosphorilation ↓	
		LXR/RXR (cholesterol metabolism) ↓	
		Protein ubiquitination pathway ↓	
		Acute phase response signaling ↓	
		Methionine degradation ↑	
		Cysteine biosynthesis ↑	
		EIF2 signaling ↓ ↑	
12 hrs	ROS concentration ↑ [A]	Flow citometry using PI + Annexin V did not detect necrosis or apoptosis	GADD45α ↑ *
	Apoptosis transcriptional response ↑↓ [δ]	LXR/RXR (cholesterol metabolism) ↓	MDM2 ↑ *
	Detoxification transcriptional response ↑↓[δ]	Protein ubiquitination pathway ↓	CYP1A1 ↑ *
	DNA damage repair transcriptional response ↑↓[δ]	Acute phase response signaling ↓	CYP1A2 ↑ *
	Cell cycle and proliferation ↑[δ]	Methionine degradation ↑	DNA damage (comet assay) *
		Cysteine biosynthesis ↑	Apoptosis transcriptional response ↑↓[δ]
		Cysteine biosynthesis ↑	Detoxification transcriptional response ↑↓[δ]
		EIF2 signaling ↓↑	DNA damage repair transcriptional response ↑↓[δ]
			Cell cycle and proliferation ↑[δ]
24 hrs	DNA damage (comet assay)*	Flow citometry using PI + Annexin V did not detect necrosis or apoptosis	MTT assay did not detect decrease in viability.*
	Micronuclei formation *	Oxidative phosphorilation ↓	CDKN1A ↑ *
	< 0.024 μM causes cell proliferation [A]	Cell cycle control of chromosomal replication ↓	CYP1A1 ↑ *
	ROS concentration ↑ [A]	Fatty Acid β-oxidation I ↓	CYP1A2 ↑ *
	Lipid peroxidation [A]	LXR/RXR (cholesterol metabolism) ↓	DNA damage (comet assay)*
	Antioxidant defense and xenobiotic efflux proteins ↑ [β]	Methionine degradation ↑	Micronuclei formation*
	Heatshock proteins ↑↓ [β]	Cysteine biosynthesis ↑	Decreased in percentage of cells in G2/M phase [χ]

Figure 60 (cont.)

24 hrs	Cytoskeleton proteins ↑ [β]	Purine Nucleotides De Novo Biosynthesis II ↑	Apoptosis transcriptional response ↑↓[ϑ]
	Energy metabolism proteins↑↓ [β]	Protein ubiquitination pathway ↓↑	Detoxification transcriptional response ↓↑[ϑ]
	Cell signaling proteins ↑↓ [β]	Superpathway of cholesterol biosynthesis ↓↑	DNA damage repair transcriptional response ↑↓[ϑ]
		Mitochondrial dysfunction ↓ ↑	Cell cycle and proliferation ↑↓[ϑ]
		Regulation of eIF4 and p70S6K Signaling ↓↑	
		EIF2 signaling ↓ ↑	
48 hrs	MTT assay detected decrease in viability. [χ]	Flow citometry using PI + Annexin V detected necrosis and apoptosis (cell death).	MTT assay detected decrease in viability. [χ]
72 hrs			MTT assay detected decrease in viability. [χ]
			DNA double strand breaks [χ]

↑= upregulation, ↓= downregulation, bold simbols indicate predominance of the condition
* (STRASER, FILIPIC, ET AL., 2011)
[A] (LIEBEL, DE OLIVEIRA RIBEIRO, ET AL., 2015)
[β] (LIEBEL, REGINA GRÖTZNER, ET AL., 2016)
[χ] (ALJA, ET AL., 2013)
[ϑ] (STRASER, ET AL., 2013)

Mitochondrial dysfuntion and oxidative phosphorylation was found as major processes evidenced by downregulation of mitochondrial proteins as early as 6 hrs and also after 24 hrs CYN treatment. Reactive oxygen species (ROS) are known to be produced by cellular metabolism or by xenobiotic stimulation of tissues. The mitochondrial membrane is a source of endogenous ROS, which are produced as a result of one-electron reduction of oxygen at the the respiratory chain complexes. On the other hand, the mitochondria possess redox systems (glutathione, thioredoxin, NADH:NAD+ and NADPH:NADP+), involved in the antioxidant defense. Intrinsic-mediated apoptosis, initializes at the mitochondrial membrane, usually by elevated levels of ROS (EL-OSTA AND CIRCU, 2016). Also as early as 6 hrs after treatment enzymes related to methionine degradation and cysteine biosynthesis were upregulated by CYN. L-cysteine is a component of the antioxidants glutathione and a thioredoxin. Reduced glutathione (GSH) plays an important role in cellular defenses against electrophiles, oxidative stress and nitrosating species.

Lipid metabolism showed a consistent downregulation after 6, 12 and 24 hrs treatment with CYN. After 24 hrs treatment with CYN, we detected mostly downregulation of fatty acid β-oxidation and several cholesterol biosynthesis pathways. LXR (liver X receptors) are transcription factors that regulate the transcription of specific genes involved in cholesterol metabolism, and act in the

nucleous complexed with retinoid X receptors (RXRs). Cellular cholesterol efflux is controlled, at least in part by these receptors (VENKATESWARAN, LAFFITTE, ET AL., 2000).

The regulation of EIF2 signaling pathways as early as 6 hrs may explain in part the effects of CYN on protein translation. The Eukaryotic Initiation Factor-2 acts as a chaperone taking the initiation-specific form of Met-tRNA to the specific ribosome location. EIF2 is comprised of subunits: alpha (36 kD), beta (38 kD), and gamma (52 kD). Phosphorilation plays an important role on the regulation of EIF2. Signaling by EIF2-Alpha kinases regulate protein synthesis in response to environmental stress (ASANO, PHAN, ET AL., 2001). Regulation of EIF2 signaling correlates with the hypothesis of some researchers that CYN's targets may not be the ribosome structure, but translation factors instead (TERAO, ET AL., 1994, FROSCIO, ET AL., 2008).

Effects of CYN on cell cycle are well documented and on the current work we detected downregulation of cell cycle control of chromosomal replication after 24 hr treatment with CYN. Cell cycle arrest evidenced by a decreased percentage of cells in G2/M phase was reported after a 24 hrs treatment with 1.2 μM CYN (ALJA, ET AL., 2013). Effects on cell cycle and DNA replication may be caused by CYN due to the direct or indirect effect on regulators, for example PCNA. The fact that PCNA is involved in the control of eukaryotic DNA replication and cell cycle is well stablished. This protein can be found positioned at the replication fork coordinating DNA replication with DNA repair and DNA damage tolerance pathways.

Finally, another consistent result along the timepoints was the regulation (mostly downregulation) of the protein ubiquitination pathway. The ubiquitin-proteasome system mantains homeostasis and protein turnover inside the cell, and it is expected that dysfunction of this pathway lead to cell toxicity and pathology in tissues. Post-translational modification by the small ubiquitin polypeptide is an enzymatic process. The stages of these enzymatic labeling can regulate the metabolic or structural role of the protein, or onset the degradation of the protein target (REYES-HERNANDEZ, MEJIA-GARCIA, ET AL., 2010, ALPI, CHAUGULE, ET AL., 2016). DNA damage or disruption of the cell cycle lead to a complex regulation of the ubiquitin-proteasome system through signaling. Protein synthesis decreases when eukaryotic cells enter a stationary phase due to lack of nutrients or accumulation of toxic substances in the environment. It has been reported that this stationary phase leads to a parallel decrease in proteasome-dependent proteolysis, by disassembly of ubiquitination pathway enzimes (BAJOREK, FINLEY, ET AL., 2003).

6.0 CONCLUTIONS

- A versatile total recovery SPE purification workflow was implemented for CYN zwitterionic species of hydrophilic nature (like CYN and 7D-CYN) using GNPC. If simultaneous purification of hydrophobic structural variants like 7D-desulfo-CYN from cell biomass is required, an additional separation step using a C18 cartridge proved to be reliable. These three variants were the only cylindrospermopsin analogs found in our lab`s strain.
- A concentration of 1 µM CYN for a maximum stimulation time of 24 hrs was defined as sublethal, because it did not induced detectable levels of apoptosis nor necrosis by flow cytometry on HepG2 cell cultures.
- A 48 hour treatment of HepG2 cells with 5 µM 7D-CYN and 7D-desulfo-CYN did not induced detectable levels of apoptosis nor necrosis by flow cytometry on HepG2 cell cultures.
- The results of the quantitative proteomics studies after a 6, 12 and 24 hour treatment with CYN, showed mostly downregulation of proteins. However there is no evidence of a complete protein synthesis inhibition after 24 hours of treatment.
- Damage to mitochondrial inner membrane and upregulation of methionine degradation are early and consistent evidences of cell toxicity in this study.
- Downregulation of cholesterol and regulation of fatty acids pathways appears as consistent findings in the interaction of CYN with the metabolic machinery of the cell.
- Regulation of transcription factors like EIF2, and regulators of DNA replication like PCNA, may play significant roles in CYN’s interaction with the proteome and protein synthesis.
- Downregulation of proteins from the ubiquitin-proteasome system may reflect DNA damage or cell cycle disruption.

7.0 FINAL PERSPECTIVES

- In order to understand the specific dynamics of CYN with hepatocyte proteins, it would be interesting to develop an experiment where CYN is bound to a stationary phase (i.e. magnetic beads) with it`s uracyl group exposed and unaltered. Next, the toxin in the stationary phase will be forced to interact with cell lysates or purified proteins (competitive binding assay). After several washing steps the proteins bound to the toxin can be digested and analyzed by LC-MS^2.

- A parallel experiment using the same CYN concentration (1 µM) and similar time points used on our shotgun proteomics experiments must be carried out to test protein synthesis inhibition in this model (HepG2 cells, *in vitro*). A pulsed SILAC experiment using H, M, L cells or only H, L cells could yield important information about the moment in which the cell`s capacity to synthezise cells decreases. If possible it would be interesting to calculate the effects of the toxin in the hepatocytes's protein turnover rate.
-

8.0 SUPPLEMENTARY MATERIAL

8.1 ASM-1 CUTURE MEDIUM PREPARATION

Preparation of the stock solutions.

The reagents must be weighed one by one in 50ml beaker, using analytical balance, dissolve them in ultrapure water (Milli-Q® water) and complete their volumes in a volumetric flask.

Stock Solution A: $NaNO_3$ (1.70 g), $MgCl_2$. 6 H_2O (0.41 g), $MgSO_4$. 7 H_2O (0.49 g), $CaCl_2$. 2 H_2O (0.29 g). Complete the volume with Milli-Q water up to 200 mL.

Stock Solution B: KH_2PO_4 (0.68 g), NaH_2PO_4 . H_2O or Na_2HPO_4 . 7 H_2O or Na_2HPO_4 . 12 H_2O (0.69 g or 1.34 g or 1.79 g). Complete the volume with Milli-Q water up to 100 mL.

Stock Solution C: H_3BO_3 (2.48 g), $MnCl_2$. 4 H2O (1.39 g), $FeCl_3$. 6 H_2O (1.08 g), $ZnCl_2$ (0.335 g), $CoCl_2$. 6 H_2O (0.019 g), $CuCl_2$ (0.0014 g). Complete the volume with Milli-Q water up to 100 mL.

Stock Solution D: EDTA.Na_2 (1.86 g), Complete the volume with Milli-Q water up to 100 mL.

Preparation of ASM-1 medium

Transfer approximately 300 mL of Milli Q® water into a volumetric flask of 1L and add the stock solutions: 20 mL of stock solution A, 2.0 mL of stock solution B, 0.1 mL of stock solution C, and 0.4 mL of stock solution D

Mix and complete volume up to 1 L with Milli Q water. Adjust pH to 8.0 using 1N NaOH or 1N HCl solution. Distribute appropriate volumes in tubes, flasks, etc., according to requirements, sterilize by autoclaving at 121 °C for 20 minutes. Identify with culture medium name, date of preparation, responsible, etc. Store at 4 °C.

8.2 ANNEXIN V AND PROPIDIUM IODIDE STAINING OF HEPG2 CELLS FOR FLOW CITOMETRY ANALYSIS

Staining Protocol

- Plate 2 x 10^5 cells/well in 6 well plates, with a final volume of 3 mL of high glucose DMEM, 10% FBS. Incubate overnight for the cells to adhere (37 °C, 5% CO_2).
- Make the desired treatment.
- Remove all medium from the wells and perform one PBS rinse. Transfer all volumes into the corresponding 5mL falcon tubes.
- Add 300 uL of trypsin to each well and incubate 5 min at 37 °C.
- Inactivate the trypsin with 2-3 mL of DMEM (containing 10% FBS). Transfer the entire contents of the wells again to the corresponding falcon tubes.
- Centrifuge at 1500 rpm 4 °C for 5 min, and discard the supernatant.
- Perform one wash of the pellet with PBS with 4% fetal bovine serum.
- Add 200 µL of binding buffer for Annexin V.
- For the double-staining positive control mix 100 µL of the cells treated with 10% DMSO (apoptosis control) and 100 µL of the cells treated with 40% MeOH (necrosis control).
- Add 5µL Annexin V (APC Annexin V, BD) and 2 uL of the propidium iodide (P4864, Sigma-Aldrich). Leave at least two control samples without staining.
- Incubate the samples 15 min in the dark at room temperature.
- Analyze samples using the flow cytometer.

Annexin V binding buffer preparation

Hepes (10 mM/L), pH 7.4, NaCl (140 mM/L), $CaCl_2$ (2.5 mM/L).

8.3 SILAC MEDIUM PREPARATION (Adapted from Professor Pierre Thibault's Lab, IRIC, Université de Montréal)

Reagents

500mL DMEM high glucose without R or K

50 mL dialyzed FBS

5.5 ml Penicillin/Streptolysin (100X)

R and K isotopes to use

R0 + K0 (Light)

R6 + K4 (Medium): R6 is $^{13}C_6$ and K4 is 4,4,5,5-D_4

R10 + K8 (Heavy): R10 is $^{13}C_6$, $^{15}N_4$ and K8 is $^{13}C_6$, $^{15}N_2$

SILAC medium preparation

For the R and K stock solutions prepare all the stock solutions (Heavy, Light and Medium) at a concentration of 84 mg/mL in PBS for R and 146 mg/mL for K.

For Light Medium:

- Add 0.5 ml Argine Light stock (84 mg/ml in PBS)
- Add 0.5 ml Lysine Light Stock (146 mg/ml in PBS)

For Heavy Medium

- Add 523.3 ul Arginine Heavy stock
- Add 518 ul Lysine Heavy stock
- Add Proline at a concentration of 100 ug/ml

For Medium Medium

- Add 514.14 ul Arginine Medium stock
- Add 509.4 ul Lysine Medium stock
- Add Proline at a concentration of 100 ug/ml

Notes: Filter sterilize alll through 0.22 µm filter and store at 4º. Supplemental proline (100 ug/mL) needs to be added to the medium to inhibit labelled arginine to proline conversion.

8.4 PROTEIN DIGESTION IN SODIUM DEOXYCHOLATE (SDC) BUFFER (Adapted from Professor Pierre Thibault's Lab, IRIC, Université de Montréal)

Cell Lysis and protein extraction

- Resuspend cell pellet in 800-1200 uL of ice cold 1% (w/v) SDC in 50 mM NH_4HCO_3 (lysis buffer).
- Transfer cell suspension in 1.5 ml screw-cap tubes and sonicate at power 3 for 5-10 sec (mammalian cells will be lysed)
- Immediately transfer sample into thermomixer and incubate at 99^{o}C for 5 min with shaking at 1,400 rpm (max speed)
- Spin sample 40,000 x g 10 min at 4^{o}C and transfer supernatant into a clean tube.

Enzymatic Digestion

- Keep aside 10-20 uL of sample for protein concentration measurement (BCA assay)
- Add 500 mM DTT to the remaining of the sample for a final conc. of 5 mM and shake at 800 rpm at 56^{o}C for 30 min. Cool down at RT.
- Add 500 mM iodoacetamide (IAA) to a final concentration of 15 mM and incubate for 30 min at RT in the dark (alternatively chloroacetamide can be used).
- Quench excess of IAA with DTT (final conc. 5 mM), leave 15 min at RT in the dark.
- Add trypsin at final conc. 5-10 ng/uL, protein:trypsin ~ 50:1 – 200:1.
- Incubate overnight at 37^{o}C and proceed with SDC removal and peptide desalting.

Desalting & Concentration

- After digestion, acidify sample by adding 30% TFA to get final pH~ 2 (check with pH indicator).
- Vortex, spin at 13,000g 5 min and transfer peptide digest solution into a clean tube.
- Condition C18 cartridge with: (i) 1 mL CAN, (ii) 1 ml of 50% ACN, 0.5% AcOH, (iii) 1 mL 0.1% TFA (use vacuum manifold, set the vacuum to adjust flow rate ~ 1 mL/min or lower).
- Apply peptide digest sample.
- Desalt peptide digest with 1 mL of 0.1% TFA;
- Elute peptide digests in 1 mL of 50% ACN, 0.5% AcOH;

- Snap freeze eluate in liquid nitrogen (important).
- Dry frozen eluate in speedvac at RT (approx. 4-6 h).
- Dried samples can be stored at -20^{o}C for at least several weeks.

8.5 OFFLINE STRONG CATION EXCHANGE (SCX) FRACTIONATION OF PEPTIDES (Adapted from Professor Pierre Thibault's Lab, IRIC, Université de Montréal)

Reagents

- SCX buffer A: 10% acetonitrile (ACN), 0.2% formic acid (FA) (v/v), keep at 4°C.
- SCX buffer B: 1M NaCl in SCX buffer A, keep at 4°C.
- "Salt steps" are prepared by mixing SCX buffers A and B.

SCX A, ul	SCX B, ul	Final NaCl, mM
990	10	10
975	25	25
960	40	40
945	55	55
930	70	70
900	100	100
850	150	150
0	1000	1000

Preparation of SCX spin columns

- cut 1 ml pipette tip ~ 2-3 mm from the orifice (you will use it to cut SDB-XC membrane);
- use it to cut small piece of Anion-SR membrane;
- place piece of Anion-SR membrane inside the 200 uL tip (yellow tip) with the help of a fused silica capillary to make a frit, necessary to retain the packing material.
- cut 13 mm from the top of yellow tip with the scissors.
- now you have empty spin column with the Anion-SR frit.
- weight your empty column on analytical balance.
- prepare suspension of Polysulfoethyl A (SCX) in MeOH.
- place 100 uL of SCX suspension into empty spin column.
- spin 13,000 x g for 1 min to remove CAN.
- weight you column and calculate exact amount of SCX in the column by mass difference, based on this measurement volume of suspension should be adjusted to get spin column with 18-22 mg of SCX.

Sample preparation

- 50 ug of peptides, desalted and dried on speedvac;
- Resuspend sample in 100 uL of SCX buffer A (vortex);
- Spin 13,000 x g for 3 min;
- Equilibrate SCX spin column with (keep centrifugation speed at 5,000 x g):
    - 100 uL of 50% ACN 0.5% FA (v/v);
    - 100 ul of SCX buffer B;
    - 2 x 100 ul of SCX buffer A;
- Apply peptide sample on top of the SCX phase, spin 5,000 x g for 15-20 min at 4^{o}C and collect flow-through fraction;
- Wash SCX column with additional 50 ul of SCX buffer A (6,000 x g) and combine this wash with flow-through fraction collected in previous step;
- Elute retained peptides with 100 ul of each “salt steps” (increasing order of salt concentration) collecting each fraction in a separate tube (keep centrifugation speed at 6,500 x g);
- dry all collected fractions (including flow-through) on speedvac (at RT);
- resuspend peptides in appropriate volume of 4% FA and analyze by LC-MS^{2}.

9.0 REFERENCES

MOREIRA, C., AZEVEDO, J., ANTUNES, A. AND VASCONCELOS, V. Cylindrospermopsin: occurrence, methods of detection and toxicology. **J Appl Microbiol**, 114, 605-620, 2013.

GALLO, P., FABBROCINO, S., CERULO, M. G., FERRANTI, P., BRUNO, M. AND SERPE, L. Determination of cylindrospermopsin in freshwaters and fish tissue by liquid chromatography coupled to electrospray ion trap mass spectrometry. **Rapid communications in mass spectrometry : RCM**, 23, 3279-3284, 2009.

BITTENCOURT-OLIVEIRA MDO, C., PICCIN-SANTOS, V., MOURA, A. N., ARAGAO-TAVARES, N. K. AND CORDEIRO-ARAUJO, M. K. Cyanobacteria, microcystins and cylindrospermopsin in public drinking supply reservoirs of Brazil. **Anais da Academia Brasileira de Ciencias**, 86, 297-310, 2014.

SADLER, R. Towards a more complete understanding of the occurrence and toxicities of the cylindrospermopsins. **AIMS Environmental Science**, 2, 827-851, 2015.

AZEVEDO, S. M., CARMICHAEL, W. W., JOCHIMSEN, E. M., RINEHART, K. L., LAU, S., SHAW, G. R. AND EAGLESHAM, G. K. Human intoxication by microcystins during renal dialysis treatment in Caruaru-Brazil. **Toxicology**, 181-182, 441-446, 2002.

YOSHIZAWA, S., MATSUSHIMA, R., WATANABE, M. F., HARADA, K., ICHIHARA, A., CARMICHAEL, W. W. AND FUJIKI, H. Inhibition of protein phosphatases by microcystins and nodularin associated with hepatotoxicity. **Journal of cancer research and clinical oncology**, 116, 609-614, 1990.

PEARSON, L., MIHALI, T., MOFFITT, M., KELLMANN, R. AND NEILAN, B. On the chemistry, toxicology and genetics of the cyanobacterial toxins, microcystin, nodularin, saxitoxin and cylindrospermopsin. **Marine drugs**, 8, 1650-1680, 2010.

TERAO, K., OHMORI, S., IGARASHI, K., OHTANI, I., WATANABE, M. F., HARADA, K. I., . . . WATANABE, M. Electron microscopic studies on experimental poisoning in mice induced by cylindrospermopsin isolated from blue-green alga Umezakia natans. **Toxicon : official journal of the International Society on Toxinology**, 32, 833-843, 1994.

FROSCIO, S. M., HUMPAGE, A. R., BURCHAM, P. C. AND FALCONER, I. R. Cylindrospermopsin-induced protein synthesis inhibition and its dissociation from acute toxicity in mouse hepatocytes. **Environmental toxicology**, 18, 243-251, 2003.

HUMPAGE, A. Toxin types, toxicokinetics and toxicodynamics. **Advances in experimental medicine and biology**, 619, 383-415, 2008.

GRIFFITHS, D. J. AND SAKER, M. L. The Palm Island mystery disease 20 years on: a review of research on the cyanotoxin cylindrospermopsin. **Environmental toxicology**, 18, 78-93, 2003.

BANKER, R., CARMELI, S., WERMAN, M., TELTSCH, B., PORAT, R. AND SUKENIK, A. Uracil moiety is required for toxicity of the cyanobacterial hepatotoxin cylindrospermopsin. **Journal of Toxicology and Environmental Health-Part A**, 62, 281-288, 2001.

MIHALI, T. K., KELLMANN, R., MUENCHHOFF, J., BARROW, K. D. AND NEILAN, B. A. Characterization of the gene cluster responsible for cylindrospermopsin biosynthesis. **Appl Environ Microbiol**, 74, 716-722, 2008.

LAWTON, L. A. AND EDWARDS, C. Conventional laboratory methods for cyanotoxins. **Advances in experimental medicine and biology**, 619, 513-537, 2008.

EAGLESHAM, G. K., NORRIS, R. L., SHAW, G. R., SMITH, M. J., CHISWELL, R. K., DAVIS, B. C., . . . MOORE, M. R. Use of HPLC-MS/MS to monitor cylindrospermopsin, a blue-green algal toxin, for public health purposes. **Environmental toxicology**, 14, 151-154, 1999.

CHONG, M. W., WONG, B. S., LAM, P. K., SHAW, G. R. AND SEAWRIGHT, A. A. Toxicity and uptake mechanism of cylindrospermopsin and lophyrotomin in primary rat hepatocytes. **Toxicon : official journal of the International Society on Toxinology**, 40, 205-211, 2002.

LOPEZ-ALONSO, H., RUBIOLO, J. A., VEGA, F., VIEYTES, M. R. AND BOTANA, L. M. Protein synthesis inhibition and oxidative stress induced by cylindrospermopsin elicit apoptosis in primary rat hepatocytes. **Chem Res Toxicol**, 26, 203-212, 2013.

ALJA, S., FILIPIC, M., NOVAK, M. AND ZEGURA, B. Double strand breaks and cell-cycle arrest induced by the cyanobacterial toxin cylindrospermopsin in HepG2 cells. **Marine drugs**, 11, 3077-3090, 2013.

FROSCIO, S. M., HUMPAGE, A. R., WICKRAMASINGHE, W., SHAW, G. AND FALCONER, I. R. Interaction of the cyanobacterial toxin cylindrospermopsin with the eukaryotic protein synthesis system. **Toxicon : official journal of the International Society on Toxinology**, 51, 191-198, 2008.

BAZIN, E., MOUROT, A., HUMPAGE, A. R. AND FESSARD, V. Genotoxicity of a Freshwater Cyanotoxin, Cylindrospermopsin, in Two Human Cell Lines: Caco-2 and HepaRG. **Environmental and Molecular Mutagenesis**, 51, 251-259, 2010.

NORRIS, R. L., SEAWRIGHT, A. A., SHAW, G. R., SENOGLES, P., EAGLESHAM, G. K., SMITH, M. J., . . . MOORE, M. R. Hepatic xenobiotic metabolism of cylindrospermopsin in vivo in the mouse. **Toxicon : official journal of the International Society on Toxinology**, 40, 471-476, 2002.

ZEGURA, B., STRASER, A. AND FILIPIC, M. Genotoxicity and potential carcinogenicity of cyanobacterial toxins - a review. **Mutation Research-Reviews in Mutation Research**, 727, 16-41, 2011.

FESSARD, V. AND BERNARD, C. Cell alterations but no DNA strand breaks induced in vitro by cylindrospermopsin in CHO K1 cells. **Environmental toxicology**, 18, 353-359, 2003.

STRASER, A., FILIPIC, M. AND ZEGURA, B. Cylindrospermopsin induced transcriptional responses in human hepatoma HepG2 cells. **Toxicology in vitro : an international journal published in association with BIBRA**, 27, 1809-1819, 2013.

LOOPER, R. E., RUNNEGAR, M. T. C. AND WILLIAMS, R. M. Syntheses of the cylindrospermopsin alkaloids. **Tetrahedron**, 62, 4549-4562, 2006.

PONIEDZIALEK, B., RZYMSKI, P. AND KARCZEWSKI, J. Cylindrospermopsin decreases the oxidative burst capacity of human neutrophils. **Toxicon : official journal of the International Society on Toxinology**, 87, 113-119, 2014.

TITZ, B., ELAMIN, A., MARTIN, F., SCHNEIDER, T., DIJON, S., IVANOV, N. V., . . . PEITSCH, M. C. Proteomics for systems toxicology. **Computational and structural biotechnology journal**, 11, 73-90, 2014.

HUNT, D. F., YATES, J. R., 3RD, SHABANOWITZ, J., WINSTON, S. AND HAUER, C. R. Protein sequencing by tandem mass spectrometry. **Proceedings of the National Academy of Sciences of the United States of America**, 83, 6233-6237, 1986.

NESVIZHSKII, A. I. AND AEBERSOLD, R. Interpretation of shotgun proteomic data - The protein inference problem. **Mol. Cell. Proteomics**, 4, 1419-1440, 2005.

BANTSCHEFF, M., LEMEER, S., SAVITSKI, M. M. AND KUSTER, B. Quantitative mass spectrometry in proteomics: critical review update from 2007 to the present. **Anal Bioanal Chem**, 404, 939-965, 2012.

BODZON-KULAKOWSKA, A., BIERCZYNSKA-KRZYSIK, A., DYLAG, T., DRABIK, A., SUDER, P., NOGA, M., . . . SILBERRING, J. Methods for samples preparation in proteomic research. **Journal of Chromatography B**, 849, 1-31, 2007.

LEUNG, H.-C. E., MAN, T.-K. AND FLORES, R. J.,H.-C. E. LEUNG,Integrative Proteomics.InTech,452,2012.

THOMPSON, A., SCHAFER, J., KUHN, K., KIENLE, S., SCHWARZ, J., SCHMIDT, G., . . . HAMON, C. Tandem mass tags: a novel quantification strategy for comparative analysis of complex protein mixtures by MS/MS. **Analytical chemistry**, 75, 1895-1904, 2003.

ROSS, P. L., HUANG, Y. N., MARCHESE, J. N., WILLIAMSON, B., PARKER, K., HATTAN, S., . . . PAPPIN, D. J. Multiplexed protein quantitation in Saccharomyces cerevisiae using amine-reactive isobaric tagging reagents. **Molecular & cellular proteomics : MCP**, 3, 1154-1169, 2004.

MARCOTTE, E. M. How do shotgun proteomics algorithms identify proteins? **Nat Biotech**, 25, 755-757, 2007.

ROEPSTORFF, P.,PROPOSAL FOR A COMMON NOMENCLATURE FOR SEQUENCE IONS IN MASS-SPECTRA OF PEPTIDES-REPLY.JOHN WILEY & SONS LTD BAFFINS LANE CHICHESTER, W SUSSEX, ENGLAND PO19 1UD,12,631-631,1985.

NEUHAUSER, N., NAGARAJ, N., MCHARDY, P., ZANIVAN, S., SCHELTEMA, R., COX, J. AND MANN, M. High Performance Computational Analysis of Large-scale Proteome Data

Sets to Assess Incremental Contribution to Coverage of the Human Genome. **J. Proteome Res.**, 12, 2858-2868, 2013.

BORTOLLI, S. D.,Guia prático para manutenção e cuidados da coleção de cianobacterias do LTPNA.Universidade de São Paulo,2011.

MEOLA, J. M. AND VANKO, M. Use of charcoal to concentrate drugs from urine before drug analysis. **Clinical chemistry**, 20, 184-187, 1974.

QIN, L. F. AND NG, I. O. Induction of apoptosis by cisplatin and its effect on cell cycle-related proteins and cell cycle changes in hepatoma cells. **Cancer letters**, 175, 27-38, 2002.

GAO, J., DONG, Y., ZHANG, B., XIONG, Y., XU, W., CHENG, Y., . . . ZHENG, G. Notch1 activation contributes to tumor cell growth and proliferation in human hepatocellular carcinoma HepG2 and SMMC7721 cells. **International journal of oncology**, 41, 1773-1781, 2012.

ONG, S. E. AND MANN, M. A practical recipe for stable isotope labeling by amino acids in cell culture (SILAC). **Nat Protoc**, 1, 2650-2660, 2006.

BENDALL, S. C., HUGHES, C., STEWART, M. H., DOBLE, B., BHATIA, M. AND LAJOIE, G. A. Prevention of amino acid conversion in SILAC experiments with embryonic stem cells. **Molecular & cellular proteomics : MCP**, 7, 1587-1597, 2008.

PETRAK, J., IVANEK, R., TOMAN, O., CMEJLA, R., CMEJLOVA, J., VYORAL, D., . . . VULPE, C. D. Deja vu in proteomics. A hit parade of repeatedly identified differentially expressed proteins. **Proteomics**, 8, 1744-1749, 2008.

WANG, P., BOUWMAN, F. G. AND MARIMAN, E. Generally detected proteins in comparative proteomics–a matter of cellular stress response? **Proteomics**, 9, 2955-2966, 2009.

STRASER, A., FILIPIC, M. AND ZEGURA, B. Genotoxic effects of the cyanobacterial hepatotoxin cylindrospermopsin in the HepG2 cell line. **Arch Toxicol**, 85, 1617-1626, 2011.

LIEBEL, S., DE OLIVEIRA RIBEIRO, C. A., DE MAGALHÃES, V. F., DA SILVA, R. D. C., ROSSI, S. C., RANDI, M. A. F. AND NETO, F. F. Low concentrations of cylindrospermopsin induce increases of reactive oxygen species levels, metabolism and proliferation in human hepatoma cells (HepG2). **Toxicology in Vitro**, 29, 479-488, 2015.

LIEBEL, S., REGINA GRÖTZNER, S., DIETRICH MOURA COSTA, D., ANTÔNIO FERREIRA RANDI, M., ALBERTO DE OLIVEIRA RIBEIRO, C. AND FILIPAK NETO, F. Cylindrospermopsin effects on protein profile of HepG2 cells. **Toxicology mechanisms and methods**, 26, 554-563, 2016.

EL-OSTA, H. AND CIRCU, M. L.,Mitochondrial ROS and Apoptosis.Springer,1-23,2016.

VENKATESWARAN, A., LAFFITTE, B. A., JOSEPH, S. B., MAK, P. A., WILPITZ, D. C., EDWARDS, P. A. AND TONTONOZ, P. Control of cellular cholesterol efflux by the nuclear oxysterol receptor LXRα. **Proceedings of the National Academy of Sciences**, 97, 12097-12102, 2000.

ASANO, K., PHAN, L., VALASEK, L., SCHOENFELD, L., SHALEV, A., CLAYTON, J., . . . HINNEBUSCH, A.,A multifactor complex of eIF1, eIF2, eIF3, eIF5, and tRNAiMet promotes initiation complex assembly and couples GTP hydrolysis to AUG recognition.Cold Spring Harbor Laboratory Press,66,403-416,2001.

REYES-HERNANDEZ, O., MEJIA-GARCIA, A., SÁNCHEZ-OCAMPO, E., CABANAS-CORTES, M., RAMIREZ, P., CHÁVEZ-GONZÁLEZ, L., . . . ELIZONDO, G. Ube2l3 gene expression is modulated by activation of the aryl hydrocarbon receptor: implications for p53 ubiquitination. **Biochemical pharmacology**, 80, 932-940, 2010.

ALPI, A. F., CHAUGULE, V. AND WALDEN, H. Mechanism and disease association of E2-conjugating enzymes: lessons from UBE2T and UBE2L3. **Biochemical Journal**, 473, 3401-3419, 2016.

BAJOREK, M., FINLEY, D. AND GLICKMAN, M. H. Proteasome disassembly and downregulation is correlated with viability during stationary phase. **Current Biology**, 13, 1140-1144, 2003.

10. ANNEXES

1- Curriculum Lattes

2- Ficha do aluno

3- Full list of regulated proteins for the final shotgun proteomics experiment

.

Carlos Andrey Gonzalez Blanco

Endereço para acessar este CV: http://lattes.cnpq.br/3534852674757703
Última atualização do currículo em 29/06/2017

Possui mestrado em Microbiologia e Química Clínica pela Universidade da Costa Rica (2007). Atualmente é doutorando pelo Departamento de Análises Clínicas e Toxicológicas da Faculdade de Ciências Farmacêuticas da Universidade de São Paulo. Tem experiência nas áreas de Toxicologia Analítica e Forense, proteômica quantitativa utilizando SILAC, cultivo celular de hepatócitos primários, análise toxicológica de drogas, substâncias voláteis, praguicidas e outros tóxicos em amostras de origem humana. **(Texto informado pelo autor)**

Identificação

Nome Carlos Andrey Gonzalez Blanco
Nome em citações bibliográficas GONZALEZ BLANCO, C.

Endereço

Endereço Profissional
Departamento de Ciências Forenses, Seção de Toxicologia Forense.
200 m nordeste, cemitério de San Joaquín de Heredia
San Joaquin de Flores
San Joaquin de Flores, - Costa Rica
Telefone: (506) 22671106
URL da Homepage: https://www.poder-judicial.go.cr/oij/index.php/ofi/departamento-de-ciencias-forenses/toxicologia

Formação acadêmica/titulação

2013
Doutorado em andamento em Ciências (Análises Clínicas e Toxicológicas).
Universidade de São Paulo, USP, Brasil.
Título: Efeitos da toxina cilindrospermopsina na expressão de proteínas de culturas celulares de hepatócitos humanos,
Orientador: Prof. Assoc. Ernani Pinto.
Bolsista do(a): CAPES - Programa de Estudantes-Convênio de Pós-Graduação, CAPES/PEC-PG, Brasil.
Palavras-chave: cilindrospermopsina; LC-MS; hepatócito primário; proteômica.
Grande área: Ciências da Saúde

2000 - 2007
Graduação em Microbiología y Química Clínica.
Universidad de Costa Rica, UCR, Costa Rica.
Título: Implementation of an analytical methodology for the detection of 2,4-D (dichlorophenoxiacetic acid) in biologiical samples for forensics purposes.
Orientador: Diego Arias Alfaro.

Formação Complementar

2014 - 2014
Extensão universitária em quantitative proteomic using SILAC. (Carga horária: 1250h).
Université de Montreal (IRIC), UDM, Canadá.

Áreas de atuação

1.
Grande área: Ciências da Saúde / Área: Farmácia / Subárea: Avaliação e analises toxicológicas.

Idiomas

Inglês	Compreende Bem, Fala Bem, Lê Bem, Escreve Bem.
Português	Compreende Bem, Fala Bem, Lê Bem, Escreve Bem.
Espanhol	Compreende Bem, Fala Bem, Lê Bem, Escreve Bem.

Prêmios e títulos

2014	Programa Santander de Bolsas de Mobilidade Internacional, Universidade de São Paulo.

Produções

Produção bibliográfica

Artigos completos publicados em periódicos

Ordenar por

Ordem Cronológica

1. **GONZALEZ BLANCO, C.**; ESQUIVEL, M. M. ; AGUILAR, G. B. . Conducción y accidente automovilístico bajo la influencia de tolueno. Revista Ciencia Forense INACIPE, v. 01, p. 23-30, 2013.
2. Arias D ; Brenes G ; **GONZALEZ BLANCO, C.** . Metodología analítica para detección de 2,4-D en muestras de sangre e contenido gástrico. Revista de Ciencias Forenses Inacipe, v. 1, p. 22-27, 2011.

Apresentações de Trabalho

1. **GONZALEZ BLANCO, C.**; PINTO, E. ; THIBAULT, P. ; KUBINIOK, P. . A sublethal concentration of the cyanotoxin Cylindrospermopsin causes primarily structural and metabolic protein upregulation on HepG2 cells. 2015. (Apresentação de Trabalho/Congresso).

Eventos

Participação em eventos, congressos, exposições e feiras

1. 7th SETAC World Congress/SETAC North America 37th Annual Meeting. Sub lethal concentrations of Cylindrospermopsin causes lipogenesis, cell cycle disruption, and activation of stress responses on hepatocytes. 2016. (Congresso).
2. Congresso Brasileiro de Toxicologia XIX. A sublethal concentration of the cyanotoxin Cylindrospermopsin causes primarily structural and metabolic protein upregulation on HepG2 cells. 2015. (Congresso).
3. IUTOX's Water Security Course.Effects of the sublethal concentrations of the cyanotoxin Cylindrospermopsin on the proteome of HepG2 cells. 2015. (Oficina).
4. IV Escola de Inverno em Toxicologia, FCF-USP.Linhas de pesquisa do laboratorio de toxinas e produtos naturais de algas. 2015. (Simpósio).
5. Canada-Brazil Molecular Sciences Workshop. 2014. (Oficina).
6. 9th South American Regional Meeting TIAFT. Conducción y accidente automovilístico bajo la influencia de tolueno: reporte de caso. 2013. (Congresso).
7. Modern Topics in Magnetic Resonance. 2013. (Congresso).
8. Seminários da Comissão de Pesquisa - FCF-USP. 2013. (Seminário).
9. The role of Mass Spectrometry in drug discovery and beyound. 2013. (Oficina).
10. Treinamento Agilent Technologies Operação do Software MassHunter.Treinamento - Operação do Software MassHunter. 2013. (Oficina).

Janus - Sistema Administrativo da Pós-Graduação

Universidade de São Paulo
Faculdade de Ciências Farmacêuticas
Documento sem validade oficial

FICHA DO ALUNO

9143 - 8679238/1 - Carlos Andrey Gonzalez Blanco

Email:	carlosgb@usp.br
Data de Nascimento:	18/02/1981
Cédula de Identidade:	RNE - V903831-1 - DF
Local de Nascimento:	Costa Rica
Nacionalidade:	Costarriquenha
Graduação:	Licenciatura en Microbiología y Química Clínica - Universidad de Costa Rica - Costa Rica - 2007

Curso:	Doutorado Direto
Programa:	Farmácia (Fisiopatologia e Toxicologia)
Área:	Toxicologia
Data de Matrícula:	22/03/2013
Início da Contagem de Prazo:	22/03/2013
Data Limite para o Depósito:	20/07/2017
Orientador:	Prof(a). Dr(a). Ernani Pinto Junior - 02/08/2016 até o presente. Email: ernani@usp.br
Proficiência em Línguas:	Inglês, Aprovado em 22/03/2013 Português, Aprovado em 22/03/2013
Prorrogação(ões):	120 dias Período de 22/03/2017 até 20/07/2017
Data de Aprovação no Exame de Qualificação:	Aprovado em 01/06/2015
Data do Depósito do Trabalho:	
Título do Trabalho:	
Data Máxima para Aprovação da Banca:	
Data de Aprovação da Banca:	
Data Máxima para Defesa:	
Data da Defesa:	
Resultado da Defesa:	
Histórico de Ocorrências:	Primeira Matrícula em 22/03/2013 Prorrogação em 15/02/2017

Aluno matriculado no Regimento da Pós-Graduação USP (Resolução nº 6542 em vigor a partir de 20/04/2013).

Última ocorrência: Prorrogação em 15/02/2017

Impresso em: 29/06/2017 11:21:25

Janus - Sistema Administrativo da Pós-Graduação

Universidade de São Paulo
Faculdade de Ciências Farmacêuticas
Documento sem validade oficial

FICHA DO ALUNO

9143 - 8679238/1 - Carlos Andrey Gonzalez Blanco

Sigla	Nome da Disciplina	Início	Término	Carga Horária	Cred.	Freq.	Conc.	Exc.	Situação
FBC5780-2/1	Análise de Dados Aplicados às Pesquisas Biológicas	20/05/2013	30/06/2013	90	6	100	B	N	Concluída
FBC5752-2/4	Danos em Biomoléculas e o seu Papel no Monitoramento da Exposição a Agentes Tóxicos	05/06/2013	09/07/2013	45	3	100	B	N	Concluída
FBC5757-4/2	Tópicos em Análises Clínicas II	06/08/2013	18/11/2013	15	1	87	A	N	Concluída
EDM5791-5/11	Metodologia do Ensino Superior (Faculdade de Educação - Universidade de São Paulo)	13/08/2013	29/11/2013	120	8	100	A	N	Concluída
FBC5793-12/1	Tópicos em Análises Clínicas I	11/03/2014	23/06/2014	15	1	80	A	N	Concluída
FBC5747-2/1	Toxicologia Forense	11/05/2015	14/06/2015	60	4	100	A	N	Concluída
FBC5712-2/2	Métodos Modernos de Proteômica na Pesquisa em Análises Clínicas e Toxicólogicas	10/08/2015	25/09/2015	60	4	100	A	N	Concluída
FBC5802-3/8	Tópicos Avançados em Toxicologia I	08/03/2016	20/06/2016	15	1	75	A	N	Concluída
FBC5803-3/8	Sistemas de Garantia da Qualidade em Laboratórios de Ensaio	15/03/2016	28/03/2016	30	2	100	A	N	Concluída
FBC5784-3/9	Tópicos Avançados em Toxicologia II	02/08/2016	14/11/2016	15	0	-	-	N	Matrícula cancelada

	Créditos mínimos exigidos		Créditos obtidos
	Para exame de qualificação	Para depósito de tese	
Disciplinas:	0	25	30
Estágios:			
Total:	0	25	30

Créditos Atribuídos à Tese: 167

Conceito a partir de 02/01/1997:

A - Excelente, com direito a crédito; B - Bom, com direito a crédito; C - Regular, com direito a crédito; R - Reprovado; T - Transferência.

Um(1) crédito equivale a 15 horas de atividade programada.

Última ocorrência: Prorrogação em 15/02/2017
Impresso em: 29/06/2017 11:21:25

Janus - Sistema Administrativo da Pós-Graduação

Universidade de São Paulo
Faculdade de Ciências Farmacêuticas
Documento sem validade oficial

FICHA DO ALUNO

9143 - 8679238/1 - Carlos Andrey Gonzalez Blanco

Comissão julgadora da tese de doutorado:

NUSP	Nome	Vínculo	Função
453826	Ernani Pinto Junior	FCF - USP	Presidente

Última ocorrência: Prorrogação em 15/02/2017
Impresso em: 29/06/2017 11:21:25

Full list of significantly regulated proteins according to the One Sample T-test. T-test was performed to the H/L datasets created after treating HepG2 cells with 1 uM CYN during 6, 12 and 24 hrs, and analyzing their tryptic digests by nano LC-MS2.

Symbol	Entrez Gene Name	Expr Log Ratio 6 hrs	Expr Log Ratio 12 hrs	Expr Log Ratio 24 hrs	Location
APOH	apolipoprotein H	-1.123	-1.55	-2.507	Extracellular Space
FGB	fibrinogen beta chain	-0.953	-1.546	-1.268	Extracellular Space
AFP	alpha fetoprotein	-0.768	-1.448	-2.498	Extracellular Space
A2M	alpha-2-macroglobulin	-0.663	-1.377	-2.172	Extracellular Space
SERPINA1	serpin family A member 1	-0.742	-1.295	-2.54	Extracellular Space
AGT	angiotensinogen	-0.414	-1.161		Extracellular Space
CST3	cystatin C	-0.535	-1.16		Extracellular Space
F2	coagulation factor II, thrombin	-0.488	-1.012	-2.042	Extracellular Space
HLA-A	major histocompatibility complex, class I A	-0.442	-1.008	-2.057	Plasma Membrane
APOE	apolipoprotein E	-0.546	-0.942	-1.816	Extracellular Space
B2M	beta-2-microglobulin	-0.541	-0.913		Plasma Membrane
C3	complement C3		-0.846	-2.088	Extracellular Space
TF	transferrin	-0.198	-0.681	-1.997	Extracellular Space
TK1	thymidine kinase 1	-0.201	-0.669		Cytoplasm
APOB	apolipoprotein B	-0.332	-0.665	-1.835	Extracellular Space
BCAM	basal cell adhesion molecule (Lutheran blood group)		-0.664	-1.033	Plasma Membrane
LYZ	lysozyme	-0.368	-0.647	-1.413	Extracellular Space
LAMA5	laminin subunit alpha 5		-0.647		Extracellular Space
ITIH2	inter-alpha-trypsin inhibitor heavy chain 2	-0.214	-0.582	-1.074	Extracellular Space
GYS1	glycogen synthase 1		-0.537		Cytoplasm
F11R	F11 receptor		-0.38	-0.511	Plasma Membrane
TFRC	transferrin receptor	-0.183	-0.376	-0.472	Plasma Membrane
CTNNA1	catenin alpha 1		-0.373	-1.044	Plasma Membrane
DNAJC7	DnaJ heat shock protein family (Hsp40) member C7		-0.316	-0.377	Cytoplasm
HDLBP	high density lipoprotein binding protein		-0.304	-0.679	Nucleus
RAVER1	ribonucleoprotein, PTB binding 1		-0.301	-0.492	Nucleus
LRPAP1	LDL receptor related protein associated protein 1		-0.295	-0.56	Plasma Membrane
EIF4H	eukaryotic translation initiation factor 4H	-0.185	-0.287	-0.473	Cytoplasm
SNX1	sorting nexin 1		-0.254		Cytoplasm
BCAS2	BCAS2, pre-mRNA processing factor		-0.25	-0.193	Nucleus
SKP1	S-phase kinase associated protein 1		-0.223	-0.365	Nucleus
EHBP1	EH domain binding protein 1		-0.219	-0.263	Cytoplasm
DYNC1LI2	dynein cytoplasmic 1 light intermediate chain 2		-0.217	-0.45	Cytoplasm
HIGD2A	HIG1 hypoxia inducible domain family member 2A		-0.214		Cytoplasm
SART1	squamous cell carcinoma antigen recognized by T-cells 1		-0.207	-0.348	Nucleus
GCN1	GCN1, eIF2 alpha kinase activator homolog		-0.18	-0.401	Cytoplasm
GNPDA1	glucosamine-6-phosphate deaminase 1		-0.178		Cytoplasm
PAPSS1	3'-phosphoadenosine 5'-phosphosulfate synthase 1		-0.165	-0.267	Cytoplasm

NAA10	N(alpha)-acetyltransferase 10, NatA catalytic subunit		-0.148		Nucleus
SDF2L1	stromal cell derived factor 2 like 1		-0.094		Cytoplasm
PDIA4	protein disulfide isomerase family A member 4		-0.071		Cytoplasm
SNRPG	small nuclear ribonucleoprotein polypeptide G		-0.022		Nucleus
HMGB2	high mobility group box 2		0.062		Nucleus
GAPDH	glyceraldehyde-3-phosphate dehydrogenase		0.109		Cytoplasm
NPM1	nucleophosmin		0.12	0.255	Nucleus
EIF5A	eukaryotic translation initiation factor 5A		0.121	0.223	Cytoplasm
RFC4	replication factor C subunit 4		0.139		Nucleus
RPS27A	ribosomal protein S27a		0.157	-0.222	Cytoplasm
POLR3C	RNA polymerase III subunit C		0.167		Nucleus
ARCN1	archain 1		0.175		Cytoplasm
MAT1A	methionine adenosyltransferase 1A	0.106	0.2	0.29	Cytoplasm
RBM12	RNA binding motif protein 12		0.225		Nucleus
NOB1	NIN1/PSMD8 binding protein 1 homolog		0.234		Nucleus
GALE	UDP-galactose-4-epimerase		0.256	0.306	Cytoplasm
PABPC1	poly(A) binding protein cytoplasmic 1	0.228	0.338	0.572	Cytoplasm
YTHDF2	YTH N6-methyladenosine RNA binding protein 2		0.351		Cytoplasm
PSME3	proteasome activator subunit 3		0.366	0.251	Cytoplasm
CUTA	cutA divalent cation tolerance homolog		1.494		Cytoplasm
ORM1	orosomucoid 1	-0.589			Extracellular Space
CHCHD2	coiled-coil-helix-coiled-coil-helix domain containing 2	-0.533			Cytoplasm
SERPINF1	serpin family F member 1	-0.512			Extracellular Space
SLC38A2	solute carrier family 38 member 2	-0.508		-1.007	Plasma Membrane
ARPC5L	actin related protein 2/3 complex subunit 5 like	-0.474			Cytoplasm
ENPP1	ectonucleotide pyrophosphatase/phosphodiesterase 1	-0.463			Plasma Membrane
SERPINA3	serpin family A member 3	-0.432			Extracellular Space
GPX2	glutathione peroxidase 2	-0.368			Cytoplasm
DNAJC8	DnaJ heat shock protein family (Hsp40) member C8	-0.364			Nucleus
NCSTN	nicastrin	-0.353			Plasma Membrane
CETN2	centrin 2	-0.333		-1.184	Nucleus
ICAM1	intercellular adhesion molecule 1	-0.328		-0.696	Plasma Membrane
CLU	clusterin	-0.305			Cytoplasm
RTN4	reticulon 4	-0.3		-0.546	Cytoplasm
LGALS3	galectin 3	-0.273		-0.396	Extracellular Space
CARHSP1	calcium regulated heat stable protein 1	-0.272		-0.203	Cytoplasm
ITGA2	integrin subunit alpha 2	-0.267		-0.571	Plasma Membrane
CYB5A	cytochrome b5 type A	-0.263		-0.407	Cytoplasm
CRIP2	cysteine rich protein 2	-0.254		-0.348	Nucleus
SCARB2	scavenger receptor class B member 2	-0.254			Plasma Membrane
SH3BGRL3	SH3 domain binding glutamate rich protein like 3	-0.25		-0.242	Nucleus
CLPP	caseinolytic mitochondrial matrix peptidase proteolytic subunit	-0.242			Cytoplasm
GOLGB1	golgin B1	-0.238		-0.281	Cytoplasm
ATP6V1E1	ATPase H+ transporting V1 subunit E1	-0.237			Cytoplasm

UBE2L3	ubiquitin conjugating enzyme E2 L3	-0.232		-0.303	Nucleus
C1QBP	complement C1q binding protein	-0.223			Cytoplasm
ITGB1	integrin subunit beta 1	-0.223			Plasma Membrane
NDUFV2	NADH:ubiquinone oxidoreductase core subunit V2	-0.221		-0.423	Cytoplasm
DNAJC9	DnaJ heat shock protein family (Hsp40) member C9	-0.221			Nucleus
EIF2A	eukaryotic translation initiation factor 2A	-0.216		-0.332	Cytoplasm
MRPL40	mitochondrial ribosomal protein L40	-0.215		-0.103	Cytoplasm
STK4	serine/threonine kinase 4	-0.213			Cytoplasm
GCSH	glycine cleavage system protein H	-0.209			Cytoplasm
RCN2	reticulocalbin 2	-0.208		-0.229	Cytoplasm
NDUFS6	NADH:ubiquinone oxidoreductase subunit S6	-0.208			Cytoplasm
NDUFS8	NADH:ubiquinone oxidoreductase core subunit S8	-0.207			Cytoplasm
GRPEL1	GrpE like 1, mitochondrial	-0.201		-0.217	Cytoplasm
PLCB1	phospholipase C beta 1	-0.195			Cytoplasm
BTF3	basic transcription factor 3	-0.194		-0.474	Nucleus
TMED9	transmembrane p24 trafficking protein 9	-0.193		-0.353	Cytoplasm
PSMA2	proteasome subunit alpha 2	-0.193		-0.289	Cytoplasm
GRSF1	G-rich RNA sequence binding factor 1	-0.191			Cytoplasm
ACP1	acid phosphatase 1, soluble	-0.19			Cytoplasm
EIF4A1	eukaryotic translation initiation factor 4A1	-0.188		-0.32	Cytoplasm
RBBP4	RB binding protein 4, chromatin remodeling factor	-0.187		-0.637	Nucleus
VBP1	VHL binding protein 1	-0.187		-0.28	Cytoplasm
EXOSC5	exosome component 5	-0.187		-0.216	Nucleus
RBX1	ring-box 1	-0.187			Cytoplasm
RPLP2	ribosomal protein lateral stalk subunit P2	-0.187			Cytoplasm
BSG	basigin (Ok blood group)	-0.184		-0.319	Plasma Membrane
AKR1B10	aldo-keto reductase family 1 member B10	-0.184		0.189	Cytoplasm
CD59	CD59 molecule	-0.18			Plasma Membrane
SLC1A5	solute carrier family 1 member 5	-0.179			Plasma Membrane
GLB1	galactosidase beta 1	-0.178			Cytoplasm
UTP18	UTP18, small subunit processome component	-0.178			Nucleus
ARPC3	actin related protein 2/3 complex subunit 3	-0.166			Cytoplasm
SSU72	SSU72 homolog, RNA polymerase II CTD phosphatase	-0.159			Other
HSPB1	heat shock protein family B (small) member 1	-0.158		-0.585	Cytoplasm
EDF1	endothelial differentiation related factor 1	-0.158		-0.462	Nucleus
APEH	acylaminoacyl-peptide hydrolase	-0.155			Cytoplasm
ATP5D	ATP synthase, H+ transporting, mitochondrial F1 complex, delta subunit	-0.153			Cytoplasm
EIF2S3	eukaryotic translation initiation factor 2 subunit gamma	-0.15		-0.177	Cytoplasm
HPD	4-hydroxyphenylpyruvate dioxygenase	-0.15			Cytoplasm
PROSC	proline synthetase cotranscribed homolog (bacterial)	-0.148			Cytoplasm

CAPZA2	capping actin protein of muscle Z-line alpha subunit 2	-0.144			Cytoplasm
DYNLRB1	dynein light chain roadblock-type 1	-0.141		-0.334	Cytoplasm
LGALS1	galectin 1	-0.141		-0.094	Extracellular Space
ATP5B	ATP synthase, H+ transporting, mitochondrial F1 complex, beta polypeptide	-0.141			Cytoplasm
PSMB1	proteasome subunit beta 1	-0.14			Cytoplasm
SDF4	stromal cell derived factor 4	-0.14			Cytoplasm
SNW1	SNW domain containing 1	-0.139		-0.213	Nucleus
PGM2	phosphoglucomutase 2	-0.138		-0.236	Cytoplasm
GLRX5	glutaredoxin 5	-0.138		-0.233	Cytoplasm
EIF6	eukaryotic translation initiation factor 6	-0.138			Cytoplasm
UQCRB	ubiquinol-cytochrome c reductase binding protein	-0.136			Cytoplasm
ACTR2	ARP2 actin related protein 2 homolog	-0.135			Plasma Membrane
UFM1	ubiquitin fold modifier 1	-0.128			Cytoplasm
EIF4E	eukaryotic translation initiation factor 4E	-0.127		-0.23	Cytoplasm
FKBP10	FK506 binding protein 10	-0.127		-0.183	Cytoplasm
PSMB3	proteasome subunit beta 3	-0.124		-0.188	Cytoplasm
EPB41L2	erythrocyte membrane protein band 4.1 like 2	-0.123			Plasma Membrane
SF3B3	splicing factor 3b subunit 3	-0.12		-0.415	Nucleus
DNAJC10	DnaJ heat shock protein family (Hsp40) member C10	-0.115		-0.163	Cytoplasm
MCM2	minichromosome maintenance complex component 2	-0.114		-0.263	Nucleus
MYDGF	myeloid derived growth factor	-0.114			Extracellular Space
YWHAB	tyrosine 3-monooxygenase/tryptophan 5-monooxygenase activation protein beta	-0.114			Cytoplasm
HSD17B10	hydroxysteroid 17-beta dehydrogenase 10	-0.113			Cytoplasm
LMAN2	lectin, mannose binding 2	-0.109		-0.392	Cytoplasm
PSMC6	proteasome 26S subunit, ATPase 6	-0.108		-0.223	Nucleus
OTUB1	OTU deubiquitinase, ubiquitin aldehyde binding 1	-0.1			Cytoplasm
PRDX5	peroxiredoxin 5	-0.098			Cytoplasm
FGA	fibrinogen alpha chain	-0.095		-0.618	Extracellular Space
RPL17	ribosomal protein L17	-0.095		-0.151	Cytoplasm
PRDX3	peroxiredoxin 3	-0.095			Cytoplasm
BAG2	BCL2 associated athanogene 2	-0.092			Cytoplasm
NSFL1C	NSFL1 cofactor	-0.089		-0.219	Cytoplasm
CAP1	adenylate cyclase associated protein 1	-0.089		-0.049	Plasma Membrane
SERBP1	SERPINE1 mRNA binding protein 1	-0.088		-0.199	Cytoplasm
PCNA	proliferating cell nuclear antigen	-0.078		-0.262	Nucleus
GNAI2	G protein subunit alpha i2	-0.078		-0.193	Plasma Membrane
CALR	calreticulin	-0.075			Cytoplasm
SPTAN1	spectrin alpha, non-erythrocytic 1	-0.069			Plasma Membrane
TXNL1	thioredoxin like 1	-0.053			Cytoplasm
CPSF7	cleavage and polyadenylation specific factor 7	0.066		0.213	Nucleus
HNRNPU	heterogeneous nuclear ribonucleoprotein U	0.071			Nucleus
ANXA11	annexin A11	0.095			Nucleus
NOP56	NOP56 ribonucleoprotein	0.102		0.226	Nucleus

PAK2	p21 (RAC1) activated kinase 2	0.109		0.171	Cytoplasm
SRSF6	serine and arginine rich splicing factor 6	0.117		0.31	Nucleus
EIF1	eukaryotic translation initiation factor 1	0.146		0.486	Cytoplasm
UPF1	UPF1, RNA helicase and ATPase	0.164		0.384	Nucleus
PEG10	paternally expressed 10	0.174			Nucleus
IRF2BP2	interferon regulatory factor 2 binding protein 2	0.186		-0.197	Nucleus
UBXN4	UBX domain protein 4	0.187			Extracellular Space
STARD10	StAR related lipid transfer domain containing 10	0.188		0.311	Cytoplasm
RAB10	RAB10, member RAS oncogene family	0.207		0.204	Cytoplasm
TMEM126A	transmembrane protein 126A	0.217			Cytoplasm
DHRS2	dehydrogenase/reductase 2	0.284		0.525	Nucleus
MT2A	metallothionein 2A	0.375			Cytoplasm
SCD	stearoyl-CoA desaturase			-1.372	Cytoplasm
RRBP1	ribosome binding protein 1			-1.208	Cytoplasm
ST6GAL1	ST6 beta-galactoside alpha-2,6-sialyltransferase 1			-1.15	Cytoplasm
PEG3	paternally expressed 3			-1.121	Nucleus
TYMS	thymidylate synthetase			-1.056	Nucleus
CADM1	cell adhesion molecule 1			-0.869	Plasma Membrane
MAN1A1	mannosidase alpha class 1A member 1			-0.836	Cytoplasm
RBP4	retinol binding protein 4			-0.834	Extracellular Space
NEU1	neuraminidase 1			-0.783	Cytoplasm
MYH9	myosin heavy chain 9			-0.742	Cytoplasm
CYP51A1	cytochrome P450 family 51 subfamily A member 1			-0.733	Cytoplasm
SLC2A1	solute carrier family 2 member 1			-0.726	Plasma Membrane
MTDH	metadherin			-0.715	Cytoplasm
P4HA2	prolyl 4-hydroxylase subunit alpha 2			-0.715	Cytoplasm
DUSP9	dual specificity phosphatase 9			-0.705	Nucleus
AMBP	alpha-1-microglobulin/bikunin precursor			-0.693	Extracellular Space
FDFT1	farnesyl-diphosphate farnesyltransferase 1			-0.692	Cytoplasm
OAT	ornithine aminotransferase			-0.69	Cytoplasm
ELOB	elongin B			-0.687	Nucleus
PLOD2	procollagen-lysine,2-oxoglutarate 5-dioxygenase 2			-0.68	Cytoplasm
GLG1	golgi glycoprotein 1			-0.647	Cytoplasm
ARHGAP18	Rho GTPase activating protein 18			-0.638	Cytoplasm
SUN2	Sad1 and UNC84 domain containing 2			-0.628	Nucleus
PPT1	palmitoyl-protein thioesterase 1			-0.627	Cytoplasm
HK2	hexokinase 2			-0.617	Cytoplasm
FAM162A	family with sequence similarity 162 member A			-0.611	Cytoplasm
MINPP1	multiple inositol-polyphosphate phosphatase 1			-0.597	Cytoplasm
SORT1	sortilin 1			-0.593	Plasma Membrane
GGCX	gamma-glutamyl carboxylase			-0.568	Cytoplasm
TMEM214	transmembrane protein 214			-0.567	Extracellular Space
TUBG1	tubulin gamma 1			-0.56	Cytoplasm
PLXNB2	plexin B2			-0.553	Plasma Membrane
MVP	major vault protein			-0.545	Nucleus
JUP	junction plakoglobin			-0.524	Plasma Membrane

IDI1	isopentenyl-diphosphate delta isomerase 1			-0.519	Cytoplasm
PDXDC1	pyridoxal dependent decarboxylase domain containing 1			-0.51	Cytoplasm
PLOD1	procollagen-lysine,2-oxoglutarate 5-dioxygenase 1			-0.505	Cytoplasm
ELOC	elongin C			-0.504	Nucleus
ADI1	acireductone dioxygenase 1			-0.503	Nucleus
DSG2	desmoglein 2			-0.503	Plasma Membrane
TOP2A	topoisomerase (DNA) II alpha			-0.501	Nucleus
ACSL4	acyl-CoA synthetase long-chain family member 4			-0.5	Cytoplasm
PSAP	prosaposin			-0.498	Extracellular Space
ATL2	atlastin GTPase 2			-0.49	Cytoplasm
NDUFA2	NADH:ubiquinone oxidoreductase subunit A2			-0.475	Cytoplasm
RFC1	replication factor C subunit 1			-0.473	Nucleus
CLNS1A	chloride nucleotide-sensitive channel 1A			-0.472	Plasma Membrane
DHFR	dihydrofolate reductase			-0.471	Nucleus
MCM3	minichromosome maintenance complex component 3			-0.468	Nucleus
C4A/C4B	complement C4B (Chido blood group)			-0.467	Extracellular Space
RRM2	ribonucleotide reductase regulatory subunit M2			-0.462	Nucleus
CNN2	calponin 2			-0.46	Cytoplasm
CYP27A1	cytochrome P450 family 27 subfamily A member 1			-0.454	Cytoplasm
SDHA	succinate dehydrogenase complex flavoprotein subunit A			-0.454	Cytoplasm
ACAA1	acetyl-CoA acyltransferase 1			-0.451	Cytoplasm
GPC3	glypican 3			-0.446	Plasma Membrane
AAMP	angio associated migratory cell protein			-0.444	Plasma Membrane
SRPK1	SRSF protein kinase 1			-0.442	Nucleus
FN1	fibronectin 1			-0.438	Extracellular Space
EMC1	ER membrane protein complex subunit 1			-0.437	Plasma Membrane
GLRX3	glutaredoxin 3			-0.434	Cytoplasm
UGT2A3	UDP glucuronosyltransferase family 2 member A3			-0.428	Other
LSS	lanosterol synthase			-0.427	Cytoplasm
SLC16A3	solute carrier family 16 member 3			-0.414	Plasma Membrane
ALDOC	aldolase, fructose-bisphosphate C			-0.41	Cytoplasm
DDX3X	DEAD-box helicase 3, X-linked			-0.401	Cytoplasm
SEC23B	Sec23 homolog B, coat complex II component			-0.4	Extracellular Space
SPTLC1	serine palmitoyltransferase long chain base subunit 1			-0.4	Cytoplasm
SAMHD1	SAM and HD domain containing deoxynucleoside triphosphate triphosphohydrolase 1			-0.396	Nucleus
TRIM71	tripartite motif containing 71			-0.395	Cytoplasm
CSNK1A1	casein kinase 1 alpha 1			-0.394	Cytoplasm
PRKAR1A	protein kinase cAMP-dependent type I regulatory subunit alpha			-0.39	Cytoplasm
SEC61B	Sec61 translocon beta subunit			-0.39	Cytoplasm
SEC24D	SEC24 homolog D, COPII coat complex component			-0.388	Cytoplasm

TTC38	tetratricopeptide repeat domain 38			-0.388	Cytoplasm
DUSP3	dual specificity phosphatase 3			-0.384	Cytoplasm
IPO9	importin 9			-0.382	Nucleus
NFS1	NFS1, cysteine desulfurase			-0.382	Cytoplasm
TFB1M	transcription factor B1, mitochondrial			-0.382	Cytoplasm
ASGR1	asialoglycoprotein receptor 1			-0.381	Plasma Membrane
RNF20	ring finger protein 20			-0.381	Nucleus
FIS1	fission, mitochondrial 1			-0.376	Cytoplasm
POLR1C	RNA polymerase I subunit C			-0.375	Nucleus
ERO1A	endoplasmic reticulum oxidoreductase 1 alpha			-0.374	Cytoplasm
MYL6	myosin light chain 6			-0.374	Cytoplasm
ASNA1	arsA arsenite transporter, ATP-binding, homolog 1 (bacterial)			-0.372	Nucleus
NUP50	nucleoporin 50			-0.368	Nucleus
RANGAP1	Ran GTPase activating protein 1			-0.366	Nucleus
A1CF	APOBEC1 complementation factor			-0.364	Nucleus
TRIM25	tripartite motif containing 25			-0.363	Cytoplasm
PAF1	PAF1 homolog, Paf1/RNA polymerase II complex component			-0.362	Nucleus
TCAF1	TRPM8 channel associated factor 1			-0.362	Plasma Membrane
UQCRC2	ubiquinol-cytochrome c reductase core protein II			-0.362	Cytoplasm
CSTB	cystatin B			-0.359	Cytoplasm
WASHC4	WASH complex subunit 4			-0.359	Cytoplasm
EPPK1	epiplakin 1			-0.358	Cytoplasm
DNAJA1	DnaJ heat shock protein family (Hsp40) member A1			-0.356	Nucleus
POLDIP3	DNA polymerase delta interacting protein 3			-0.356	Nucleus
PIN4	peptidylprolyl cis/trans isomerase, NIMA-interacting 4			-0.354	Nucleus
RAD23B	RAD23 homolog B, nucleotide excision repair protein			-0.353	Nucleus
CWC27	CWC27 spliceosome associated protein homolog			-0.35	Nucleus
AIP	aryl hydrocarbon receptor interacting protein			-0.345	Nucleus
GPT2	glutamic--pyruvic transaminase 2			-0.345	Cytoplasm
UROD	uroporphyrinogen decarboxylase			-0.344	Cytoplasm
DNAJA3	DnaJ heat shock protein family (Hsp40) member A3			-0.342	Cytoplasm
USP10	ubiquitin specific peptidase 10			-0.341	Cytoplasm
EMC7	ER membrane protein complex subunit 7			-0.339	Cytoplasm
GRN	granulin precursor			-0.334	Extracellular Space
PLS3	plastin 3			-0.33	Cytoplasm
EPN1	epsin 1			-0.329	Plasma Membrane
TUBB3	tubulin beta 3 class III			-0.325	Cytoplasm
CRNKL1	crooked neck pre-mRNA splicing factor 1			-0.322	Nucleus
DUT	deoxyuridine triphosphatase			-0.322	Nucleus
PTGES2	prostaglandin E synthase 2			-0.322	Cytoplasm
DDX23	DEAD-box helicase 23			-0.32	Nucleus
STXBP2	syntaxin binding protein 2			-0.319	Plasma Membrane
SRP9	signal recognition particle 9			-0.317	Cytoplasm

PDCD5	programmed cell death 5			-0.314	Nucleus
PSMA7	proteasome subunit alpha 7			-0.314	Cytoplasm
MUT	methylmalonyl-CoA mutase			-0.312	Cytoplasm
P3H1	prolyl 3-hydroxylase 1			-0.312	Nucleus
MCM5	minichromosome maintenance complex component 5			-0.31	Nucleus
UQCRC1	ubiquinol-cytochrome c reductase core protein I			-0.309	Cytoplasm
DHX30	DExH-box helicase 30			-0.308	Nucleus
NDUFA6	NADH:ubiquinone oxidoreductase subuni A6			-0.307	Cytoplasm
PAH	phenylalanine hydroxylase			-0.306	Cytoplasm
KPNA2	karyopherin subunit alpha 2			-0.304	Nucleus
PGRMC2	progesterone receptor membrane component 2			-0.303	Nucleus
ARL2	ADP ribosylation factor like GTPase 2			-0.302	Cytoplasm
PFDN5	prefoldin subunit 5			-0.302	Nucleus
HNRNPM	heterogeneous nuclear ribonucleoprotein M			-0.299	Nucleus
MCM4	minichromosome maintenance complex component 4			-0.299	Nucleus
ATP6V1A	ATPase H+ transporting V1 subunit A			-0.298	Plasma Membrane
SNX12	sorting nexin 12			-0.298	Cytoplasm
NPC2	NPC intracellular cholesterol transporter 2			-0.297	Extracellular Space
KANK1	KN motif and ankyrin repeat domains 1			-0.294	Nucleus
TM9SF2	transmembrane 9 superfamily member 2			-0.292	Plasma Membrane
SEC13	SEC13 homolog, nuclear pore and COPII coat complex component			-0.291	Cytoplasm
TLN1	talin 1			-0.291	Plasma Membrane
ACSS2	acyl-CoA synthetase short-chain family member 2			-0.29	Cytoplasm
EXOSC6	exosome component 6			-0.29	Nucleus
ECI2	enoyl-CoA delta isomerase 2			-0.289	Cytoplasm
STMN1	stathmin 1			-0.289	Cytoplasm
PPP6C	protein phosphatase 6 catalytic subunit			-0.285	Nucleus
CCAR1	cell division cycle and apoptosis regulato 1			-0.283	Nucleus
NDUFS1	NADH:ubiquinone oxidoreductase core subunit S1			-0.283	Cytoplasm
ACAT2	acetyl-CoA acetyltransferase 2			-0.282	Cytoplasm
CUL4B	cullin 4B			-0.276	Nucleus
FARSA	phenylalanyl-tRNA synthetase alpha subunit			-0.273	Cytoplasm
MSH2	mutS homolog 2			-0.272	Nucleus
MRPL44	mitochondrial ribosomal protein L44			-0.27	Cytoplasm
UQCRFS1	ubiquinol-cytochrome c reductase, Rieske iron-sulfur polypeptide 1			-0.27	Cytoplasm
COPS4	COP9 signalosome subunit 4			-0.269	Cytoplasm
NUCB1	nucleobindin 1			-0.269	Cytoplasm
NDUFS3	NADH:ubiquinone oxidoreductase core subunit S3			-0.267	Cytoplasm
TM9SF4	transmembrane 9 superfamily member 4			-0.265	Cytoplasm
RNF213	ring finger protein 213			-0.261	Cytoplasm
IKBIP	IKBKB interacting protein			-0.259	Cytoplasm
QPRT	quinolinate phosphoribosyltransferase			-0.259	Cytoplasm

SRSF9	serine and arginine rich splicing factor 9			-0.259	Nucleus
TWF1	twinfilin actin binding protein 1			-0.259	Cytoplasm
CKB	creatine kinase B			-0.258	Cytoplasm
PSMA4	proteasome subunit alpha 4			-0.258	Cytoplasm
SEC61A1	Sec61 translocon alpha 1 subunit			-0.258	Cytoplasm
HNMT	histamine N-methyltransferase			-0.256	Cytoplasm
NDUFB10	NADH:ubiquinone oxidoreductase subuni B10			-0.255	Cytoplasm
P4HA1	prolyl 4-hydroxylase subunit alpha 1			-0.255	Cytoplasm
IK	IK cytokine, down-regulator of HLA II			-0.254	Extracellular Space
CHMP4B	charged multivesicular body protein 4B			-0.251	Cytoplasm
FDPS	farnesyl diphosphate synthase			-0.251	Cytoplasm
NSF	N-ethylmaleimide sensitive factor, vesicle fusing ATPase			-0.251	Cytoplasm
HCFC1	host cell factor C1			-0.249	Nucleus
PSMD2	proteasome 26S subunit, non-ATPase 2			-0.249	Cytoplasm
LRPPRC	leucine rich pentatricopeptide repeat containing			-0.248	Cytoplasm
CPSF2	cleavage and polyadenylation specific factor 2			-0.246	Nucleus
SNRPA1	small nuclear ribonucleoprotein polypeptide A'			-0.244	Nucleus
TPD52L2	tumor protein D52 like 2			-0.243	Cytoplasm
CDK6	cyclin dependent kinase 6			-0.242	Nucleus
PSMC3	proteasome 26S subunit, ATPase 3			-0.242	Nucleus
NUP107	nucleoporin 107			-0.241	Nucleus
ACIN1	apoptotic chromatin condensation inducer 1			-0.24	Nucleus
EIF2B4	eukaryotic translation initiation factor 2B subunit delta			-0.24	Cytoplasm
SOD1	superoxide dismutase 1			-0.24	Cytoplasm
ACADVL	acyl-CoA dehydrogenase, very long chain			-0.239	Cytoplasm
CRTAP	cartilage associated protein			-0.239	Extracellular Space
EHD1	EH domain containing 1			-0.239	Cytoplasm
VTA1	vesicle trafficking 1			-0.239	Cytoplasm
COPG2	coatomer protein complex subunit gamma 2			-0.238	Cytoplasm
IPO5	importin 5			-0.238	Nucleus
ALDH2	aldehyde dehydrogenase 2 family (mitochondrial)			-0.237	Cytoplasm
SSR1	signal sequence receptor subunit 1			-0.236	Cytoplasm
PSMC4	proteasome 26S subunit, ATPase 4			-0.235	Nucleus
IQGAP1	IQ motif containing GTPase activating protein 1			-0.234	Cytoplasm
CDC37	cell division cycle 37			-0.233	Cytoplasm
LAMP1	lysosomal associated membrane protein 1			-0.233	Plasma Membrane
ACLY	ATP citrate lyase			-0.232	Cytoplasm
PPP1CA	protein phosphatase 1 catalytic subunit alpha			-0.232	Cytoplasm
RPL36	ribosomal protein L36			-0.231	Cytoplasm
MSH6	mutS homolog 6			-0.23	Nucleus
PSMB4	proteasome subunit beta 4			-0.23	Cytoplasm
ATP5H	ATP synthase, H+ transporting, mitochondrial Fo complex subunit D			-0.229	Cytoplasm

NUMA1	nuclear mitotic apparatus protein 1			-0.229	Nucleus
GTF3C5	general transcription factor IIIC subunit 5			-0.228	Nucleus
SF3B2	splicing factor 3b subunit 2			-0.228	Nucleus
TMX1	thioredoxin related transmembrane protein 1			-0.227	Cytoplasm
ALDH6A1	aldehyde dehydrogenase 6 family member A1			-0.225	Cytoplasm
DECR1	2,4-dienoyl-CoA reductase 1			-0.224	Cytoplasm
OGFOD1	2-oxoglutarate and iron dependen oxygenase domain containing 1			-0.223	Cytoplasm
RBBP7	RB binding protein 7, chromatin remodeling factor			-0.22	Nucleus
NAPA	NSF attachment protein alpha			-0.218	Cytoplasm
TXNDC5	thioredoxin domain containing 5			-0.217	Cytoplasm
HDAC1	histone deacetylase 1			-0.216	Nucleus
PMPCA	peptidase, mitochondrial processing alpha subunit			-0.216	Cytoplasm
MRPS9	mitochondrial ribosomal protein S9			-0.214	Cytoplasm
AGFG2	ArfGAP with FG repeats 2			-0.213	Other
CTNNB1	catenin beta 1			-0.212	Nucleus
PRMT1	protein arginine methyltransferase 1			-0.211	Nucleus
BCCIP	BRCA2 and CDKN1A interacting protein			-0.209	Nucleus
LGALS3BP	galectin 3 binding protein			-0.209	Plasma Membrane
NDUFB8	NADH:ubiquinone oxidoreductase subuni B8			-0.209	Cytoplasm
PPP1R8	protein phosphatase 1 regulatory subuni 8			-0.209	Nucleus
RPL38	ribosomal protein L38			-0.209	Cytoplasm
RPS17	ribosomal protein S17			-0.209	Cytoplasm
PSMA3	proteasome subunit alpha 3			-0.208	Cytoplasm
ANXA4	annexin A4			-0.207	Plasma Membrane
SF3B1	splicing factor 3b subunit 1			-0.207	Nucleus
ATOX1	antioxidant 1 copper chaperone			-0.205	Cytoplasm
TARDBP	TAR DNA binding protein			-0.204	Nucleus
PEF1	penta-EF-hand domain containing 1			-0.203	Cytoplasm
SULT1A3/SU	sulfotransferase family 1A member 3			-0.203	Cytoplasm
TPD52	tumor protein D52			-0.203	Cytoplasm
ALDH1A1	aldehyde dehydrogenase 1 family member A1			-0.202	Cytoplasm
ESYT1	extended synaptotagmin 1			-0.201	Cytoplasm
HNRNPL	heterogeneous nuclear ribonucleoprotei L			-0.201	Nucleus
PPA2	pyrophosphatase (inorganic) 2			-0.201	Cytoplasm
RAB11B	RAB11B, member RAS oncogene family			-0.2	Cytoplasm
VIL1	villin 1			-0.2	Cytoplasm
SNX6	sorting nexin 6			-0.199	Cytoplasm
KPNA3	karyopherin subunit alpha 3			-0.198	Nucleus
PSMA1	proteasome subunit alpha 1			-0.197	Cytoplasm
ALYREF	Aly/REF export factor			-0.195	Nucleus
FTO	FTO, alpha-ketoglutarate dependent dioxygenase			-0.195	Nucleus
PGAM1	phosphoglycerate mutase 1			-0.195	Cytoplasm
METAP2	methionyl aminopeptidase 2			-0.194	Cytoplasm

ANP32E	acidic nuclear phosphoprotein 32 family member E			-0.193	Nucleus
SMC1A	structural maintenance of chromosomes 1A			-0.193	Nucleus
SPR	sepiapterin reductase (7,8-dihydrobiopterin:NADP+ oxidoreductase)			-0.193	Cytoplasm
DDX47	DEAD-box helicase 47			-0.191	Nucleus
GFM1	G elongation factor mitochondrial 1			-0.191	Cytoplasm
GALK1	galactokinase 1			-0.19	Cytoplasm
RAB1B	RAB1B, member RAS oncogene family			-0.19	Cytoplasm
RHOA	ras homolog family member A			-0.189	Cytoplasm
CAPZA1	capping actin protein of muscle Z-line alpha subunit 1			-0.188	Cytoplasm
NAE1	NEDD8 activating enzyme E1 subunit 1			-0.188	Cytoplasm
PGP	phosphoglycolate phosphatase			-0.188	Other
NUP93	nucleoporin 93			-0.186	Nucleus
RPL35	ribosomal protein L35			-0.186	Cytoplasm
ACSL3	acyl-CoA synthetase long-chain family member 3			-0.185	Cytoplasm
ATG4B	autophagy related 4B cysteine peptidase			-0.185	Cytoplasm
DYNC1LI1	dynein cytoplasmic 1 light intermediate chain 1			-0.185	Cytoplasm
HSP90AA1	heat shock protein 90 alpha family class A member 1			-0.185	Cytoplasm
PSMC2	proteasome 26S subunit, ATPase 2			-0.185	Nucleus
RRP1	ribosomal RNA processing 1			-0.185	Nucleus
BCLAF1	BCL2 associated transcription factor 1			-0.184	Nucleus
PLEC	plectin			-0.184	Cytoplasm
RPS10	ribosomal protein S10			-0.183	Cytoplasm
SKIV2L2	Ski2 like RNA helicase 2			-0.18	Nucleus
DDB1	damage specific DNA binding protein 1			-0.179	Nucleus
DNAJB1	DnaJ heat shock protein family (Hsp40) member B1			-0.179	Nucleus
PSMD11	proteasome 26S subunit, non-ATPase 11			-0.177	Cytoplasm
ECHS1	enoyl-CoA hydratase, short chain 1			-0.176	Cytoplasm
CALM1 (incl	calmodulin 1			-0.175	Cytoplasm
LMO7	LIM domain 7			-0.175	Cytoplasm
PSMC1	proteasome 26S subunit, ATPase 1			-0.175	Nucleus
MGME1	mitochondrial genome maintenance exonuclease 1			-0.174	Cytoplasm
SUCLA2	succinate-CoA ligase ADP-forming beta subunit			-0.171	Cytoplasm
RPL10	ribosomal protein L10			-0.17	Cytoplasm
TIMM13	translocase of inner mitochondrial membrane 13			-0.17	Cytoplasm
NDUFV1	NADH:ubiquinone oxidoreductase core subunit V1			-0.169	Cytoplasm
MCM6	minichromosome maintenance complex component 6			-0.168	Nucleus
CALU	calumenin			-0.167	Cytoplasm
FASN	fatty acid synthase			-0.167	Cytoplasm
RUVBL2	RuvB like AAA ATPase 2			-0.167	Nucleus
SERPINB9	serpin family B member 9			-0.167	Cytoplasm

CPSF1	cleavage and polyadenylation specific factor 1			-0.165	Nucleus
VAT1	vesicle amine transport 1			-0.162	Plasma Membrane
POLR2B	RNA polymerase II subunit B			-0.161	Nucleus
ANXA2	annexin A2			-0.158	Plasma Membrane
PITPNB	phosphatidylinositol transfer protein beta			-0.158	Cytoplasm
HNRNPA3	heterogeneous nuclear ribonucleoprotein A3			-0.156	Nucleus
PECR	peroxisomal trans-2-enoyl-CoA reductase			-0.156	Cytoplasm
LAD1	ladinin 1			-0.154	Extracellular Space
PGK1	phosphoglycerate kinase 1			-0.154	Cytoplasm
CBX3	chromobox 3			-0.153	Nucleus
HMGCS1	3-hydroxy-3-methylglutaryl-CoA synthase 1			-0.153	Cytoplasm
PEPD	peptidase D			-0.151	Cytoplasm
CAPZB	capping actin protein of muscle Z-line beta subunit			-0.147	Cytoplasm
MYH10	myosin heavy chain 10			-0.146	Cytoplasm
RBM4	RNA binding motif protein 4			-0.146	Nucleus
GBE1	1,4-alpha-glucan branching enzyme 1			-0.145	Cytoplasm
NACA	nascent polypeptide-associated complex alpha subunit			-0.145	Cytoplasm
TRAP1	TNF receptor associated protein 1			-0.145	Cytoplasm
DBI	diazepam binding inhibitor, acyl-CoA binding protein			-0.143	Cytoplasm
TKFC	triokinase and FMN cyclase			-0.143	Cytoplasm
RPL9	ribosomal protein L9			-0.142	Nucleus
TMED10	transmembrane p24 trafficking protein 10			-0.142	Cytoplasm
CHMP5	charged multivesicular body protein 5			-0.141	Cytoplasm
TJP2	tight junction protein 2			-0.141	Plasma Membrane
UBE2N	ubiquitin conjugating enzyme E2 N			-0.139	Cytoplasm
PSMD7	proteasome 26S subunit, non-ATPase 7			-0.138	Cytoplasm
RPS19	ribosomal protein S19			-0.138	Cytoplasm
SLIRP	SRA stem-loop interacting RNA binding protein			-0.137	Cytoplasm
MANF	mesencephalic astrocyte derived neurotrophic factor			-0.136	Extracellular Space
PSMD4	proteasome 26S subunit, non-ATPase 4			-0.136	Cytoplasm
TIMM50	translocase of inner mitochondrial membrane 50			-0.136	Cytoplasm
PSMA6	proteasome subunit alpha 6			-0.135	Cytoplasm
ERP29	endoplasmic reticulum protein 29			-0.132	Cytoplasm
RPL13	ribosomal protein L13			-0.132	Nucleus
APRT	adenine phosphoribosyltransferase			-0.131	Cytoplasm
RPS13	ribosomal protein S13			-0.131	Cytoplasm
EIF4G1	eukaryotic translation initiation factor 4 gamma 1			-0.129	Cytoplasm
MIF	macrophage migration inhibitory factor (glycosylation-inhibiting factor)			-0.129	Extracellular Space
RNPEP	arginyl aminopeptidase			-0.129	Cytoplasm
EIF3G	eukaryotic translation initiation factor 3 subunit G			-0.128	Cytoplasm
SEH1L	SEH1 like nucleoporin			-0.128	Cytoplasm
TXNDC17	thioredoxin domain containing 17			-0.128	Cytoplasm

TBCA	tubulin folding cofactor A			-0.127	Cytoplasm
ABCF1	ATP binding cassette subfamily F member 1			-0.126	Cytoplasm
LONP1	lon peptidase 1, mitochondrial			-0.124	Cytoplasm
RPL7	ribosomal protein L7			-0.124	Nucleus
SUCLG2	succinate-CoA ligase GDP-forming beta subunit			-0.122	Cytoplasm
MRPS30	mitochondrial ribosomal protein S30			-0.121	Cytoplasm
COPB2	coatomer protein complex subunit beta 2			-0.12	Cytoplasm
FABP1	fatty acid binding protein 1			-0.12	Cytoplasm
PRKDC	protein kinase, DNA-activated, catalytic polypeptide			-0.12	Nucleus
SPTBN1	spectrin beta, non-erythrocytic 1			-0.12	Plasma Membrane
SF3A1	splicing factor 3a subunit 1			-0.117	Nucleus
HNRNPH3	heterogeneous nuclear ribonucleoprotein H3			-0.116	Nucleus
ROCK2	Rho associated coiled-coil containing protein kinase 2			-0.115	Cytoplasm
SMU1	DNA replication regulator and spliceosomal factor			-0.115	Nucleus
ADH5	alcohol dehydrogenase 5 (class III), chi polypeptide			-0.114	Cytoplasm
RHOC	ras homolog family member C			-0.114	Plasma Membrane
HSP90AB1	heat shock protein 90 alpha family class B member 1			-0.111	Cytoplasm
PDIA6	protein disulfide isomerase family A member 6			-0.111	Cytoplasm
RPS5	ribosomal protein S5			-0.111	Cytoplasm
RPS14	ribosomal protein S14			-0.108	Cytoplasm
ASPSCR1	ASPSCR1, UBX domain containing tether for SLC2A4			-0.105	Cytoplasm
GLOD4	glyoxalase domain containing 4			-0.103	Cytoplasm
PGM1	phosphoglucomutase 1			-0.103	Cytoplasm
RPL14	ribosomal protein L14			-0.1	Cytoplasm
RPL7A	ribosomal protein L7a			-0.099	Cytoplasm
ELAVL1	ELAV like RNA binding protein 1			-0.098	Cytoplasm
EFTUD2	elongation factor Tu GTP binding domain containing 2			-0.094	Nucleus
COPE	coatomer protein complex subunit epsilon			-0.091	Cytoplasm
PDHB	pyruvate dehydrogenase (lipoamide) beta			-0.091	Cytoplasm
RPL8	ribosomal protein L8			-0.089	Cytoplasm
ATP5C1	ATP synthase, H+ transporting, mitochondrial F1 complex, gamma polypeptide 1			-0.088	Cytoplasm
RPL23	ribosomal protein L23			-0.086	Cytoplasm
PRPF8	pre-mRNA processing factor 8			-0.084	Nucleus
MAPK1	mitogen-activated protein kinase 1			-0.08	Cytoplasm
RPS21	ribosomal protein S21			-0.076	Cytoplasm
HSPA1A/HS	heat shock protein family A (Hsp70) member 1A			-0.075	Cytoplasm
RPSA	ribosomal protein SA			-0.073	Cytoplasm
ALDOA	aldolase, fructose-bisphosphate A			-0.07	Cytoplasm
RPS20	ribosomal protein S20			-0.069	Cytoplasm

ETFB	electron transfer flavoprotein beta subunit			-0.067	Cytoplasm
GANAB	glucosidase II alpha subunit			-0.067	Cytoplasm
HSPA8	heat shock protein family A (Hsp70) member 8			-0.066	Cytoplasm
CCT8	chaperonin containing TCP1 subunit 8			-0.065	Cytoplasm
ACTN4	actinin alpha 4			0.023	Cytoplasm
LDHA	lactate dehydrogenase A			0.05	Cytoplasm
TUFM	Tu translation elongation factor, mitochondrial			0.056	Cytoplasm
PSAT1	phosphoserine aminotransferase 1			0.059	Cytoplasm
CSNK2A1	casein kinase 2 alpha 1			0.062	Nucleus
HSPD1	heat shock protein family D (Hsp60) member 1			0.071	Cytoplasm
UGGT1	UDP-glucose glycoprotein glucosyltransferase 1			0.071	Cytoplasm
PEBP1	phosphatidylethanolamine binding protein 1			0.073	Cytoplasm
ACTN1	actinin alpha 1			0.074	Cytoplasm
ALDH1B1	aldehyde dehydrogenase 1 family member B1			0.076	Cytoplasm
EPRS	glutamyl-prolyl-tRNA synthetase			0.078	Cytoplasm
HSP90B1	heat shock protein 90 beta family member 1			0.079	Cytoplasm
RPS23	ribosomal protein S23			0.08	Cytoplasm
CNDP2	CNDP dipeptidase 2 (metallopeptidase M20 family)			0.086	Cytoplasm
NANS	N-acetylneuraminate synthase			0.087	Cytoplasm
FLNA	filamin A			0.088	Cytoplasm
ACTG1	actin gamma 1			0.089	Cytoplasm
FDXR	ferredoxin reductase			0.089	Cytoplasm
FUBP1	far upstream element binding protein 1			0.09	Nucleus
THUMPD1	THUMP domain containing 1			0.092	Nucleus
CES2	carboxylesterase 2			0.093	Cytoplasm
YWHAZ	tyrosine 3-monooxygenase/tryptophan 5-monooxygenase activation protein zeta			0.093	Cytoplasm
NSUN2	NOP2/Sun RNA methyltransferase family member 2			0.094	Nucleus
SPATA18	spermatogenesis associated 18			0.096	Cytoplasm
ANXA5	annexin A5			0.097	Plasma Membrane
ARHGDIA	Rho GDP dissociation inhibitor alpha			0.098	Cytoplasm
ACO2	aconitase 2			0.099	Cytoplasm
NME2	NME/NM23 nucleoside diphosphate kinase 2			0.101	Nucleus
HDGF	hepatoma derived growth factor			0.102	Extracellular Space
PARK7	Parkinsonism associated deglycase			0.103	Nucleus
GOT2	glutamic-oxaloacetic transaminase 2			0.104	Cytoplasm
TCEA1	transcription elongation factor A1			0.104	Nucleus
FLNB	filamin B			0.105	Cytoplasm
RNH1	ribonuclease/angiogenin inhibitor 1			0.105	Cytoplasm
OGDH	oxoglutarate dehydrogenase			0.106	Cytoplasm
PFAS	phosphoribosylformylglycinamidine synthase			0.107	Cytoplasm
UBA1	ubiquitin like modifier activating enzyme 1			0.108	Cytoplasm
FKBP4	FK506 binding protein 4			0.11	Nucleus

PIR	pirin			0.112	Nucleus
ATIC	5-aminoimidazole-4-carboxamide ribonucleotide formyltransferase/IMP cyclohydrolase			0.113	Cytoplasm
HNRNPUL1	heterogeneous nuclear ribonucleoprotein U like 1			0.114	Nucleus
WDR1	WD repeat domain 1			0.114	Extracellular Space
GLUD1	glutamate dehydrogenase 1			0.115	Cytoplasm
GSTO1	glutathione S-transferase omega 1			0.115	Cytoplasm
TARS	threonyl-tRNA synthetase			0.12	Nucleus
IGF2BP3	insulin like growth factor 2 mRNA binding protein 3			0.122	Cytoplasm
TES	testin LIM domain protein			0.122	Plasma Membrane
DYNC1I2	dynein cytoplasmic 1 intermediate chain 2			0.123	Cytoplasm
DAZAP1	DAZ associated protein 1			0.126	Other
AFG3L2	AFG3 like matrix AAA peptidase subunit 2			0.127	Cytoplasm
ST13	suppression of tumorigenicity 13 (colon carcinoma) (Hsp70 interacting protein)			0.127	Cytoplasm
CPNE3	copine 3			0.128	Cytoplasm
HSPH1	heat shock protein family H (Hsp110) member 1			0.128	Cytoplasm
CMPK1	cytidine/uridine monophosphate kinase 1			0.131	Nucleus
RAB7A	RAB7A, member RAS oncogene family			0.132	Cytoplasm
DKC1	dyskerin pseudouridine synthase 1			0.133	Nucleus
HNRNPD	heterogeneous nuclear ribonucleoprotein D			0.133	Nucleus
MRTO4	MRT4 homolog, ribosome maturation factor			0.133	Cytoplasm
LMNB1	lamin B1			0.134	Nucleus
NOP10	NOP10 ribonucleoprotein			0.134	Nucleus
SRM	spermidine synthase			0.134	Cytoplasm
HSPA5	heat shock protein family A (Hsp70) member 5			0.135	Cytoplasm
SPATS2L	spermatogenesis associated serine rich 2 like			0.135	Nucleus
SSBP1	single stranded DNA binding protein 1			0.136	Cytoplasm
CAMK2D	calcium/calmodulin dependent protein kinase II delta			0.138	Cytoplasm
MYO1B	myosin IB			0.139	Cytoplasm
TSR1	TSR1, ribosome maturation factor			0.142	Nucleus
AKR1C3	aldo-keto reductase family 1 member C3			0.143	Cytoplasm
ILF3	interleukin enhancer binding factor 3			0.143	Nucleus
MDH2	malate dehydrogenase 2			0.144	Cytoplasm
RAC1	ras-related C3 botulinum toxin substrate 1 (rho family, small GTP binding protein Rac1)			0.144	Plasma Membrane
PUS1	pseudouridylate synthase 1			0.145	Nucleus
HSPA4L	heat shock protein family A (Hsp70) member 4 like			0.146	Cytoplasm
EEF1D	eukaryotic translation elongation factor 1 delta			0.147	Cytoplasm
ACOT7	acyl-CoA thioesterase 7			0.148	Cytoplasm
PMM2	phosphomannomutase 2			0.148	Cytoplasm

RAE1	ribonucleic acid export 1			0.149	Nucleus
NUP153	nucleoporin 153			0.15	Nucleus
TXN	thioredoxin			0.15	Cytoplasm
USP7	ubiquitin specific peptidase 7			0.15	Nucleus
HNRNPA2B	heterogeneous nuclear ribonucleoprotein A2/B1			0.151	Nucleus
PDPR	pyruvate dehydrogenase phosphatase regulatory subunit			0.151	Cytoplasm
SFPQ	splicing factor proline and glutamine rich			0.152	Nucleus
SRSF1	serine and arginine rich splicing factor 1			0.155	Nucleus
XPO1	exportin 1			0.155	Nucleus
CRYZ	crystallin zeta			0.157	Cytoplasm
WARS	tryptophanyl-tRNA synthetase			0.157	Cytoplasm
BUB3	BUB3, mitotic checkpoint protein			0.158	Nucleus
IGF2BP1	insulin like growth factor 2 mRNA binding protein 1			0.159	Cytoplasm
AKR1A1	aldo-keto reductase family 1 member A1			0.162	Cytoplasm
LYAR	Ly1 antibody reactive			0.164	Plasma Membrane
UTP14A	UTP14A small subunit processome component			0.164	Nucleus
PRKCSH	protein kinase C substrate 80K-H			0.166	Cytoplasm
RALY	RALY heterogeneous nuclear ribonucleoprotein			0.169	Nucleus
FBL	fibrillarin			0.17	Nucleus
PLOD3	procollagen-lysine,2-oxoglutarate 5-dioxygenase 3			0.17	Cytoplasm
CTSB	cathepsin B			0.174	Cytoplasm
ABAT	4-aminobutyrate aminotransferase			0.175	Cytoplasm
CS	citrate synthase			0.175	Cytoplasm
NXF1	nuclear RNA export factor 1			0.176	Nucleus
NOP58	NOP58 ribonucleoprotein			0.177	Nucleus
GART	phosphoribosylglycinamide formyltransferase, phosphoribosylglycinamide synthetase phosphoribosylaminoimidazole synthetase			0.179	Cytoplasm
TKT	transketolase			0.18	Cytoplasm
PCK2	phosphoenolpyruvate carboxykinase 2 mitochondrial			0.181	Cytoplasm
RPRD1B	regulation of nuclear pre-mRNA domain containing 1B			0.182	Nucleus
AFDN	afadin, adherens junction formation factor			0.184	Nucleus
THRAP3	thyroid hormone receptor associated protein 3			0.185	Nucleus
GEMIN5	gem nuclear organelle associated protein 5			0.186	Nucleus
SLC25A13	solute carrier family 25 member 13			0.187	Cytoplasm
GGH	gamma-glutamyl hydrolase			0.189	Cytoplasm
BZW2	basic leucine zipper and W2 domains 2			0.19	Cytoplasm
THOP1	thimet oligopeptidase 1			0.191	Cytoplasm
GAA	glucosidase alpha, acid			0.192	Cytoplasm
PPIF	peptidylprolyl isomerase F			0.192	Cytoplasm
NCL	nucleolin			0.193	Nucleus
GSR	glutathione-disulfide reductase			0.196	Cytoplasm

RDX	radixin			0.196	Cytoplasm
REXO2	RNA exonuclease 2			0.196	Cytoplasm
OLA1	Obg like ATPase 1			0.198	Cytoplasm
OPLAH	5-oxoprolinase (ATP-hydrolysing)			0.198	Cytoplasm
BZW1	basic leucine zipper and W2 domains 1			0.199	Cytoplasm
DDX21	DExD-box helicase 21			0.2	Nucleus
YWHAE	tyrosine 3-monooxygenase/tryptophan 5-monooxygenase activation protein epsilon			0.2	Cytoplasm
NONO	non-POU domain containing, octamer-binding			0.201	Nucleus
SLC25A5	solute carrier family 25 member 5			0.201	Cytoplasm
NAT10	N-acetyltransferase 10			0.203	Nucleus
TMED7	transmembrane p24 trafficking protein 7			0.203	Cytoplasm
DDX39B	DExD-box helicase 39B			0.204	Nucleus
VARS	valyl-tRNA synthetase			0.204	Cytoplasm
PRKAR2A	protein kinase cAMP-dependent type II regulatory subunit alpha			0.205	Cytoplasm
TXNRD1	thioredoxin reductase 1			0.206	Cytoplasm
ADAR	adenosine deaminase, RNA specific			0.208	Nucleus
HGD	homogentisate 1,2-dioxygenase			0.208	Cytoplasm
PNP	purine nucleoside phosphorylase			0.208	Nucleus
USP9X	ubiquitin specific peptidase 9, X-linked			0.21	Plasma Membrane
GMDS	GDP-mannose 4,6-dehydratase			0.212	Cytoplasm
ME2	malic enzyme 2			0.212	Cytoplasm
RBM14	RNA binding motif protein 14			0.212	Nucleus
TOMM70	translocase of outer mitochondrial membrane 70			0.213	Cytoplasm
DHX15	DEAH-box helicase 15			0.214	Nucleus
GARS	glycyl-tRNA synthetase			0.214	Cytoplasm
HNRNPA1	heterogeneous nuclear ribonucleoprotein A1			0.214	Nucleus
SRSF2	serine and arginine rich splicing factor 2			0.214	Nucleus
SRSF7	serine and arginine rich splicing factor 7			0.216	Nucleus
FIP1L1	factor interacting with PAPOLA and CPSF1			0.218	Nucleus
S100P	S100 calcium binding protein P			0.218	Cytoplasm
TRMT10C	tRNA methyltransferase 10C, mitochondrial RNase P subunit			0.219	Cytoplasm
CARM1	coactivator associated arginine methyltransferase 1			0.22	Nucleus
GNB2	G protein subunit beta 2			0.22	Plasma Membrane
EEF2	eukaryotic translation elongation factor 2			0.221	Cytoplasm
UBE2M	ubiquitin conjugating enzyme E2 M			0.221	Cytoplasm
NAP1L1	nucleosome assembly protein 1 like 1			0.226	Nucleus
TROVE2	TROVE domain family member 2			0.227	Nucleus
LTA4H	leukotriene A4 hydrolase			0.229	Cytoplasm
YTHDF3	YTH N6-methyladenosine RNA binding protein 3			0.229	Cytoplasm
HNRNPA0	heterogeneous nuclear ribonucleoprotein A0			0.231	Nucleus
MSI2	musashi RNA binding protein 2			0.231	Cytoplasm
HSPA4	heat shock protein family A (Hsp70) member 4			0.233	Cytoplasm

JAGN1	jagunal homolog 1			0.236	Cytoplasm
MAT2A	methionine adenosyltransferase 2A			0.236	Cytoplasm
PFN1	profilin 1			0.238	Cytoplasm
BCAT1	branched chain amino acid transaminase 1			0.24	Cytoplasm
CSDE1	cold shock domain containing E1			0.243	Cytoplasm
PDLIM5	PDZ and LIM domain 5			0.248	Cytoplasm
SSB	Sjogren syndrome antigen B			0.25	Nucleus
GSPT1	G1 to S phase transition 1			0.251	Cytoplasm
AHCY	adenosylhomocysteinase			0.252	Cytoplasm
CMBL	carboxymethylenebutenolidase homolog			0.252	Cytoplasm
EML4	echinoderm microtubule associated protein like 4			0.254	Cytoplasm
PPM1G	protein phosphatase, Mg2+/Mn2+ dependent 1G			0.255	Nucleus
MTPN	myotrophin			0.258	Nucleus
DPP4	dipeptidyl peptidase 4			0.261	Plasma Membrane
FUS	FUS RNA binding protein			0.261	Nucleus
HSD17B11	hydroxysteroid 17-beta dehydrogenase 11			0.262	Cytoplasm
CBR4	carbonyl reductase 4			0.264	Cytoplasm
BLVRA	biliverdin reductase A			0.266	Cytoplasm
NAA15	N(alpha)-acetyltransferase 15, NatA auxiliary subunit			0.268	Nucleus
EEA1	early endosome antigen 1			0.269	Cytoplasm
HNRNPDL	heterogeneous nuclear ribonucleoprotein D like			0.269	Nucleus
LARP1	La ribonucleoprotein domain family member 1			0.269	Cytoplasm
SLC25A6	solute carrier family 25 member 6			0.269	Cytoplasm
TRA2B	transformer 2 beta homolog (Drosophila)			0.273	Nucleus
GDI2	GDP dissociation inhibitor 2			0.276	Cytoplasm
GNL3	G protein nucleolar 3			0.276	Nucleus
SYNCRIP	synaptotagmin binding cytoplasmic RNA interacting protein			0.277	Nucleus
GMPS	guanine monophosphate synthase			0.278	Nucleus
HNRNPR	heterogeneous nuclear ribonucleoprotein R			0.281	Nucleus
ITPR2	inositol 1,4,5-trisphosphate receptor type 2			0.282	Cytoplasm
ESD	esterase D			0.285	Cytoplasm
PAFAH1B1	platelet activating factor acetylhydrolase 1b regulatory subunit 1			0.285	Cytoplasm
HNRNPAB	heterogeneous nuclear ribonucleoprotein A/B			0.286	Nucleus
NNT	nicotinamide nucleotide transhydrogenase			0.286	Cytoplasm
NQO1	NAD(P)H quinone dehydrogenase 1			0.287	Cytoplasm
PA2G4	proliferation-associated 2G4			0.287	Nucleus
ABCE1	ATP binding cassette subfamily E member 1			0.29	Cytoplasm
EIF4A2	eukaryotic translation initiation factor 4A2			0.29	Cytoplasm
NOP16	NOP16 nucleolar protein			0.29	Nucleus
SBDS	SBDS ribosome assembly guanine nucleotide exchange factor			0.29	Nucleus

LCMT1	leucine carboxyl methyltransferase 1			0.292	Cytoplasm
NUDT5	nudix hydrolase 5			0.301	Cytoplasm
RBM22	RNA binding motif protein 22			0.302	Nucleus
HIBCH	3-hydroxyisobutyryl-CoA hydrolase			0.303	Cytoplasm
EIF1AX	eukaryotic translation initiation factor 1A, X-linked			0.314	Cytoplasm
NOP2	NOP2 nucleolar protein			0.317	Nucleus
EEF1A1	eukaryotic translation elongation factor 1 alpha 1			0.319	Cytoplasm
ILKAP	ILK associated serine/threonine phosphatase			0.328	Cytoplasm
CELF1	CUGBP Elav-like family member 1			0.331	Cytoplasm
RBM3	RNA binding motif (RNP1, RRM) protein 3			0.333	Cytoplasm
TPT1	tumor protein, translationally-controlled 1			0.345	Cytoplasm
PUS7	pseudouridylate synthase 7 (putative)			0.352	Other
LBR	lamin B receptor			0.354	Nucleus
PABPC4	poly(A) binding protein cytoplasmic 4			0.358	Cytoplasm
LPP	LIM domain containing preferred translocation partner in lipoma			0.36	Nucleus
APEX1	apurinic/apyrimidinic endodeoxyribonuclease 1			0.362	Nucleus
RBMX	RNA binding motif protein, X-linked			0.365	Nucleus
GCLC	glutamate-cysteine ligase catalytic subunit			0.37	Cytoplasm
STIM1	stromal interaction molecule 1			0.37	Plasma Membrane
FAM120A	family with sequence similarity 120A			0.371	Cytoplasm
MAN2A1	mannosidase alpha class 2A member 1			0.371	Cytoplasm
TACO1	translational activator of cytochrome c oxidase I			0.371	Cytoplasm
SNRPN	small nuclear ribonucleoprotein polypeptide N			0.38	Nucleus
NADK2	NAD kinase 2, mitochondrial			0.383	Cytoplasm
CHTOP	chromatin target of PRMT1			0.397	Nucleus
CIRBP	cold inducible RNA binding protein			0.404	Nucleus
ASNS	asparagine synthetase (glutamine-hydrolyzing)			0.412	Cytoplasm
EIF5	eukaryotic translation initiation factor 5			0.444	Cytoplasm
RPF2	ribosome production factor 2 homolog			0.45	Nucleus
H1F0	H1 histone family member 0			0.458	Nucleus
RGN	regucalcin			0.459	Nucleus
SAMM50	SAMM50 sorting and assembly machinery component			0.477	Cytoplasm
ARSA	arylsulfatase A			0.489	Cytoplasm
ABCB1	ATP binding cassette subfamily B member 1			0.491	Plasma Membrane
VDAC2	voltage dependent anion channel 2			0.522	Cytoplasm
YBX1	Y-box binding protein 1			0.546	Nucleus